ASSESSING THE NEURAL CORRELATES, SOURCES AND CONSEQUENCES OF THE ATTENTIONAL RHYTHM

A Dissertation
Submitted to the Graduate Faculty
of the
North Dakota State University
of Agriculture and Applied Science

By

Andrea Bocincova

In Partial Fulfillment of the Requirements
for the Degree of
DOCTOR OF PHILOSOPHY

Major Department:
Psychology

April 2019

Fargo, North Dakota

North Dakota State University
Graduate School

Title

ASSESSING THE NEURAL CORRELATES, SOURCES AND CONSEQUENCES OF THE ATTENTIONAL RHYTHM

By

Andrea Bocincova

The Supervisory Committee certifies that this ***disquisition*** complies with North Dakota State University's regulations and meets the accepted standards for the degree of

DOCTOR OF PHILOSOPHY

SUPERVISORY COMMITTEE:

Dr. Jeffrey Johnson
Chair

Dr. Benjamin Balas

Dr. Paul Rokke

Dr. Simone Ludwig

Approved:

April 08, 2019
Date

Dr. Mark Nawrot
Department Chair

ABSTRACT

Evidence suggests that even when sustained at a single location, spatial attention waxes and wanes over time. These fluctuations are cyclic, lasting about 125-200 ms (i.e., ~4-8 Hz), and are characterized by alternating periods of focused attention to a single location together with exploratory periods during which attention is prone to switching to a new source of stimulation. Despite an increasing interest in this temporal property of spatial attention, multiple aspects of rhythmic attentional sampling remain to be explored. In this dissertation, I introduce and examine three unexplored areas related to this topic. The first area, addressed in Experiment 1, concerns the potential neural oscillatory signatures of attentional rhythmicity. Precisely, it assesses the role of a well-established oscillatory correlate of selective attention, alpha band power, in rhythmic switching of attention over time. The second area focuses on the neural sources controlling rhythmic attentional sampling. More specifically, the goal of Experiment 2 is to establish causal evidence for the involvement of an important attentional hub in generating the attentional rhythm using transcranial magnetic stimulation. Finally, the last area examines the consequences of attentional rhythmicity on the encoding and storage of information in working memory. In particular, Experiment 3 provides evidence that rhythmic changes in spatial attention affect the quality with which information is encoded into working memory. Finally, Experiment 4 assesses whether attention rhythmically cycles between items stored in WM in a manner similar to the cycling observed when attention is directed to the external world. In summary, the work included in this dissertation makes an important contribution to extending our understating of the attentional rhythm and introduces multiple avenues for further research necessary in this area.

ACKNOWLEDGEMENTS

Over the past five years, I have had the incredible opportunity to be a part of the Department of Psychology at North Dakota State University. The work included in this dissertation would have not been possible without the support of the faculty and staff of this department for which I am very grateful. I would like to express my gratitude to the members of my dissertation committee, Dr. Benjamin Balas, Dr. Paul Rokke and Dr. Simone Ludwig for their help with refining the ideas for this dissertation and their words of encouragement. I am also thankful to Dr. Benjamin Balas for introducing me to the secrets of programming that gave me the type of independence in my research I cannot imagine working without.

The biggest thank you goes to my advisor, Dr. Jeffrey Johnson, for giving me a chance to learn that research is my passion. During the years I worked under his supervision, he always had my best interests in mind. He was persistent in teaching me how to be a better researcher even if the process seemed painful sometimes because it was too early for me to see the big picture. He allowed me to make mistakes and learn from them, teaching me independence and accountability as a result. Aside from his academic guidance, he also cared about my well-being, provided emotional support and reminded me numerous times that things were never as tragic as they seemed (often with humor and empirical data). He always kept his door open when I needed it. Looking back, I wish I had taken more opportunities to tell him how great of an advisor he was to me.

Many thanks also go to my fellow graduate students and post docs, some of which became my friends for life. I would especially like to thank Shanda Lauer for showing me how to be strong and how to navigate graduate school with grace and positivity (and a pinch of sarcasm), and Amanda van Lamsweerde for being an incredible coworker and a friend who was

always there for me when I needed advice or needed to vent my frustrations. I am also indebted to the current and prior members of the Johnson Cognitive Neuroscience Lab, especially Stephanie Leach, who were essential to my successful completion of this work. I am also grateful to the members of the staff for their help and friendship; I cannot even count the number of times Dan Gu, Enrique Alvarez-Vazquez, Ganesh Padmanabhan and Alyson Saville saved my day.

I owe a life-long thank you to my parents and my brother. I would like to thank my dad for encouraging my curiosity from an early age and for his never-ending support. I thank my mom for always celebrating my success and cheering me up when I felt defeated. To my brother, I thank for paving my way to success and always taking care of me. I love them all for never making me feel guilty for pursuing my goals even if it meant moving away across the ocean.

Finally, I am forever indebted to my husband, Jonathan Calix. He was there for me during the highs, the lows and everything in between, listening, guiding, helping, celebrating, encouraging, and doing everything to keep me happy. There are no words that can do justice to how much his support meant to me. He truly is the best thing in my life.

TABLE OF CONTENTS

LIST OF FIGURES

LIST OF ABBREVIATIONS

SOA	Stimulus Onset Asynchrony
CTC	Communication Through Coherence
ABOP	Alpha Band Oscillatory Power
EEG	Electroencephalogram
FEF	Frontal Eye Fields
LIP	Lateral Intraparietal Area
VFC	Ventral Frontal Cortex
TPJ	Temporoparietal Junction
TMS	Transcranial Magnetic Stimulation
WM	Working Memory
IEM	Inverted Encoding Model
CTF	Channel Tuning Function
IRB	Institutional Review Board
LCD	Liquid Crystal Display
CMS	Common Mode Sense electrode
DRL	Driven Right Leg (DRL) electrode
EOG	Electrooculogram
PSD	Power Spectrum Density
IRASA	Irregular-Resampling Auto-Spectral Analysis
SD	Standard Deviation
CI	Confidence Interval
SEM	Standard Error of the Mean
TMS	Transcranial Magnetic Stimulation

rTMS	Repetitive Transcranial Magnetic Stimulation
cTBS	Continuous Theta Burst Stimulation
RT	Reaction Time
MRI	Magnetic Resonance Imagining
ANOVA	Analysis of Variance
LVF	Left Visual Field
RVF	Right Visual Field

LIST OF APPENDIX FIGURES

INTRODUCTION

The Role of Attention and its Implications for the Nature of Attentional Processing

The visual systems of humans and other animals continuously receive stimulation from numerous sources that compete for the brain's limited processing resources. In order to tackle such highly dynamic environments, attentional processes have developed to structure the moment-to-moment perceptual experience by selecting and facilitating the processing of only currently relevant information from the sensory stream (see Desimone & Duncan, 1995 for review). According to the classic view of attention, this metaphorically happens by moving a spotlight of attention around the visual field and facilitating the processing of stimuli within the 'beam of light' (Crick, 1984; Posner & Petersen, 1990; Treisman, 1982). We all subjectively experience this between eye fixations when we overtly switch attention from one object or location in our visual space to another.

Interestingly, more recent experimental findings show that even if overt attention is continuously sustained at a single location, covert selective attention continues to sample periodically from multiple potentially relevant sources, in a manner similar to the process of overt ocular exploration (see Zoefel & VanRullen, 2017 for a review). According to this newer view, the spotlight of attention is intrinsically rhythmic with periods of attention directed to the attended stimulus periodically overlaid with periods of "exploration" during which attention is prone to be attracted to other sources of stimulation (Figure 1A). This periodicity allows the spotlight to flexibly sample from multiple information sources at different phases of its oscillation (Figure 1B). Such attentional reweighting is not subjectively experienced under normal circumstances, but happens within a single and/or between multiple objects/locations every ~125-200 ms, i.e., at a frequency of 4-8 Hz, which corresponds to a theta oscillatory

rhythm (Fiebelkorn, Saalmann, & Kastner, 2013; Landau, Schreyer, van Pelt, & Fries, 2015; Song, Meng, Chen, Zhou, & Luo, 2014).

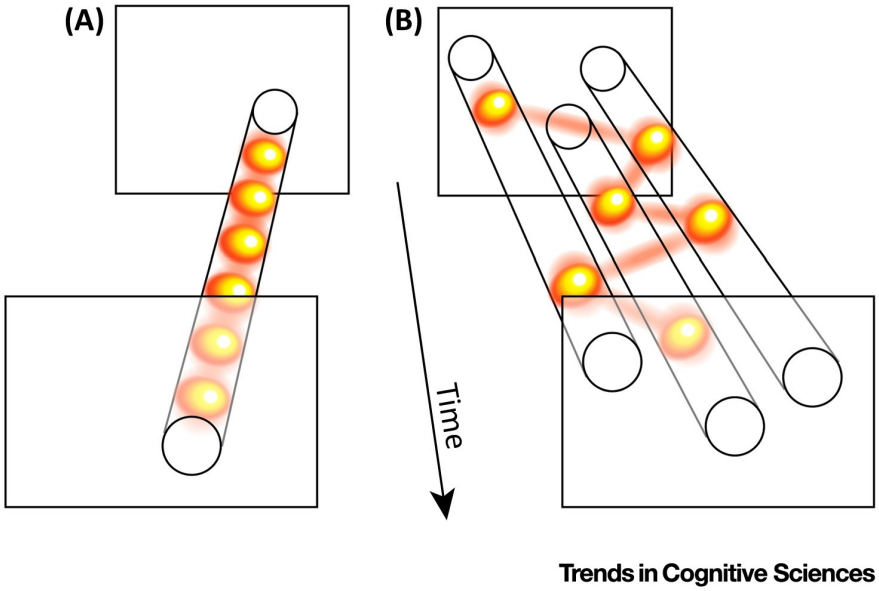

Figure 1. Blinking spotlight of attention (VanRullen, 2016)[1]. To flexibly monitor the environment, attentional processing fluctuates rhythmically between cycles of directed attention and exploration resulting in periodic sampling of a single object/location (A) or rhythmic serial sampling between multiple sources/objects (B).

Using psychophysics, the rhythmic sampling of attention can be revealed through the implementation of so-called attentional reset. If attention naturally oscillates between two different locations in a serial manner, i.e., sampling from one location at one point in time (i.e., at a particular phase of an ongoing oscillation) and sampling from the other location at a different point in time, an attention-grabbing stimulus presented near one of the locations/objects can be used to generate a consistent phase alignment across trials (Figure 2A). As a result of this reset, a measure of attentional allocation to the location on the same and opposite side of the resetting stimulus at different stimulus-onset-asynchronies (SOAs) reveals a pattern of cyclic fluctuations

[1] Reprinted from Trends in Cognitive Sciences, 20, VanRullen, R., Perceptual Cycles, 723–735, 2016, with permission from Elsevier.

in performance (Figure 2C). This cyclic pattern is not generated by the resetting stimulus, but rather reflects an intrinsic rhythm present even in the absence of an external event (Busch & VanRullen, 2010; Landau & Fries, 2012).

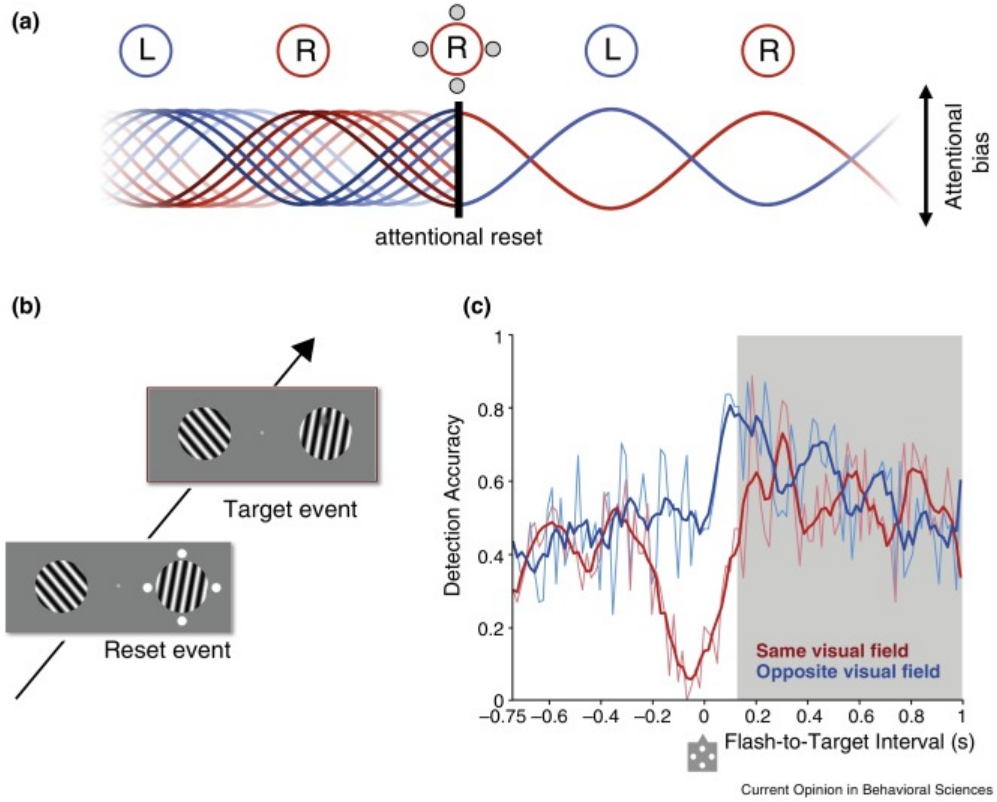

Figure 2. Revealing the rhythmic fluctuations in attentional bias (Herbst & Landau, 2016)[2]. (A) An attention-grabbing stimulus is used to align the phase of ongoing attentional sampling across trials. (B) A measure of performance is collected at varying intervals following the reset stimulus and at locations congruent and incongruent with the flash. (C) Plotting behavioral performance at increasing SOAs following the resetting event reveals a pattern of attentional sampling shifting rhythmically between the two attended objects every ~200 ms.

Attentional Rhythmicity and Oscillations

The experimentally observed rhythm of attentional sampling seems to parallel physiological rhythms of brain activation referred to as neural oscillations. In fact, rhythmic

[2] Reprinted from Current Opinion in Behavioral Sciences, 8, Herbst, S., K., Landau, A., N., Rhythms for cognition: the case of temporal processing, 85–93, 2016, with permission from Elsevier.

attentional sampling is potentially a direct consequence of the oscillatory nature of neural activity. The resting membrane potential of individual neurons fluctuates over time and the firing rates of groups of interconnected neurons tend to naturally synchronize. According to the Communication Through Coherence theory (CTC; Fries, 2005, 2015), communication between neuronal groups is established through their rhythmic synchronization, which creates temporal windows during which transfer of information is more effective. Interestingly, it has been shown that the activity of neurons in early visual areas tends to vary with the phase of relatively slow oscillations (Spaak, Bonnefond, Maier, Leopold, & Jensen, 2012). Findings like these continue to demonstrate that the processing of incoming inputs varies systematically as a function of oscillatory phase (Buschman & Kastner, 2015; Siegel, Donner, Oostenveld, Fries, & Engel, 2008), and the potential of neural oscillations to modulate the effectiveness of information transfer makes them an ideal candidate mechanism for implementing selective attention.

Supporting the possibility of an oscillatory mechanism for attention, studies of selective attention by Mathewson et al. (2009) and Busch, Dubois, and VanRullen (2009) showed that participants were more likely to perceive hard-to-see targets at a single location when the targets were presented at a particular phase of a theta-alpha (4-10 Hz) oscillation and were more likely to miss them when presented at the opposite phase. In like manner, in a study by Busch and VanRullen (2010), participants were required to detect hard-to-see objects that could appear at two locations, one attended and one unattended. Even though behavioral and neural measures showed that attention was directed to the attended location, detection performance at the attended location was predicted by the phase of a theta (~7 Hz) oscillation. This suggests that, even when apparently ‘sustained’ at a single location, the effects of attention wax and wane over time in a

rhythmic fashion. These studies point towards the possibility that the cycling patterns of attention revealed in behavioral data are driven by underlying neural oscillatory activity.

Extending the role of oscillatory rhythms in attention further, it has been proposed that the above-described attentional rhythm interacts with other brain oscillatory rhythms; more specifically, gamma and alpha oscillations. According to CTC (Fries, 2015), neural networks naturally synchronize in the alpha frequency band, which prevents communication and keeps the activity within the local network basically invisible to other networks. These "local" neural representations can be sampled (in theta rhythm) by attention, which releases the network from inhibition by de-synchronizing alpha (Clayton, Yeung, & Cohen Kadosh, 2015). Sampled representations are then represented in gamma band activity that effectively transfers information across the network. In line with this proposal, Landau et al. (2015) demonstrated that when two locations were simultaneously monitored, stimulus-related gamma-band (>40 Hz) oscillations were modulated by the phase of a 4 Hz theta oscillation.

Unlike for gamma activity, evidence for the role of alpha activity in the attentional rhythm has yet to be well established (however, see discussion of Fiebelkorn, Pinsk, & Kastner, 2018 below). The role of alpha-band activity is well studied in more traditional effects of attention. For example, numerous studies have reported decreases in alpha band oscillatory power (ABOP; i.e., alpha de-synchronization) in visual areas representing attended information and increased ABOP in areas representing distractors (e.g., Fries, Reynolds, Rorie, & Desimone, 2001; Sauseng et al., 2005). In other words, alpha oscillations seem to enhance attentional selection through the inhibition of task-irrelevant information (Klimesch, 2012). However, the importance of alpha in generating rhythmic shifts in attention has not been examined.

Additionally, all of the studies providing evidence for the existence of the neural correlate of the attentional rhythm only explored the relationship between underlying neural oscillations and target-related processing; however, none of these studies directly tracked how changes in neural oscillations relate to rhythmic changes in attention over time. To begin exploring this, Jia, Liu, Fang and Luo (2017; see also Jensen & Vissers, 2017 for additional analyses of the data) tracked the allocation of attention following spatial cues that indicated the likely location of an upcoming target with different levels of validity (100%, 75% and 50%). At the same time, they used electroencephalography (EEG) together with temporal response function analysis to analyze the processing of two continuously visible objects over time. They found that attended and unattended objects were sampled sequentially depending on their task-relevance at a rate of about 2 Hz (Jensen & Vissers, 2017). To my knowledge, this is the only study to date that has focused on the neural signature of attentional rhythmicity in the temporal dimension. The majority of studies assessing neural correlates of attentional sampling focus on target-related processing and, as a result, provide important information about neural activity immediately preceding the target, but do not provide information about how these neural correlates unfold over time.

To address the lack of research in this area, Experiment 1 examined the role of ABOP in rhythmic attention using an inverted encoding modeling approach (e.g., Foster, Sutterer, Serences, Vogel, & Awh, 2017) to track the rhythmic allocation of attention over time.

Neural Substrates of the Rhythm of Attention

The role of the brain's oscillatory rhythms in generating the rhythmic signature of attention is becoming clearer; however, its neural source is still elusive. Generally, attention is supported by activity within a distributed network of brain regions that can be organized into two

systems (Corbetta & Shulman, 2002). The dorsal fronto-parietal network, including the frontal eye fields (FEF) and lateral intraparietal area (LIP), primarily supports top-down control of visual attention; i.e., selection of stimuli and responses on the basis of current goals. The ventral fronto-parietal network, including the ventral frontal cortex (VFC) and temporoparietal junction (TPJ) serves to 'break' the goal-directed activity supported by the first system and orient attention towards unexpected and potentially behaviorally significant stimuli. Because attention relies on a network of brain areas, communication between these different hubs is of crucial importance.

As I described above, existing theories and empirical evidence suggest that oscillatory brain activity supports communication between different brain regions (Fries, 2005, 2015; Helfrich & Knight, 2016; Siegel, Donner, & Engel, 2012). Moreover, theta-band (4-8 Hz) oscillatory activity, which corresponds to the sampling frequency of selective attention revealed through psychophysics, is a likely candidate for implementing top-down control by directing the flow of relevant information through the brain (Cavanagh & Frank, 2014; Phillips, Vinck, Everling, & Womelsdorf, 2014; Sellers et al., 2016; Szczepanski et al., 2014). One possibility is that communication among the nodes of the proposed attentional network and its top-down influence on lower-level visual areas is driving the signature theta rhythm of attention.

Two recent studies were among the first to attempt to address the question of the neural underpinnings of the attentional rhythm. In the first study, Helfrich et al. (2018) measured brain signals intracranially while participants performed an attention detection task. They showed that participants' ability to detect targets was predicted by the phase of theta recorded from channels in the fronto-parietal network at the time of target appearance. Moreover, activity in higher frequency bands (gamma >30 Hz), which likely reflect neuronal spiking activity, were

rhythmically modulated at theta frequency providing additional evidence that fluctuations in detection performance were related to rhythmic changes in neural excitability. In the second study, Fielberkorn, Pink and Kastner (2018) recorded from two hubs of the fronto-parietal attentional network in two macaque monkeys, the FEF and LIP, and found that the dynamic interplay between these two areas accounted for the observed rhythmic shifts in spatial attention. More specifically, they found that the phase of theta oscillations in the fronto-parietal network coordinated two rhythmically alternating states of the network. The first state was characterized by suppressed shifting of attention; in other words, by a state of sustained attention to the cued location. This state was dominated by beta-band (16-35 Hz) activity in the FEF and gamma-band activity reflecting active processing and improved performance in the LIP. The second state, corresponding to a shifting focus of attention, was characterized by an increase of alpha-band activity in the LIP, which was proposed to reflect reduced processing of target stimuli and a worsening of behavioral performance. According to these results, theta oscillations generated in the FEF propagate to more posterior areas and serve the purpose of organizing activity within the attentional network, potentially generating the theta signature observed in behavioral data. In contrast to this proposal, a multi-unit recording study of activity in monkey extra-striate area V4 showed that theta-rhythmic activity can arise from local competitive interactions within neuronal receptive fields, rather than reflecting long-range influences (Kienitz et al., 2018). Future studies will be needed to reconcile these findings.

Interestingly, the brain region implicated in directing attentional shifts in non-human primates, the FEF, has also been shown to exert feedback control over how information is routed through the cortex in humans (Popov, Kastner, & Jensen, 2017). Moreover, it has been shown that transcranial magnetic stimulation (TMS)-induced disruption of the FEF results in a reduction

of EEG correlates of anticipatory attention (Sauseng, Feldheim, Freunberger, & Hummel, 2011). Importantly, the extent of disruption of fronto-parietal communication indexed by fronto-parietal alpha coupling predicted decrements in behavioral performance, suggesting that this disruption had functional significance. Despite this clear link between the FEF and the allocation of attention, no human study has directly tested the role of FEF in mediating rhythmic shifts of attention. If FEF orchestrates the rhythmic shifts of attention, disruption of the FEF should result in a degradation of the attentional rhythm. This possibility was explored in Experiment 2.

The Role of Attention in Working Memory

Our ability to selectively attend to relevant information in the environment while ignoring information that is irrelevant is closely related to our ability to hold information "in mind" when it is no longer present in the environment, an ability known as working memory (WM; Baddeley, 1992; D'Esposito & Postle, 2015). Previous evidence has shown that information we attend to is more likely to be stored in WM, and information that we hold in WM biases attention towards matching information in the environment (Downing, 2000; Downing & Dodds, 2004; Olivers, Peters, Houtkamp, & Roelfsema, 2011; Pashler & Shiu, 1999; Woodman & Luck, 2002). Despite the close relationship between attention and WM, and growing evidence for periodic fluctuations in attention, the effects of the proposed attentional rhythm on WM have not been well examined.

There are several reasons to think that periodic fluctuations in attention may be relevant to WM. First of all, when and what we attend to in the environment influences the quality of what is encoded into WM (Awh & Pashler, 2000; Makovski & Jiang, 2007; Schmidt, Vogel, Woodman, & Luck, 2002; Vogel, Woodman, & Luck, 2005). For example, providing spatial cues about where a to-be-remembered object will be presented increases memory accuracy (Schmidt et al., 2002). As a result of the rhythmic nature of attentional allocation to space and

the relationship between WM encoding and attention, it could be the case that the efficiency of encoding information into WM fluctuates in a similar fashion. To test this prediction, Experiment 3 probed the effect of rhythmic attentional fluctuations on WM encoding.

Secondly, research has shown that maintaining information in WM involves sustained attention to the internal representations of remembered objects in the same way that attention is allocated to sources of stimulation in the environment (Awh & Jonides, 2001; Awh, Jonides, & Reuter-Lorenz, 1998; Chun & Johnson, 2011). An unexplored aspect of attentional deployment during WM maintenance is whether attention is distributed equally across multiple maintained representations, or whether it switches periodically between representations in a manner similar to the cycling of attention between items in the external world. Experiment 4 explored whether such periodic switching exists among the items held in WM by testing whether an attentional reset presented during the active maintenance of information in WM reveals cyclic fluctuations in access to WM representations.

In summary, this dissertation explores three different aspects of rhythmic attentional sampling. Experiment 1 assesses whether attentional sampling can be tracked over time using well-established oscillatory correlates of spatial attention (i.e., alpha band oscillatory power). Experiment 2 then explores the involvement of the frontal eye fields, an important attention network hub, in generating the attentional rhythm. Finally, Experiments 3 and 4 explore whether rhythmic attentional sampling also extends to the processes of encoding and storing information in WM. In particular, Experiment 3 tests whether the rhythmically changing allocation of attention in time and space affects the quality with which information is encoded into WM. Experiment 4 then explores whether attentional resources devoted to the active maintenance of information in WM are rhythmic in nature.

EXPERIMENT ONE: ASSESSING THE NEURAL OSCILLATORY SIGNATURES OF RHYTHMIC ALLOCATION OF SPATIAL ATTENTION

Introduction

Thus far, the majority of studies assessing the oscillatory correlates of rhythmic fluctuations in attention have adopted experimental designs in which an attention-grabbing stimulus is used to reset attentional sampling (Figure 2). This effectively resets the phase of the attention cycle, allowing us to know where attention is at a given moment in time. However, to date, the temporal evolution of the neural correlates underlying such attentional cycling have not been well characterized (for a first step in this direction, see Jia et al., 2017). Existing neural evidence for the presence of rhythmic attention cycling comes from studies examining target-related activity (e.g., Busch et al., 2009; Landau et al., 2015). These studies are capable of capturing pre-stimulus neural activity (~500 ms prior to stimulus onset) and relating its characteristics to the subsequent detection of a target. However, they only provide a snapshot of ongoing dynamic neural activity at a moment in time.

Previous studies assessing effects of directed spatial attention over time have shown sustained alpha band oscillatory power (ABOP) de-synchronization in the hemisphere contralateral to the attended location (e.g., Sauseng et al., 2005; Kelly, Lalor, Reilly, & Foxe, 2006; Rihs, Michel, & Thut, 2007). Such sustained effects, however, seem to be at odds with the proposed rhythmically fluctuating nature of spatial attention. One possible explanation of these sustained ABOP effects is that they are a result of trial averaging. If attention samples between spatial locations and this sampling is not constrained in any way (e.g., by using a resetting stimulus), the time course of attentional allocation will vary between trials and will be obscured once trials are averaged to increase signal-to-noise ratio. If this is the case, using a resetting

stimulus should align the phase of the attentional rhythm and reveal rhythmic fluctuations in ABOP between hemispheres contralateral versus ipsilateral to the location of the resetting stimulus.

Another possibility is that attentional sampling relies on oscillatory correlates that are different from the ones supporting directed spatial attention. Some studies exploring the rhythmic sampling of attention have reported general attentional benefits at the attended location (e.g., lower detection thresholds and larger attention-related event-related responses reported by Busch & VanRullen, 2010) in addition to rhythmic fluctuations of attentional effects. It may be the case that ABOP de-synchronization is a signature of this general effect of attention, but it may not track the rhythmic changes in attentional allocation.

To explore the possibility that ABOP represents an oscillatory correlate of attentional sampling, the current experiment assessed the ABOP signature in an experimental design that was conducive to observing its rhythmic changes, possibly reflecting rhythmic sampling of attention. In addition to assessing changes of ABOP over time, the present experiment also used a more sensitive, multivariate inverted encoding modeling (IEM) approach to reconstruct the focus of spatial attention as it cycles between two locations over time. This approach assumes that stimulus representations can be reconstructed from neural signals measuring population-level neural activity. In general, the IEM is trained to model a relationship between stimulus feature values (e.g., spatial location) and their associated neural activity based on a hypothesized neural response function. The derived model is then used to reconstruct the feature value of a novel stimulus feature based on its neural representation (Figure 3). In this particular case, the model takes advantage of the fact that the topographic distribution of alpha-band power over parietal and occipital brain regions changes depending on the current locus of spatial attention

(e.g., Sauseng et al., 2005; Kelly et al., 2006; Rihs et al., 2007) and uses it to reconstruct the attended location. Previous studies implementing IEM have shown that this approach can be used to successfully track the focus of spatial attention over the course of a trial (Foster, Sutterer, et al., 2017). More importantly, it is capable of tracking the allocation of attention to more than one location, in which case the derived index of attentional allocation is sensitive to which location is currently attended and unattended (Foster, Bsales, Jaffe, & Awh, 2017). These characteristics of the IEM make this approach suitable for assessing the rhythmicity of attention during sampling of two locations over time.

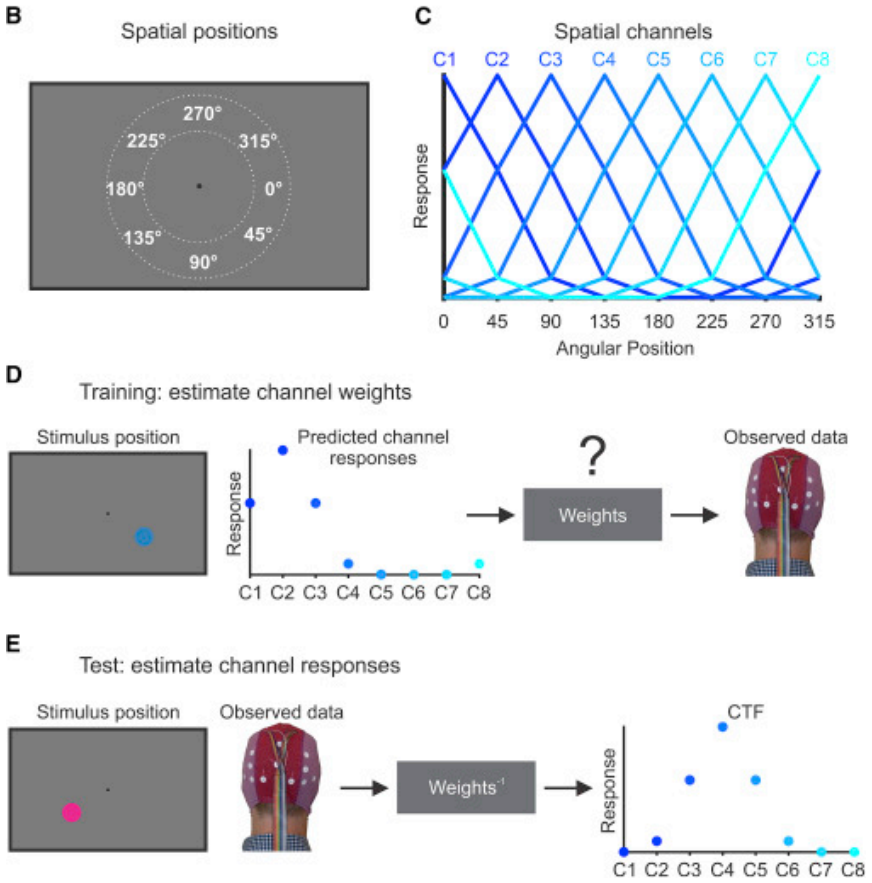

Figure 3. A schematic depiction of the reconstruction of spatial positions using inverted encoding modeling (Foster, Sutterer, et al., 2017)[3]. (B) Eight spatial positions and (C) their hypothesized neural responses in eight spatially tuned channels. (D) During training, IEM uses the predicted spatial channel responses to generate a set of weights representing the relative contribution of each of the spatial channels to the observed data. (E) In the test phase, the derived weights are then used to reconstruct the feature value (represented by the channel tuning function; CTF) of a novel, independent stimulus feature from observed data. Reprinted from Foster et al. (2017).

The goal of Experiment 1 was to test whether well-established oscillatory correlates of directed attention (i.e., contralateral alpha band power desynchronization; e.g., Sauseng et al., 2005; Kelly et al., 2006; Rihs et al., 2007) can be used to track the rhythmic sampling of attention over time and whether IEM utilizing the topographic pattern of ABOP can track the

[3] Reprinted from Psychological Science, 28, Foster, J. J., Sutterer, D. W., Serences, J. T., Vogel, E. K., & Awh, E., Alpha-Band Oscillations Enable Spatially and Temporally Resolved Tracking of Covert Spatial Attention, 929–941, 2017, with permission from SAGE Publications.

rhythmic allocation of attention to two spatial locations over the course of a trail. If ABOP can serve as a signature of attentional sampling, I hypothesized that a reset of attentional sampling should produce a pattern of ABOP de-synchronization and re-synchronization that alternate throughout the delay period. Additionally, because the reconstructed channel responses obtained through IEM are sensitive to the current focus of attention, I hypothesized that resetting the phase of attentional sampling should generate rhythmic fluctuations in observed channel tuning functions that are similar to fluctuations previously observed in behavioral data. In other words, topographic patterns of ABOP reflecting the momentary focus of attention should change in a rhythmic fashion over the course of a trial.

Materials and Methods

Participants. Fourteen undergraduate and graduate students (13 female; 20-32 years M = 23.9, SD = 4.2) were recruited from North Dakota State University to participate in this study for course credit or monetary compensation ($15/hr). Three participants were dropped due to poor behavioral performance (the percentage of false alarms for two participants was >30% and, for one participant, the percentage of hits in RVF was <10%). One participant was dropped due to a high percentage of rejected trials due to EEG artifacts. All participants were required to have normal or corrected to normal vision, normal color vision and no prior or current neurological or mental disorders, determined by self-report. Each participant provided written informed consent and all experimental protocols were approved by the North Dakota State University IRB.

Materials and procedure. Stimulus presentation and response recording were controlled by a PC running Matlab (Mathworks, Inc.) with Psychophysics Toolbox extensions (Brainard, 1997; D.G. Pelli, 1997). Stimuli were presented on the surface of a 24” LCD monitor (BenQ Model XL2430-B) with a refresh rate of 144 Hz at a viewing distance of 57 cm.

Participants performed an attention task during which they were asked to report the presence of a target that could appear at one of two possible locations. The experimental stimuli consisted of two circular, black and white noise patches (black R=0, G=0, B=0; white R=255, G=255, B=255) subtending 1.6° of visual angle in diameter presented against medium gray background (R=128, G=128, B=128) and positioned 3.8° of visual angle from central fixation point, and a target stimulus, a black circle (0.8° of visual angle) appearing in the center of one of the noise patches with variable contrast. The two noise patches were presented around fixation in separate visual hemifields (angular positions of locations in the right visual field 40°, 90°, 140° and left visual field 220°, 270°, 320°) at locations that varied independently of one another. To reset attentional sampling, an unfilled white circle (R=255, G=255, B=255) with a border 0.1° of visual angle wide, was flashed for 33 ms around one of the noise patches.

The target was present on only half of the experimental trials and was presented at a random time during the interval 200-1400 ms after the flash. In a separate session conducted prior to the main experimental session, the contrast of the target was adjusted for each participant to a 50% threshold (i.e., to a contrast that produces correct responses on 50% of trials) using a staircase procedure (Brainard, 1997; Denis G. Pelli & Farell, 1995; Watson & Pelli, 1983). Stimuli and overall task sequence for this phase of the experiment were identical to the experimental procedure described below, with the exception that the task-irrelevant flash was omitted.

Experimental procedure. The sequence of trial events can be seen in Figure 4. A fixation cross was presented in the middle of the screen at the beginning of each block and remained on the screen until the block's end. At the beginning of each trial, two noise patches were presented on the screen, one to the left and one to the right of fixation and remained on the screen until the

end of a trial. Following an interval of 1000-1300 ms, a task-irrelevant flash was presented for 33 ms around one of the noise patches. This flash occurred randomly and with equal likelihood at the location of one of the two noise patches. On half of the experimental trials, a target was presented at the center of one of the noise patches following a variable SOA (200 – 1400 ms). The target was equally likely to appear at either of the two attended locations and appeared randomly with regards to the task-irrelevant flash (50% congruent, 50% incongruent). Participants were instructed to respond by pressing the space bar as soon as they saw the target or, if no target was present, to withhold a response, waiting until the noise patches disappeared at the end of the trial. Participants received feedback after each experimental block notifying them about the number of correctly (hits) and incorrectly (false alarms) reported targets. Participants with an overall false alarm rate higher than 15% and an overall hit rate lower than 20% were removed from further analysis. The experiment consisted of 576 total trials separated into 18 blocks. Participants completed 16 practice trials prior to the experiment. The full experiment took ~2.5 h to complete.

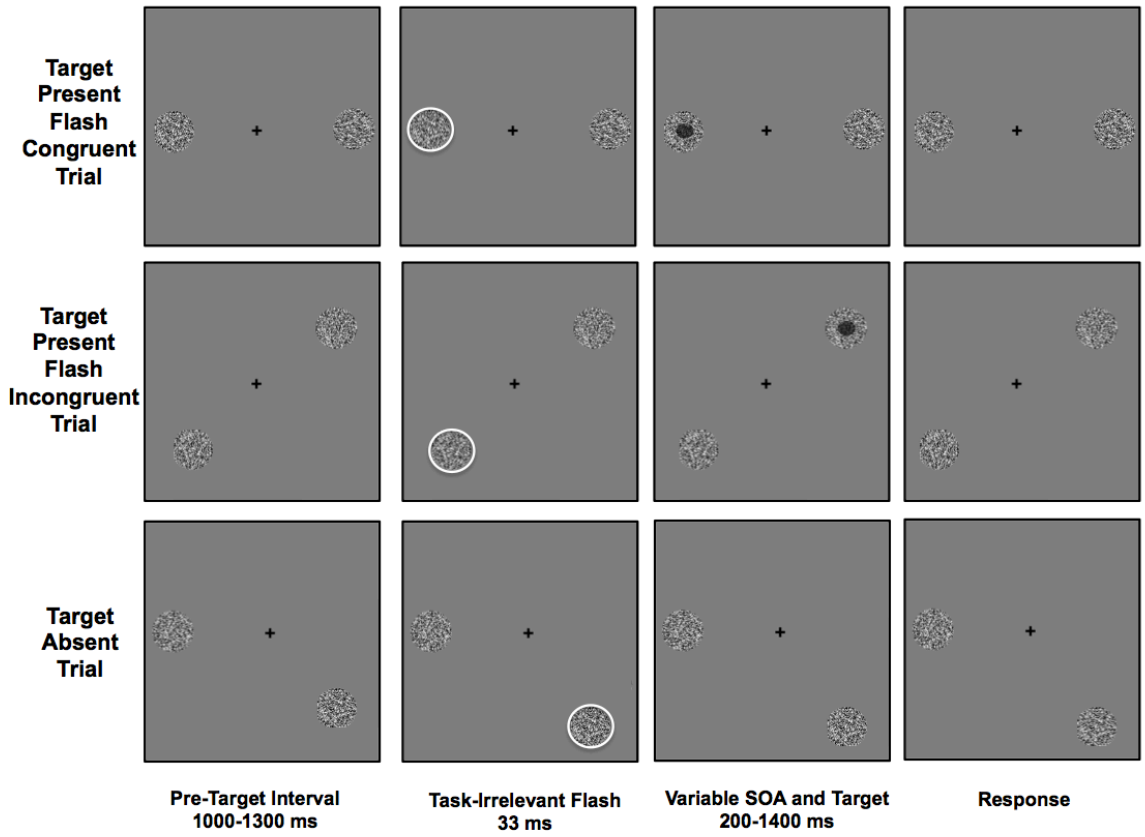

Figure 4. Behavioral task trial sequence for Experiment 1. Participants were asked to attend to two circular noise patches presented to the left and right of fixation and respond to the appearance of a target (target present on 50% of the trials). A task-irrelevant flash was used to reset attentional sampling prior to the appearance of the target.

EEG data acquisition and preprocessing. EEG was recorded using active Ag/AgCl electrodes (BioSemi Active Two) positioned at the left and right mastoids and 64 scalp sites according to the standards of the modified international 10/20 system (American Electroencephalographic Society, 1994). The common mode sense (CMS) electrode was located at site C1, with a driven right leg (DRL) electrode located at site C2. To track eye movements and blinks, the electrooculogram (EOG) was recorded from electrodes placed above and below each eye and ~1cm to the left and right of the external canthi of each eye. EEG and EOG was recorded with a sampling rate of 512 Hz and band-pass filter of 0.01-100 Hz.

Data were processed off-line using the EEGLab open source Matlab-based toolbox (Delorme and Makeig, 2004) and custom-written analysis scripts in Matlab (MathWorks, Inc.,

Natic, MA, USA). All signals were re-referenced to the algebraic average of the left and right mastoids, downsampled to 256 Hz, and epoched into 4000-ms long segments (i.e., trials) spanning the time interval 2000 ms before to 2000 ms after the task-irrelevant flash. To detect eye movements and blinks in the epoched data, EOG signals were combined to derive bipolar vertical and horizontal channels. To avoid any contamination of data by eye blinks or muscle movements, any trials containing amplitude changes larger than 80 μV in the vertical bipolar EOG channel and 120 μV in any other channel within a moving window of 200 ms were removed. Additionally, to prevent contamination due to eye movements, a step function was used to detect amplitude changes larger than 25 μV in the horizontal bipolar EOG channel. Participants were removed from further analysis if the number of trials rejected exceeded 30% of total trials. The average rejection rate was 10.95±9.85% of total trials.

Time-frequency analysis. All raw EEG data were Laplace transformed prior to time-frequency analysis to reduce volume conduction and maximize the spatial resolution of the signal (Carvalhaes & de Barros, 2015). Oscillatory power was extracted in two different ways. For the purpose of analyzing the lateralized effects of attention, power in a range of frequencies between 2-50 Hz was extracted using Morlet wavelet convolution as implemented in the FieldTrip toolbox (Oostenveld, Fries, Maris, & Schoffelen, 2011). For the purpose of the IEM analysis, instantaneous alpha-band oscillatory power (ABOP) values were extracted by first bandpass-filtering (8-14 Hz) the Laplace transformed signal using a two-way least squares finite impulse response filter using EEGLab toolbox function eegfilt.m (see Foster, Sutterer, Serences, Vogel, & Awh, 2016 for the same approach). This function uses a zero-phase forward and reverse operation that eliminates phase shifting caused by the use of forward-only filters. The filtered data, $f(t)$, will then be Hilbert transformed (MATLAB Signal Processing Toolbox) to

produce the complex analytic signal, $A(t)e^{i\varphi(t)}$, where $A(t)$ is the instantaneous amplitude and $\varphi(t)$ is the instantaneous phase. Frequency specific instantaneous amplitudes were extracted from the complex analytical signal using the following MATLAB syntax:

$$\boldsymbol{hilbert}(\boldsymbol{eegfilt}(\boldsymbol{data}, \boldsymbol{F_{sample}}, \boldsymbol{f_1}, \boldsymbol{f_2})')'$$

where $data$ is a 2D matrix of EEG data (number of trials x number of time points), F_{sample} is the sampling frequency (256 Hz) and f_1 and f_2 are the lower and higher bounds of the frequency band of interest, respectively. Total power was calculated as the squared absolute value of the resulting complex signal.

Behavioral performance. Detection accuracy was calculated as the proportion of reported targets on target-present trials. Detection accuracy was calculated across all SOAs (average detection accuracy) and also separately for each SOA and the left and right visual field.

Lateralized effects of attention. To test whether the task-irrelevant flash attracts attention and produces a reset in attentional sampling, post-flash lateralization of ABOP was examined in a subset of posterior electrodes symmetrically positioned to the left or right of midline. The electrodes of interest were determined by visually inspecting the topographic distribution of ABOP during the pre-flash interval (i.e., 1000 ms from the appearance of noise patches) across the flash-congruent and flash-incongruent conditions. Total power across these electrodes from trials with a task-irrelevant flash appearing in the left versus right visual field was averaged separately and normalized to decibels (10*log*10 (power/baseline power)) using a baseline of 500 - 100 ms before the flash. Significant differences in power between the subset of contralateral and ipsilateral electrodes for flash-right and flash-left conditions was evaluated

using a cluster-based permutation analysis applied to the time-frequency data using FieldTrip (Oostenveld et al., 2011).

Inverted encoding model. To examine variations in location-based attentional prioritization between the two attended locations during the delay interval, IEM was used to reconstruct information about each spatial location from the topographic distribution of ABOP across posterior electrodes (Foster, Bsales, et al., 2017). The assumption behind this model is that the power recorded at each electrode corresponds to a weighted sum of the outputs of separate spatially tuned neural populations, with each of these populations or channels tuned to a different angular position. The response profile of each of spatial channel was modeled as a half sinusoid raised to the 5th power (number of location bins – 1):

$$\boldsymbol{R = sin(0.5\theta)^5}$$

where θ is the angular position (ranging from 0 to 359°), and R is the channel response in arbitrary units. The response profile was shifted so that the peak response of each spatial channel was centered over a different location bin (40°, 90°, 140°, 220°, 270°, 320°).

To recover spatial locations, the alpha-band power data were divided into separate training and test data sets using the following procedure. To equate the number of trials across location bins, the bin with the lowest number of trials was identified and this number was used to randomly subsample trials from all other bins. The trials were then divided into 3 blocks with equal number of trials and averaged. Data from 2 blocks were used as training data set (B_1) and the 1 left-out block was used as test data set (B_2). Importantly, no trial was ever assigned to both training and test data set making the sets independent. The process of subsampling and division of trials into blocks was repeated 10 times to ensure that all available trials were used.

Additionally, the partitioning of data into training and test data sets was cross-validated, which means that each block served as a training and test data set.

During training, the training data, B_1, were used to estimate a weight matrix, W, which represents the relative contribution of the six spatial channels to the observed power at each electrode:

$$\boldsymbol{B_1 = WC_1},$$

where B_1 is the training data (number of electrodes x number of training blocks), C_1 is the predicted channel response (6 spatial channels x number of training blocks), and W is a weight matrix (electrodes x 6 spatial channels) that corresponds to a linear mapping between channel and electrode space. The weight matrix was derived using least-squares estimation using the following equation:

$$\widehat{\boldsymbol{W}} = \boldsymbol{B_1 C_1{}^T \left(C_1 C_1{}^T\right)^{-1}}$$

In the test stage, the model was inverted to transform the test data B_2 (number of electrodes x number of test blocks) into estimated channel responses C_2 (6 spatial channels x number of test blocks) with the use of the weight matrix $\widehat{W}$ derived during the training phase as follows:

$$\boldsymbol{C_2 = \left(\widehat{W}^T \widehat{W}\right)^{-1} \widehat{W}^T B_2}$$

The resulting channel response functions were then circularly shifted to a common center such that the center channel (i.e., 0°) was the channel tuned for the location of the noise patch of interest (separately for flash-congruent and flash-incongruent locations). The shifted-channel-

response function were then averaged to obtain CTFs averaged across the six stimulus location bins.

The IEM procedure was performed at each time point from 200 ms prior to 1400 ms after the task-irrelevant flash and for each participant separately. Note that CTFs were reconstructed separately for flash-congruent and flash-incongruent locations using only target-absent trials. When reconstructing the flash-congruent location, trials were organized into bins (1-6) based on the location of the noise patch that appeared in the same location as the flash. When reconstructing the flash-incongruent location, trials were organized into bins (1-6) based on the location of the noise patch opposite to the flash.

Channel Tuning Function Selectivity. To quantify how spatially selective the CTFs are, linear regression was used to estimate CTF slopes by averaging together spatial location channels equidistant from 0°. Greater CTF slope corresponds to greater spatial selectivity.

To evaluate the statistical significance of channel selectivity, obtained CTF slopes were compared to a surrogate null distribution separately for each time point. The null distribution was generated using a non-parametric Monte Carlo randomization procedure involving randomly reassigning bin labels across trials and estimating CTFs from the scrambled datasets using the same procedure as described above. This was repeated 1,000 times and the resulting CTF values were used to derive a null distribution of t-statistics for each time-point. One-tailed t-tests was used to evaluate the probability of obtaining a null distribution t-statistic that is greater than or equal to the observed t-statistic. If this probability was less than 0.01, CTF selectivity was considered statistically above chance.

Spectral analysis of behavioral performance. To evaluate fluctuations in performance with respect to the location and time of the task-irrelevant flash, percentage of correctly detected

targets, i.e., detection accuracy was calculated separately for the flash-congruent and flash-incongruent conditions and for left and right visual field. Because the timing of the target presentation was randomized, not all time points will contain behavioral estimates. To calculate a continuous time-series of behavioral performance, a 100-ms long moving window spanning 200 ms to 1400 ms post flash in steps of 1 ms was used to yield a time-series with a sampling rate of 1000 Hz (for similar approach, see Helfrich et al., 2018). The time-series was then smoothed, any missing data were interpolated using a 25-point boxcar moving average, and the resulting time-series was tapered by applying a Hanning window. Spectral estimates of the time-series data for individual subjects were obtained using Fast Fourier Transform (fft; Delorme & Makeig, 2004). To increase frequency resolution, each 1200-ms epoch was zero-padded to obtain 10s of data per trial (4400 ms on each end of the epoch). The squared absolute value of the resulting complex number represented power values for frequencies *f* determined as follows:

$$\boldsymbol{f = linspace\left(0, \frac{sampling\ rate}{2}, floor\left(\frac{length(data)}{2} + 1\right)\right)}$$

where f is a linearly spaced vector of values from 0 to Nyquist frequency (i.e., sampling rate divided by 2) with N points (i.e., length of the zero-padded data divided by two, rounded down and plus 1) (Cohen, 2014). Power values were scaled by 1/(sampling rate*data length) to calculate power spectral density (PSD), representing the power present in the signal as a function of frequency (i.e., the quantity of power for each frequency component). Normalized PSD was then calculated by dividing the spectral power by its maximum power value.

Spectral analysis of CTF selectivity for flash-congruent and flash-incongruent locations. If CTF selectivity tracks shifts in attentional prioritization, CTF slopes should show

rhythmic fluctuations at a rate that mirrors that observed for behavioral estimates of attentional sampling between the two attended locations in the theta band (4-8 Hz). To test this prediction, the same analysis described above was applied to the CTF selectivity time-series from 400-1400 ms after the flash event.

Statistical significance of power spectrum distributions using non-parametric permutation testing. The statistical significance of the observed power spectrum distribution was evaluated against a null distribution generated by randomly shuffling the time-series (behavioral or CTF series) and repeating the FFT analysis described above 1,000 times. For every participant, the power spectrum distribution was z-scored relative to the median and standard deviation of the null-distribution (for similar approach, see Helfrich et al., 2018). The highest z-score within the 2-10 Hz range was selected as the individual peak frequency for each participant, and the observed mean z-score across participants was then compared against a one-tailed p-value of .05 (z-score = 1.645). I also implemented irregular resampling (IRASA, Wen & Liu, 2016) as another way to account for background 1/f activity and non-oscillatory (fractal) components contributing to the power spectrum distribution (parameters: time window = 75% length of the original signal, step size = 50 ms). For each individual participant, individual peak frequency was defined as the strongest peak that exceeded the 1/f within a 2-10 Hz range.

Phase-lag analysis of time-series data. If attention samples between the two locations in a serial manner, fluctuations in the time series data (behavioral performance, CTF slopes) for the flash-congruent and flash-incongruent conditions should have an anti-phase relationship. For this analysis, phase angle values were extracted from the complex numbers in individual peak frequencies determined during the spectral analysis described above. Phase differences between flash-congruent and flash-incongruent conditions were calculated. The angular difference was

then projected as a unit vector on a circle, generating a distribution of vectors. The extent to which these vectors were clustered (i.e., non-uniformly distributed) along a particular angle represented a phase-locking value calculated as the length of the average vector using the following formula

$$\textbf{\textit{phase-locking value}} = \textbf{\textit{abs}}(\textbf{\textit{mean}}(\textbf{\textit{exp}}(1\textbf{\textit{i}} * \textbf{\textit{k}})))$$

where k is a vector of the individual participant phase angle differences expressed as vectors in complex space (Cohen, 2014). The phase-locking value was compared to a null-distribution of phase-locking values calculated from angle differences generated during permutation testing (see above). The phase-locking value was considered statistically significant if it exceeded the 95th percentile of the null distribution ($p < .05$). The angle of the average vector defined the average phase lag between the flash-congruent and flash-incongruent conditions. A phase lag of 180° would suggest a perfect anti-phase relationship.

Results

Behavioral performance. To evaluate behavioral performance, average detection accuracy was first calculated as the average proportion of correctly reported targets across all SOAs and as function of congruency (flash-congruent, flash-incongruent). The average detection accuracy was $M = .44$, $SD = 0.11$. There were no significant differences in target contrast or in the average detection accuracy between the left (contrast: $M = 33.90$, $SD = 7.05$; detection accuracy: $M = 40.00$, $SD = 11.63$) and the right (contrast: $M = 35.40$, $SD = 6.24$; detection accuracy: $M = 47.70$, $SD = 15.35$) visual fields $t(9) = -1.342$, $p = 0.213$, d = 0.424, CI [-4.029, 1.029], $t(9) = -1.496$, $p = 0.169$, d = 0.473, CI [-19.343, 3.943] respectively.

To test for the presence of rhythmic fluctuations in behavioral performance, detection accuracy was calculated as a function of flash-to-target SOA. Permutation-based spectral analysis of the detection accuracy time series revealed a peak in the theta frequency range (4-8 Hz) for both the left [flash-congruent: 6.74 Hz, z-score = 1.90, p = .03; flash-incongruent 6.51 Hz, z-score = 1.74, p = .04] and the right visual field [flash-congruent 5.48 Hz, z-score = 2.19, p = .01; flash-incongruent: 6.17 Hz, z-score = 1.35, p = .09; Figure 5A] suggesting the presence of rhythmic fluctuations in attentional deployment to the two sampled locations. The IRASA procedure produced similar results (see Figure A1A).

To analyze the phase relationship between the flash-congruent and flash-incongruent conditions, phase angle values were extracted for the peak frequency separately for the two conditions and LVF and RVF. Their angle difference was then calculated and projected onto a unit circle separately for each individual participant. The resulting mean vector direction revealed a phase lag of 112.61° between the flash-congruent and flash-incongruent fluctuation for the LVF and 302.88° for the RVF. However, neither of these phase lags was significant with respect to the null distribution (LVF: phase-locking value = 0.36, null distribution phase-locking value = .55, p > .05; RVF: phase-locking value = 0.20, null distribution phase-locking value = .53, p > .05; Figure 5B).

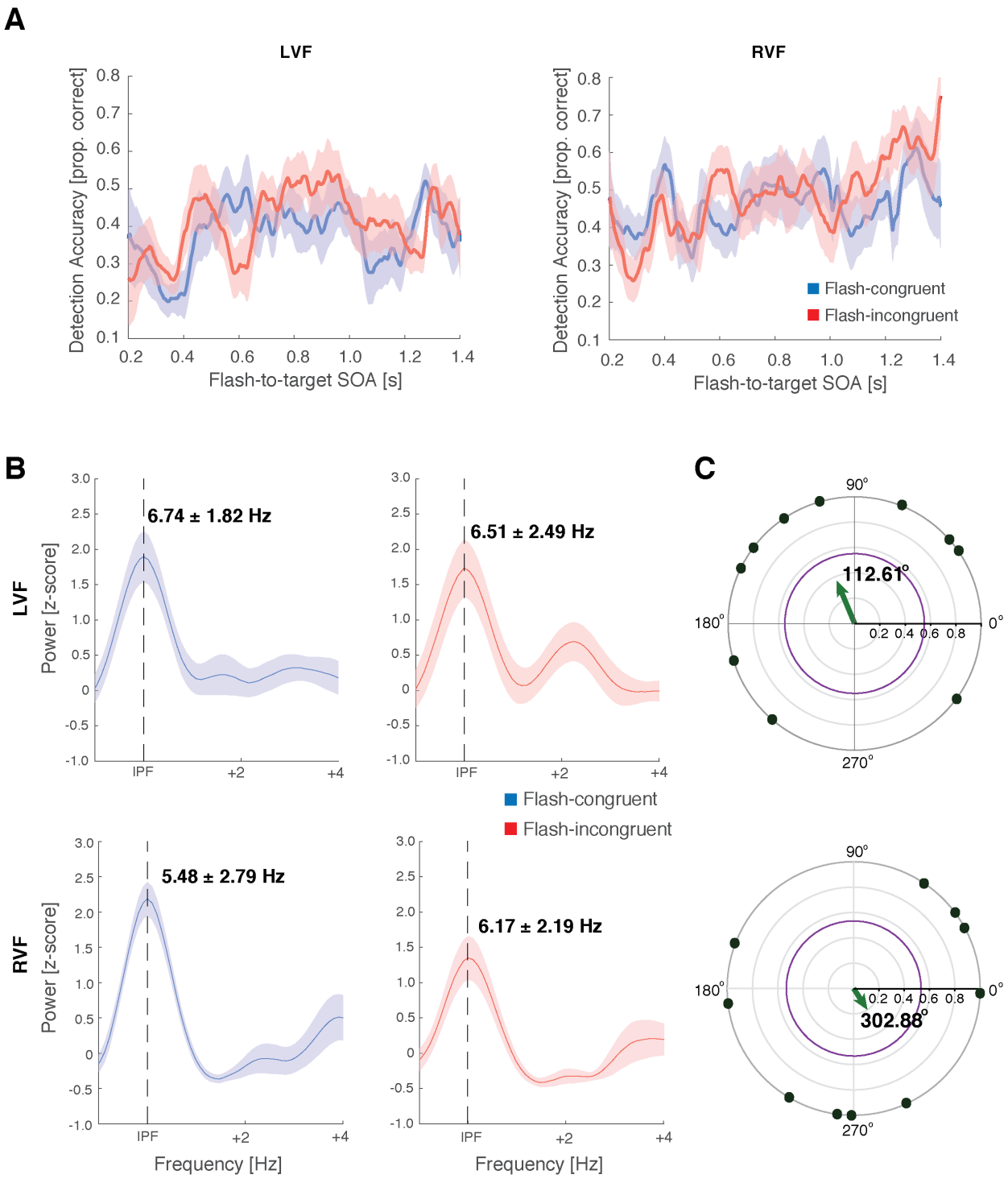

Figure 5. The results of spectral and phase analysis of detection accuracy. (A) Detection accuracy data for the left and right visual fields. (B) Peak aligned power spectral density for the flash-congruent (blue) and flash-incongruent (red) detection accuracy for LVF (top) RVF (bottom). Peaks in theta range (4-8Hz) provide evidence for the presence of rhythmic fluctuations in detection accuracy. Z-scored power was derived using permutation testing. Shaded areas correspond to ±1 SEM. (C) Phase-lag analysis of the phase relationship between

the flash-congruent and flash-incongruent conditions for LVF and RVF. There was no significant shift in phase between the flash-congruent and flash-incongruent conditions (phase-locking value equal to p = .05 shown in purple, actual phase-locking value shown in green).

Lateralized effects of attention. In line with previous evidence suggesting that ABOP tracks the allocation of attention, an attentional shift elicited by the task-irrelevant flash should result in a temporary de-synchronization of ABOP in electrodes contralateral to the visual hemifield where the flash occurred. To evaluate this possibility, first, a subset of electrodes sensitive to ABOP changes following the presentation of the two locations was selected using a section of data preceding the appearance of the flash and averaged across conditions. A total of 14 electrodes was selected based on the topography of ABOP (Figure 6) that were symmetrically distributed over the left (P3,P5,P7,P9,PO3,PO7,O1) and right (P4,P6,P8,P10,PO4,P08,O2) hemisphere.

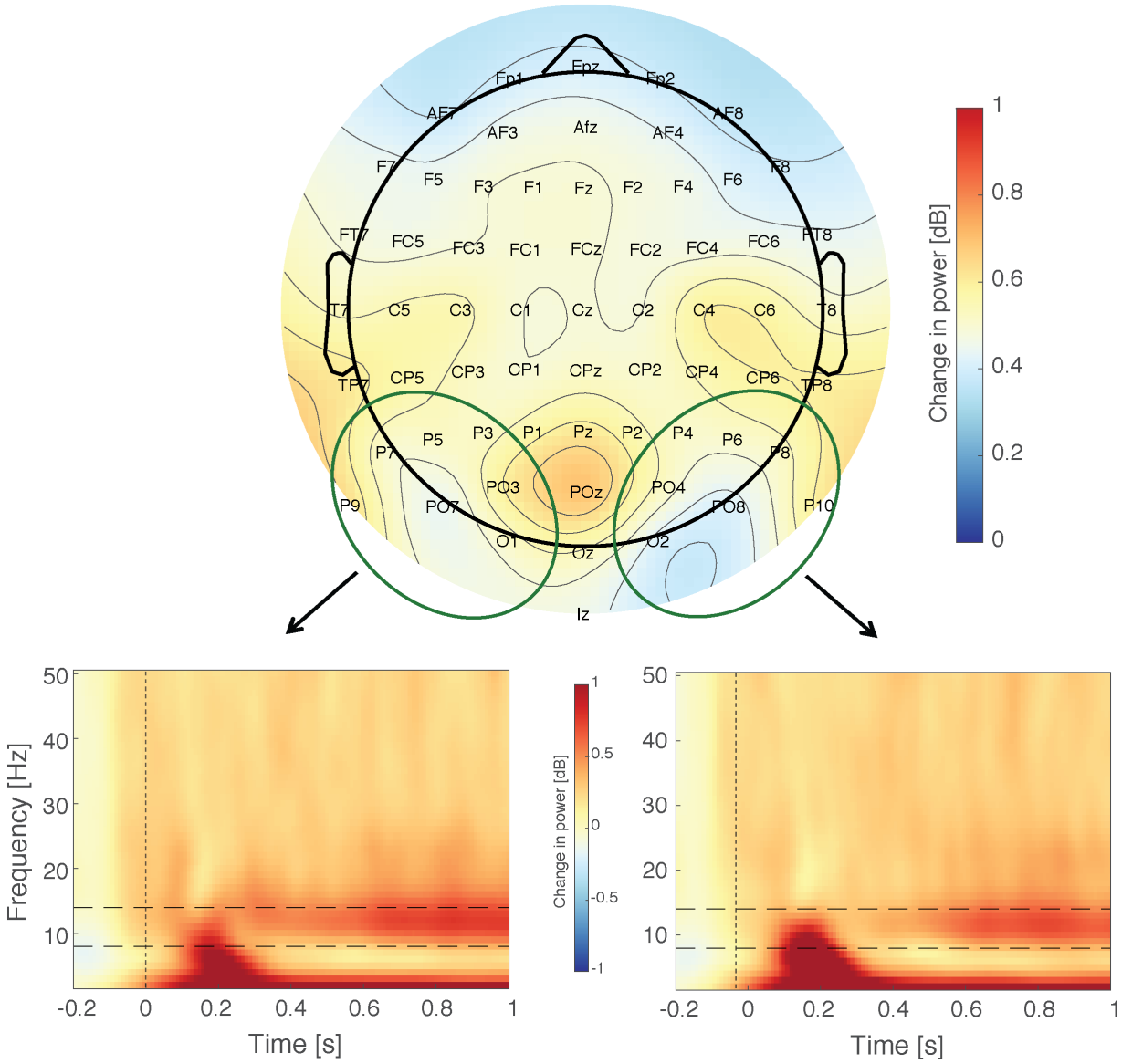

Figure 6. Grand average of alpha band power (8-14 Hz). (A) The topographical distribution of the pre-flash average ABOP (0-1000 ms following the appearance of the two to-be-attended locations). (B) Time-frequency plots of power fluctuations following the appearance of the to-be-remembered locations for the electrodes circled in green. Alpha frequency band (8-14 Hz) is marked by dashed lines.

To test whether the task-irrelevant flash produced an attentional shift towards the location of the flash and whether this shift resulted in rhythmic shifts in attentional allocation between the two attended locations, cluster-based permutation analysis was applied to the contralateral-ipsilateral difference in ABOP separately for the left and right flash conditions. Permutation testing yielded several clusters (Figure 7) among which there was a visible ABOP de-

synchronization (decrease in alpha power in contralateral versus ipsilateral electrodes) following the initial evoked response (~100-300 ms) in theta frequency (4-8 Hz) band elicited by the flash. However, none of the clusters remained significant when corrected for multiple comparisons. This attentional shift was only temporary, lasting only up to ~500 ms following the flash, suggesting that the flash produced only a short-term attentional shift as was expected for an uninformative cue. In contrast to my prediction, however, there was no clear visible pattern of ABOP alternations, as would be expected if ABOP tracked rhythmic shifts in attention. Interestingly, a pattern of alternations in power was hinted at in lower frequencies (theta frequency band, 4-8 Hz), and appeared to occur every ~200 ms, in line with the rate of attentional sampling reported in behavioral studies.

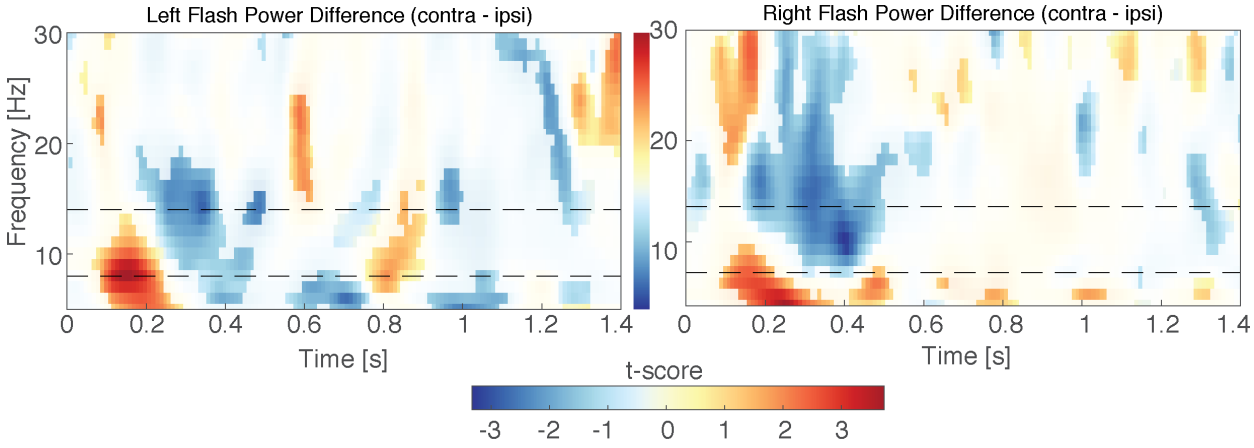

Figure 7. Time-frequency plots of t-scores comparing contralateral versus ipsilateral power separately for the left and right flash conditions. Alpha frequency band (8-14 Hz) is marked by dashed lines. Clusters are not corrected for multiple comparisons.

Channel tuning function selectivity. The pattern of evoked and total ABOP in the two clusters of posterior electrodes defined above (Figure 6) was used to reconstruct CTFs for the flash-congruent and flash-incongruent locations (Figure 8A). As expected, temporary allocation of attention to the flash-congruent location following the flash lead to more selective CTFs for the flash-congruent versus the flash-incongruent locations during the initial ~400 ms post-flash

(Figure 8B). This was true for the CTFs reconstructed from both evoked and total power. Importantly, total power CTF selectivity for both flash-congruent and flash-incongruent locations was above chance (with brief interruptions) until the end of the trial, suggesting that CTFs successfully tracked attentional allocation during the trial.

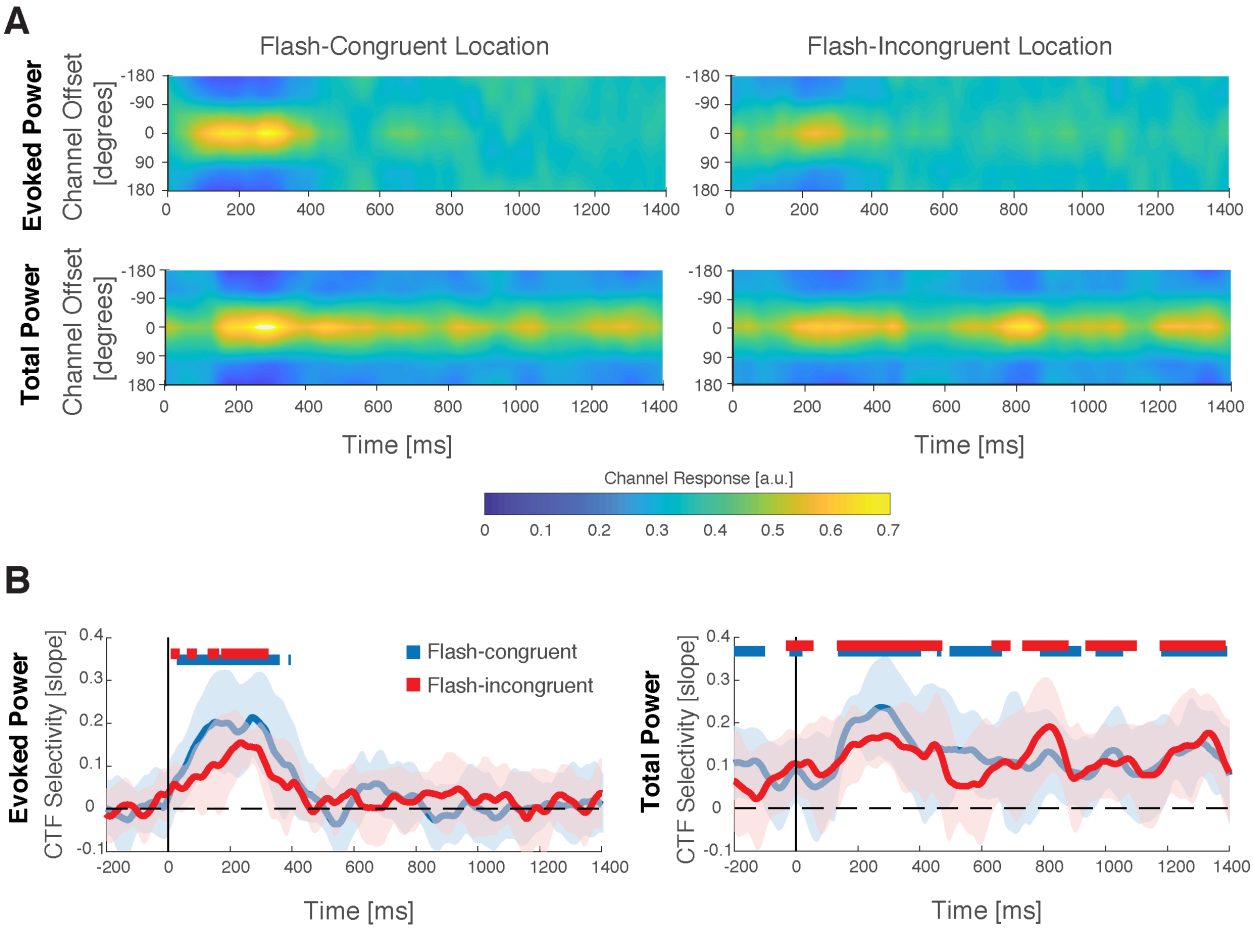

Figure 8. The results of inverted encoding modeling of the FOA using ABOP. (A) Center-shifted channel response for evoked (top) and total (bottom) for the flash-congruent and flash-incongruent locations. (B) CTF selectivity over time for flash-congruent (blue) and flash-incongruent (red) locations separately for evoked and total power. Solid bars on the top of the plots correspond to CTF selectivity time intervals that were significantly above chance. Shaded areas correspond to ±1 SEM.

Spectral analysis of total power CTF selectivity for flash-congruent and flash-incongruent locations. To evaluate whether CTF selectivity (i.e., slopes) for the flash-congruent and flash-incongruent locations varied as a function of periodic attentional allocation towards the

two spatial locations, the total power CTF slopes time series were subjected to spectral analysis. The permutation-based spectral analysis yielded a significant peak in theta range (4-8 Hz) [flash-congruent: 4.79 Hz, z-score = 11.13, $p < .001$; flash-incongruent 5.68 Hz, z-score = 8.53, $p < .001$; Figure 9A] suggesting the presence of rhythmic fluctuations in attentional deployment to the two sampled locations. The IRASA procedure produced similar results (see Figure A1B).

Phase-lag analysis of total power CTF selectivity for flash-congruent and flash-incongruent locations. To evaluate the relationship between the phases of the total power CTF slopes, phase angle values were extracted for the peak frequency for the flash-congruent and flash-incongruent location separately for each participant. The angle difference between the two values was then calculated and projected onto a unit circle separately for each individual participant. The resulting mean vector direction revealed a phase lag of 349.71°, pointing towards an in-phase rather than the expected anti-phase relationship. However, this phase lag was not significant with respect to the null distribution (phase-locking value = 0. 37, null distribution phase-locking value = .55, $p > .05$; Figure 9B).

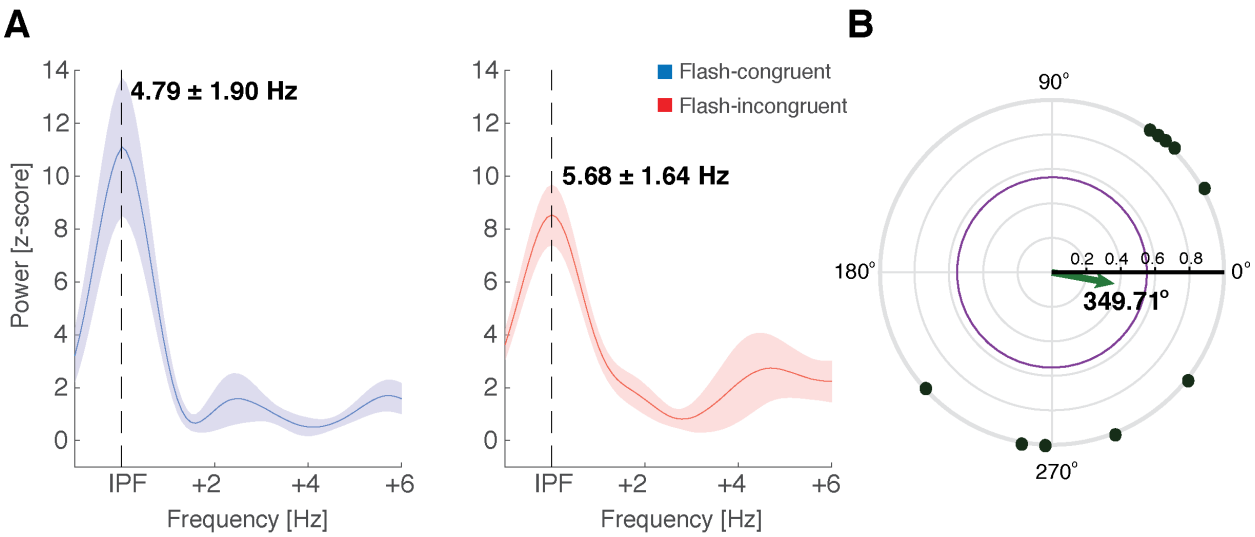

Figure 9. The results of spectral and phase analysis of total power CTF selectivity. (A) Peak aligned power spectral density for flash-congruent and flash-incongruent CTF selectivity. Both flash-congruent (left) and flash-incongruent (right) location's CTF slopes contained a significant peak in theta frequency band. Z-scored power was derived using permutation testing. Shaded areas correspond to ±1 SEM. (B) Phase-lag analysis of the phase relationship between the flash-congruent and flash-incongruent conditions. There was no significant shift in phase between the flash-congruent and flash-incongruent conditions (phase-locking value equal to p = .05 shown in purple, actual phase-locking value shown in green).

Discussion

An important step in our understanding of the proposed attentional rhythm is uncovering its neural correlates. Previous studies examining the neural oscillatory correlates of attentional sampling have suggested that the phase of neural oscillations in theta band could drive rhythmic fluctuations in the effects of attention (e.g., target detection accuracy or target response times; Helfrich et al., 2018; Landau & Fries, 2012; Landau et al., 2015). At the same time, another line of research focusing on more traditional, sustained effects of attention has consistently assigned an important role to a different oscillatory band, specifically the alpha band (8-14 Hz) and its power. In these studies, changes in the topography of alpha band power were shown to track to the allocation of attention in space (Foster, Sutterer, et al., 2017). Despite these consistent reports of the importance of ABOP in attention, the role of ABOP in the sampling rhythm of attention

has not yet been established. The goal of Experiment 1 was therefore to examine the role of ABOP in attentional sampling and to assess the possibility of reconstructing rhythmic changes in attentional allocation over time from ABOP using inverted encoding models.

In order to study the attentional rhythm in the neural signal, it was important to first establish its presence in behavior. The analysis of detection accuracy demonstrated the presence of previously reported rhythmic attentional sampling over the two attended locations in the theta frequency range (4-8 Hz). A closer examination of the behavioral data also revealed that individual participants varied in the rate of their attentional sampling as evidenced by between-participant variability in the individual peak frequency (see Figure AF2). As a potential result of this individual variability in the time intervals between attentional samples, no clear rhythmic signature was observed in ABOP. Specifically, grand-averaged data of ABOP did not show rhythmic waxing and vanning between the contralateral and ipsilateral hemispheres as was expected.

Surprisingly, there was a hint of a pattern of rhythmic fluctuations in lower frequencies, specifically in the theta frequency band (4-8 Hz) instead of the predicted alpha band (8-14 Hz). Similarly, one previous study published as a preprint (Crouzet & VanRullen, 2017) has reported a shift in the relative EEG power spectrum when participants were asked to monitor two instead of one image. The authors observed more power in the delta-theta band range when two images were monitored compared to relatively more power in the alpha band range when one image was attended. The authors have taken this as evidence for a splitting of the natural attentional "clock" that operates at 8 Hz in a way that each alternate cycle is directed to a different location, leading to a slower, 4 Hz cycle (see VanRullen, 2016 for more on this argument). This could suggest that the neural oscillatory frequency corresponding to attentional sampling may change depending on

the number of items that are sampled; however, this possibility was not directly tested here. The lack of rhythmic changes in ABOP may also indicate that this frequency is not be a suitable index for tracking the rhythmic sampling of attention, but may rather reflect more static aspects of attentional deployment (Busch & VanRullen, 2010).

In contrast to the findings from the hemispheric differences in ABOP, spectral analysis of the results of inverted encoding modeling of the focus of attention revealed the presence of attentional sampling in the theta frequency range. Unlike hemispheric differences in ABOP, evidence for the presence of rhythmic sampling in this case was established for each individual participant, which preserved differences in peak frequency across participants. However, there was no clear phase shift between the attentional fluctuations observed over the two locations in either the behavioral or neural data that would suggest that these two locations were sampled in a serial manner as previously proposed. One possible explanation for the lack of a phase shift could be that the flash did not effectively align the phase of the cycle. In fact, the temporary shift of attention evidenced by ABOP de-synchronization following the resetting stimulus was not significant at the group level, which could mean that the resetting stimulus may have not elicited a phase reset for all of the participants.

In summary, Experiment 1 has successfully replicated previous behavioral results suggesting the presence of rhythmic sampling when attention was directed to two spatial locations. Additionally, the present experiment showed that, despite the lack of a group-level signature of rhythmic sampling in the pattern of hemispheric differences in ABOP, the pattern of individual participant ABOP topography could be used to reconstruct the time course of the allocation of the focus of attention. More importantly, this time course has shown signs of rhythmic fluctuations observed in the behavioral data. Future work will be necessary to address

and extend certain aspects of the current findings. First of all, it is necessary to clarify the reasons for the lack of the predicted phase-relationship between the flash-congruent and flash-incongruent conditions. Secondly, future studies should replicate the findings from the inverted encoding modeling in a larger sample with larger trial numbers and directly test the relationship between the neural and behavioral rhythms. Finally, future research should examine the relationship between changes in ABOP and the phase of lower frequency oscillations that have been proposed to underlie the phasic influence of higher-order brain areas on perception (Cavanagh & Frank, 2014).

EXPERIMENT TWO: INVESTIGATING THE NEURAL SOURCES OF RHYTHMIC ATTENTIONAL SAMPLING

Introduction

The goal of Experiment 1 was to identify the neural oscillatory correlates of rhythmic attentional sampling previously observed at the level of behavior. The goal of Experiment 2 was then to identify the neural mechanisms supporting this rhythmicity. Existing evidence from non-human primates suggests that the FEF controls serial, covert shifts of attention during visual search (Buschman & Miller, 2009) and has been implicated as the source of a top-down signal directing the rhythmic sampling of attention (Fiebelkorn et al., 2018). Despite some corroborating evidence from humans pointing towards the role of fronto-central cortical areas in rhythmic sampling of attention (e.g., Busch et al., 2009; Dugué, Marque, & VanRullen, 2011), this evidence is correlational in nature. To more clearly establish a functional role for particular cortical areas in the rhythmic cycling of attention, causal evidence is necessary. Transcranial magnetic stimulation (TMS) is a non-invasive brain stimulation technique that can be used to temporarily induce a 'virtual lesion' in a targeted brain area, making it possible to assess its contribution to specific behaviors (Pascual-Leone, Bartres-Faz, & Keenan, 1999).

In contrast to the lack of causal evidence for areas involved in attentional cycling, there is existing evidence suggesting a clear functional role for FEF in other, related aspects of attention, such as sustained attention and attentional disengagement. For example, Esterman et al. (2015) delivered repetitive TMS (rTMS) to either the left or right FEF while participants performed a go/no-go attention task and showed that disruption of activity in the right FEF resulted in a disruption of sustained attention. Another study by Heinen et al. (2017) tested the role of FEF in attentional disengagement from the current focus of attention using continuous theta burst

stimulation (cTBS), a type of TMS that has been shown to reduce activity in the targeted area for up to 30 minutes after application (Nyffeler et al., 2006). In their experiment, cTBS applied to the right FEF was found to impair visual discrimination selectively in the left hemifield when attention was sustained, but impaired visual discrimination in both hemifields following attention shifts. This suggests a bilateral role of right FEF in shifting attention and, potentially, in orchestrating rhythmic shifts of attention.

The goal of the current study was to test the role of the right FEF in the rhythmic cycling of spatial attention. The right FEF has been shown to predominantly control attention across the visual field, whereas the left FEF has shown only contralateral or limited impact (Hung, Driver, & Walsh, 2011; Ruff et al., 2008; Silvanto, Lavie, & Walsh, 2006). To assess the causal role of the FEF in attentional sampling, cTBS was applied offline (i.e., before the completion of the task) to the right FEF to temporarily attenuate its function, and the rhythm of attentional sampling was assessed behaviorally. TMS stimulation of the FEF has been found to increase the threshold for perceiving near-threshold targets (Chanes, Quentin, Tallon-Baudry, & Valero-Cabré, 2013). This could produce differences in the difficulty of target detection tasks following TMS of the FEF versus a control area. To avoid this outcome, the proposed experiment implemented a behavioral task with easy-to-see targets, and analysis of periodic changes in reaction time (RT) to assess rhythmic sampling. FEF cTBS has also been shown to cause a general slowing of RT in tasks with fixed cue-target intervals (Marshall, O'Shea, Jensen, & Bergmann, 2015); however, the effect of such slowing on attentional sampling at variable cue-target intervals has not been examined. If cTBS only causes general slowing in RT, but does not disrupt the sampling process, I expected to observe increased RTs across all stimulus onset asynchronies, but a preserved pattern of fluctuations (i.e., waxing and waning of RTs with

increasing SOA). If FEF plays a causal role in the generation of rhythmic shifts of spatial attention, the attentional rhythm should be disrupted following TMS. This disruption could be manifested in at least three ways: 1) by a total removal of rhythmic attentional sampling, which would be revealed by a lack of a significant frequency peak in the derived power spectrum, 2) by decreasing the strength of attentional sampling, which would be reflected in overall lower differences between the high and low peaks of the observed behavioral oscillation (i.e. by a reduction in the amplitude of observed oscillations), or 3) by causing a shift in the frequency of attentional sampling, which would be suggested by the presence of a significant frequency peak, but at a different frequency than observed in the no-TMS condition (e.g., decreasing from 4-5 samples per second to only 1-2 samples).

Materials and Methods

Participants. Twelve undergraduate and graduate students (8 female; 19-36 years M = 25.1, SD = 5.2) were recruited from North Dakota State University to participate in this study for course credit or monetary compensation ($20/h). Participant selection criteria and recruitment procedures were identical to those described for Experiment 1.

Procedure. All participants eligible for the experiment completed three different experimental sessions on separate days. Prior to the experimental sessions, an anatomical magnetic resonance imaging (MRI) scan for each participant was acquired. During the first session, each participant completed a behavioral session without TMS stimulation to establish a baseline measure of individual attentional rhythm. Afterwards, a motor threshold was determined to set TMS intensity and the stimulation targets (right FEF and vertex) were localized anatomically. The right FEF anatomical coordinates were identified on the basis of individual anatomy from whole-brain T1-weighted anatomical MRIs for each participant separately prior to

the experimental session. The FEF was anatomically defined as the intersection of the superior precentral sulcus and the superior frontal sulcus (Paus, 1996). The vertex anatomical coordinates were defined as the junction of the two central sulci (Marshall et al., 2015). During the second and third sessions, TMS was applied to either the right FEF or the vertex prior to completion of the behavioral task, with the order of targets counter-balanced across participants.

Attention task. Stimulus presentation and response recording was controlled by a PC running Presentation® (Version 18.0, Neurobehavioral Systems, Inc., Berkeley, CA, www.neurobs.com). Stimuli were presented on the surface of a 19" cathode ray tube monitor with a refresh rate of 100 Hz, at a viewing distance of 57 cm.

Participants completed a reaction time behavioral task called the Starry Night Test (see Figure 10; Deouell, Sacher, & Soroker, 2005; Szczepanski et al., 2014; Helfrich et al., 2018), in which they were cued to covertly attend to either the left or right visual field (LVF and RVF respectively) using a centrally presented arrow. At a random time 1000-2000 ms after the cue, a small blue square (0.65° of visual angle) appeared at either the cued (60% of trials) or uncued (40% of trials) location and participants were asked to press a button as soon as they saw it. Targets appeared on a dynamic background of red distracters (0.4° visual angle) each appearing in a random location within a virtual cell (display was divided into a 6x7 invisible grid with 42 virtual cells) and never overlapping a distracter. At the beginning of each trial, the distracters were randomly set to be visible or invisible. With random intervals of 50-250 ms throughout the trial, one distractor at a time was chosen at random and its status was flipped (if the distractor was previously visible, it became invisible and vice versa), giving the appearance of twinkling starlight. The task consisted of 480 total trials (+10 practice trials) separated into 12 blocks and lasted ~30 min. The length of the experiment was kept deliberately short to fit within the window

of maximal cTBS efficacy (Nyffeler et al., 2006). The average time necessary to complete the behavioral task following the stimulation was 35.61±1.93 minutes. There was no significant difference in the time necessary to complete the behavioral task between the FEF (M = 35.42, SD = 2.19) and vertex (M = 35.00, SD = 1.21) stimulation sessions: $t(11) = 1.101$, $p = .295$, d = 0.321, CI [-0.417, 1.250].

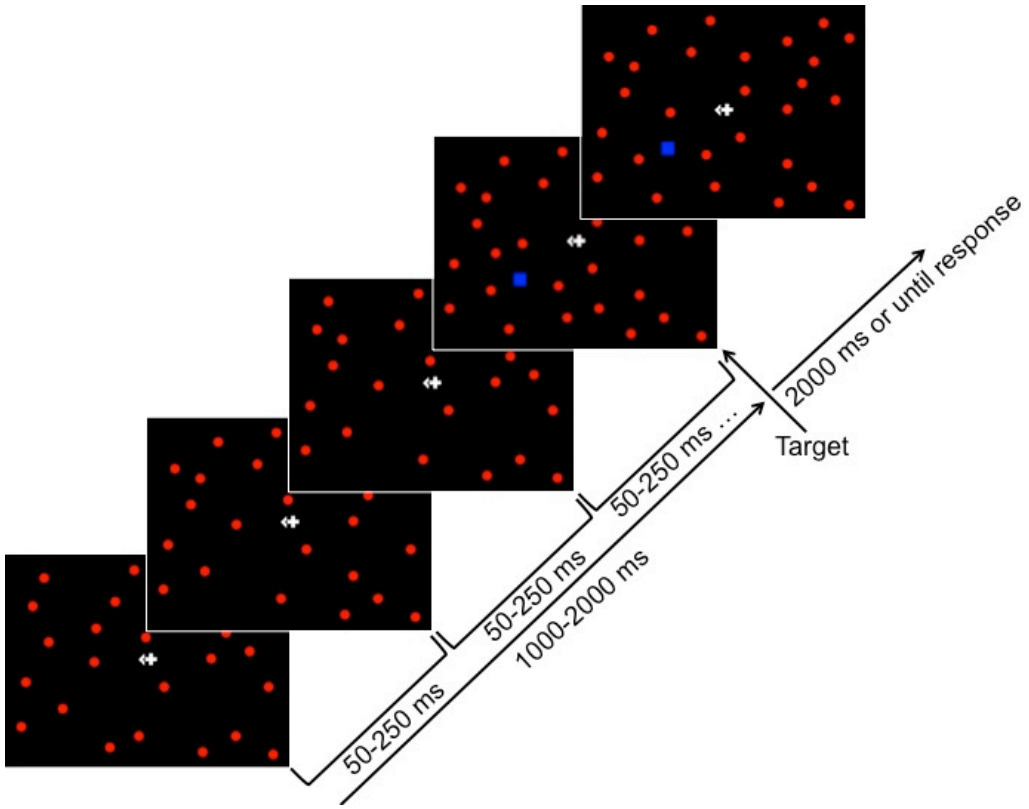

Figure 10. Starry Night Test trial sequence for Experiment 2. Each trial started with the appearance of a fixation cross in the middle of the screen and a set of distractors. Additionally, an arrow pointing either to the left or right was presented at fixation and remained on the screen until the end of the trial. Following a variable cue-target SOA (1000 - 2000 ms), a blue square appeared either to the left or right of fixation and remained on the screen for 2000 ms or until the participant responded. Participants were asked to only respond to targets appearing within the cued hemifield and withhold responses to targets appearing in the uncued hemifield. The response was followed by a 500 ms inter-trial interval.

Structural MRI. Prior to participation, whole brain T1-weighted anatomical MRI scans were acquired for each participant with a GE Signa HD 1.5-T MRI scanner (206 axial slices, with a resolution of 1 mm).

Administration of TMS. TMS was delivered with a Magstim Super Rapid^2 Plus 1 magnetic stimulator fit with an air-cooled, focal bipulse, figure of eight 70-mm stimulating coil (Magstim, Whitland, UK). TMS targeting and online guidance was achieved using a Visor2 neuronavigation system (Advanced Neuro Technology, Enschede, The Netherlands) that uses infrared-based frameless stereotaxy to map the position of the coil and the participant's head within the reference space of the individual's high-resolution anatomical MRI. During right FEF stimulation, the coil was held at a 45° angle from the vertical midline. During vertex stimulation, the coil was held in line with the longitudinal fissure separating the hemispheres, with the coil handle facing backwards.

Determination of resting motor threshold. For each individual participant, active motor threshold (AMT) was determined as the minimum stimulator output required to produce a finger movement on 5/10 single pulses delivered to the hand area of the primary motor cortex prior to the experiment. The average resting motor threshold was $M = 47.50$, $SD = 0.09$.

FEF cTBS. cTBS stimulation was delivered offline to FEF and vertex (in separate sessions) prior to the completion of the behavioral task. Specifically, short 50 Hz bursts of three pulses were applied at a frequency of 5 Hz (i.e., a 200 ms intertrain interval) for 40 s (i.e., 600 pulses in total) at 80% of each participant's AMT (Huang et al., 2005). During the cTBS and for 1 min afterward, participants remained seated and maintain fixation.

Eyetracking. Eye movements of the left eye were tracked using the Eyelink 1000 system (SR Research Ltd., Mississauga, Canada). Trials contaminated by eye movements, defined as a deviation from central fixation larger than 1° of visual angle during the period 500 ms prior to target until response, were excluded from further analysis. The average rejection rate was 9.76±1.75% of trials). There were no significant differences [$F(2,22) = 1.266$, , $p = .302$, $\eta_p^2 =$

.103] in rejection rates between the baseline (M = 10.36, SD = 1.83), FEF (M = 9.35, SD = 1.48) and vertex (M = 9.58, SD = 1.90) conditions.

Spectral analysis of behavioral performance. To evaluate fluctuations in reaction time (RT) with respect to the length of the cue-target SOA, a time series of RTs was calculated. Prior to calculation, any RTs 2 SDs longer than the mean were removed from the analysis. Because the timing of the target presentation was randomized, not all time points contained behavioral estimates. To calculate a continuous time-series of behavioral performance a 100-ms long moving window spanning 1000 ms to 2000 ms post cue in steps of 1 ms was used to yield a time-series with a sampling rate of 1000 Hz (for similar approach, see Helfrich et al., 2018). The time-series were then smoothed and any missing data interpolated using a 25-point boxcar moving average. Spectral estimates of the time-series data for individual subjects were obtained using Fast Fourier Transform (fft; Delorme & Makeig, 2004) and corrected for background 1/f activity and non-oscillatory (fractal) components, as described in Experiment 1. Statistical significance of individual power spectrum distributions was evaluated using non-parametric permutation testing, as described for Experiment 1.

Comparison of power and frequency of individual peak frequencies between experimental conditions. Firstly, to assess whether cTBS to right FEF disrupted the rhythm of attentional sampling by decreasing its amplitude (i.e., the difference between high and low peaks), power for individual peak frequencies were compared between baseline, control and cTBS conditions using repeated measures ANOVA. Secondly, to test whether cTBS to right FEF disrupted the rhythm of attentional sampling by shifting its sampling frequency, individual peak frequencies were compared between baseline, control and cTBS conditions using repeated measures ANOVA.

Results

Reaction Time (RT). Reaction time was calculated as the time elapsed between the appearance of a target and the response. Mean RT (averaged across all cue-target SOAs) was not significantly different [$F(2,22) = 3.067$, $p = .067$, $\eta_p^2 = .218$] between the baseline ($M = 536.79$, $SD = 26.35$), FEF ($M = 520.93$, $SD = 44.02$) and vertex ($M = 521.75$, $SD = 32.54$) conditions, suggesting that cTBS delivered to the FEF did not produce a general slowing of RT. Mean RTs were also analyzed separately for the right and left visual fields to evaluate whether right FEF stimulation produced a hemifield-specific disruption. There was no evidence for a hemifield-specific disruption (see Figure 11) for either the left visual field [$F(2,22) = 1.314$, $p = .289$, $\eta_p^2 = .107$] or the right visual field [$F(2,22) = 5.045$, $p = .016$, $\eta_p^2 = .314$; RTs in baseline condition ($M = 541.49$, $SD = 27.07$) were significantly slower compared to the vertex condition ($M = 520.84$, $SD = 30.65$, $p = .017$), but not the FEF ($M = 521.39$, $SD = 43.25$, $p = .076$), no difference between the vertex and FEF conditions ($p = .948$)].

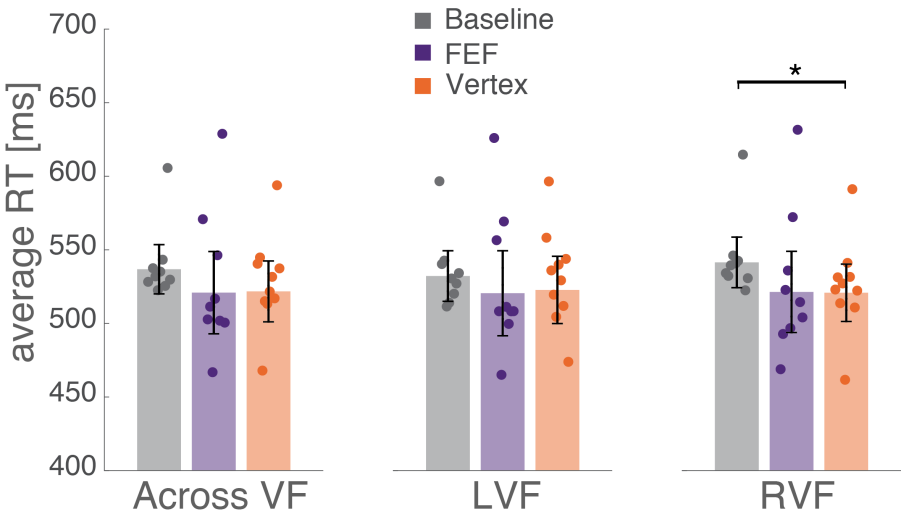

Figure 11. Mean RTs for baseline, FEF and vertex conditions plotted across visual fields and separately for the LVF and RVF. There were no significant differences in RTs between conditions suggesting the presence of cTBS-triggered RT slowing. There was a significant difference in RTs between the baseline and vertex condition (marked with an '*') in the RVF that potentially resulted from task practice. Error bars correspond to 95% CI.

Spectral analysis of behavioral performance. To evaluate the presence of rhythmic fluctuations in RTs, the RT time series were subjected to spectral analysis that yielded an estimate of peak frequency (in Hz) for each individual participant (see example from a single participant in Figure 12 or Figure A4 for all participants). The peak frequency was selected as the largest peak with respect to a permutation-generated null distribution (i.e., a peak with the largest z-score) and the amplitude of this peak corresponded to the z-scored power of the peak (Figure 13A). To evaluate whether cTBS resulted in a significant shift in the frequency of attentional sampling, the peak frequencies were compared across the three conditions (baseline, FEF, vertex). There was no significant difference in peak frequency [$F(2,22) = 0.258$, $p = .775$, $\eta_p^2 = .023$] between the baseline ($M = 6.34$, $SD = 2.23$), FEF ($M = 6.46$, $SD = 2.20$) and vertex ($M = 7.11$, $SD = 2.52$) conditions (Figure 13B). This suggests that cTBS delivered to the right FEF did not significantly affect the frequency of rhythmic sampling. However, cTBS seemed to affect the power of the rhythmic fluctuations. Specifically, the combined z-scored power for the peak frequency for both the baseline ($M_{z\text{-score}} = 1.77$, $SD_{z\text{-score}} = 1.21$, $p = .04$) and vertex ($M_{z\text{-score}} = 1.83$, $SD_{z\text{-score}} = 1.04$, $p = .03$) conditions were significant, suggesting the presence of a rhythmic fluctuation in the theta range (baseline: 6.34 Hz, vertex: 7.11). However, there was no significant oscillation present for the FEF condition ($M_{z\text{-score}} = 1.12$, $SD_{z\text{-score}} = 0.85$, $p = .13$), suggesting a lack of theta-rhythmic fluctuation for this condition. The individual z-score power values for the different conditions were also compared using a repeated-measures ANOVA. Because the FEF-specific disruption was driven by a subset of participants, the ANOVA did not yield a significant drop in power in FEF compared to baseline and vertex [$F(2,22) = 1.606$, $p = .223$, $\eta_p^2 = .127$; Figure 13B]. A direct comparison between the two TMS conditions (FEF versus vertex) showed a marginally significant group-level difference between the two conditions: $t(11)$

= -2.10, p = .06, d = .607, CI [-1.454, 0.034]. A similar pattern of results was produced when spectral estimates were corrected for 1/f noise using IRASA procedure compared to permutation testing described above (see Figure A3).

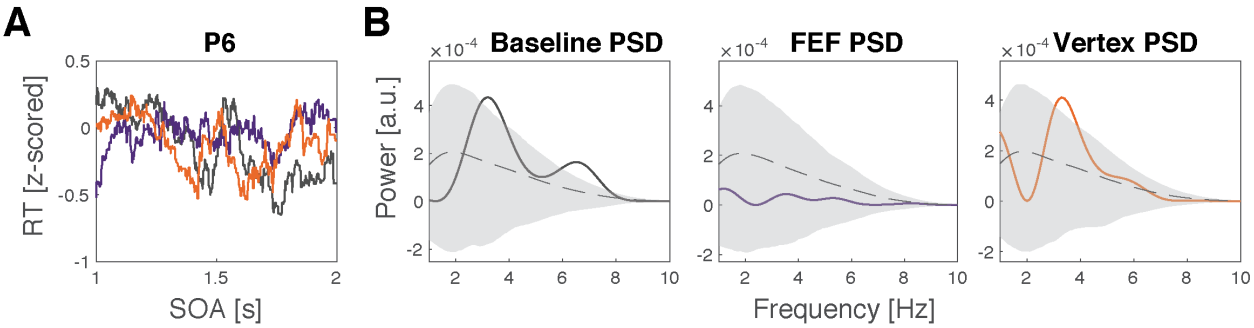

Figure 12. An example of individual participant data and the results of the spectral analysis for the baseline (gray), FEF (purple) and vertex (orange) conditions. (A) Time-series of z-scored RTs for the three experimental conditions. (B) PSD for the three experimental conditions. Dashed lines represent mean PSD for the null-distribution. Shaded areas correspond to 95% CI.

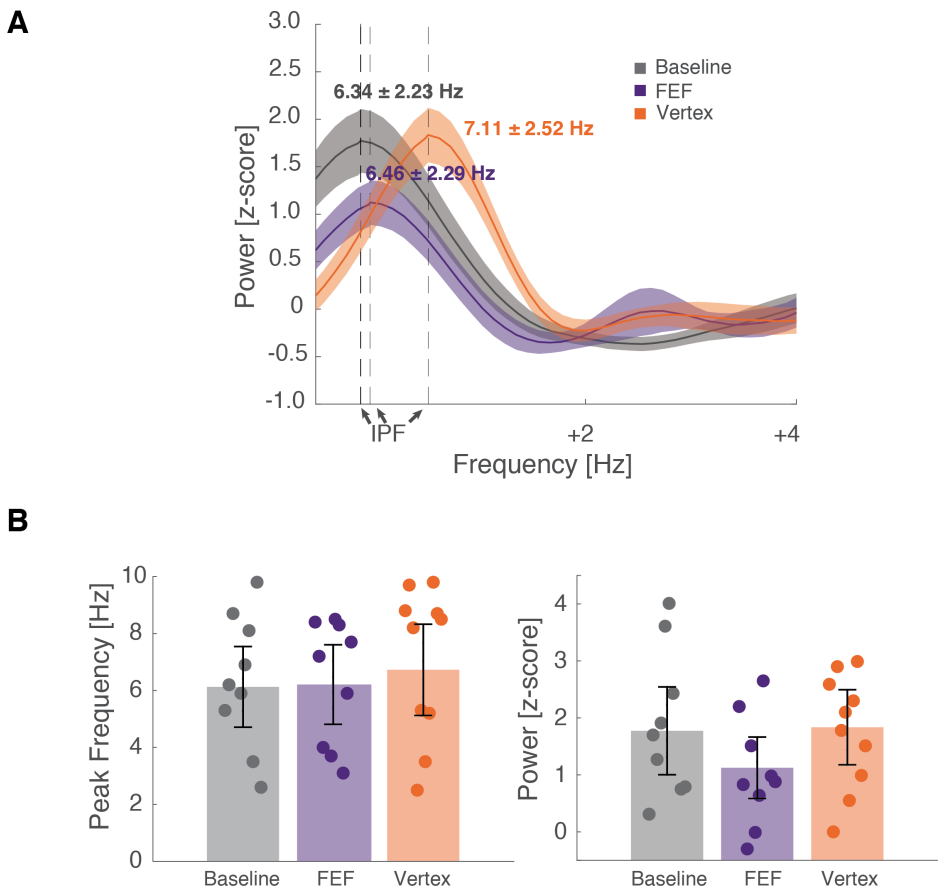

Figure 13. The results of spectral analysis of RT time series for baseline, FEF and vertex conditions. (A) Peak aligned power spectral density for the three conditions. Z-scored power was derived using permutation testing. Shaded areas correspond to ±1 SEM. (B) Bar plots of the average peak frequency and power for baseline, FEF and vertex conditions. There is a visible decrease in z-scored power in the FEF condition compared to the baseline and vertex conditions. Even though the drop in power in the FEF conditions rendered this combined peak insignificant (p = .13), this decrease did not render the power observed in the FEF condition statistically different from the power observed in the baseline and vertex conditions. Error bars correspond to 95% CI.

Discussion

The goal of Experiment 2 was to evaluate the role of the right FEF in rhythmic sampling of attention. FEF has previously been shown to play an important role in orienting visual attention as well as controlling eye-movement behavior (Vernet, Quentin, Chanes, Mitsumasu, & Valero-Cabré, 2014), but no published study has tested its involvement in the generation of rhythmic sampling of attention. To do so, I used cTBS to temporarily disrupt the function of the

right FEF and behaviorally evaluated the presence of attentional sampling following TMS stimulation. The results of the FEF condition were then compared to a condition with no TMS stimulation (baseline) and a condition in which TMS was delivered to a control area (vertex). I predicted that if FEF is causally involved in the generation of the attentional rhythm, disruption of this area could result in three different scenarios: 1) a complete removal of rhythmic sampling, 2) a reduction in the amplitude of the attentional sampling, and/or 3) a shift in the rate (frequency) of attentional sampling.

In line with the first hypothesized scenario, cTBS delivered to the right FEF resulted in a lack of a significant rhythmic signature that was specific to this condition, suggesting that TMS-induced disruption of the FEF lead to a degradation of the sampling rhythm. This disruption was driven by a decrease in amplitude of the sampling rhythm following TMS delivered to the right FEF in a subset of participants (scenario 2). Interestingly, there was no significant change in the rate of the sampling (scenario 3) providing no evidence for a shift in the sampling frequency resulting from FEF disruption. Overall, these findings point towards a role of the right FEF in the generation of the attentional rhythm.

It is important to note that the TMS-induced disruption of the attentional rhythm was only present in some of the participants (5 out of 12) and it remains unclear why this was the case. One potential explanation could be that the function of the right FEF was only successfully disrupted in these participants. This possibility is not unusual given that previous studies attempting to localize the FEF reported failure to produce disruption in FEF for a proportion of participants (e.g., 3 out of 10 participants in Ro, Farnè, & Chang, 2002). Because no independent measure of FEF disruption was collected, this possibility cannot be ruled out or confirmed. In contrast to a previous study by Marshall et al. (2015), there was also no effect of TMS on the

average RT in either the entire group or in the subgroup that could be used as an indicator of TMS efficiency. Future studies will be needed to examine the relationship between the effect of TMS on attentional sampling and other measures of FEF function, such as saccade slowing (Ro et al., 2002) and EEG correlates of attentional deployment (Marshall et al., 2015).

To summarize, the findings of the current study are among the first pieces of causal evidence suggesting the involvement of the FEF in the generation of rhythmic sampling of attention (see also preprint by Dugue, Beck, Marque, & VanRullen, 2018). Future studies will be needed in order to establish the exact cause of the degradation of the attentional rhythm following TMS to the right FEF. For example, disengagement of the FEF could result in a weaker deployment of attentional resources during different phases of the attentional cycle, leading to decreased benefits and detriments observed at different phases (i.e., decrease in amplitude of the rhythm). Another possibility could be that the FEF acts to reset attentional sampling, and its disruption leads to a poor alignment of the phase of attentional sampling. Additionally, the effect of FEF disruption will need to be examined with respect to other neural indices of this process, such as the strength and phase of oscillatory coupling between frontal and posterior brain areas (Fiebelkorn et al., 2018; Helfrich et al., 2018).

EXPERIMENT THREE: UNDERSTANDING THE IMPLICATIONS OF ATTENTIONAL RHYTHMICITY ON ENCODING INTO WORKING MEMORY

Introduction

The amount of information that can be maintained in WM is strictly limited (~3-4 simple objects; Cowan, 2001; Luck & Vogel, 1997), and as a result, the focus of attention at any given moment has a strong influence on what information is encoded and ultimately stored in WM (Schmidt et al., 2002; Woodman, Vecera, & Luck, 2003). For example, when provided with spatial cues about where task-relevant information will be presented, humans are capable of selectively allocating attention to only this information (e.g., Vogel, McCollough, & Machizawa, 2005), thus reducing the overall number of items stored. An unanswered question is whether, in the absence of such information, the natural rhythmic sampling of attention causes variability in encoding across the sampled locations. More specifically, information presented at the sampled location in the "good" phase of the attention cycle should be encoded into WM more accurately compared to information presented at the "poor" phase of the cycle (i.e., when attention is deployed to other locations). In line with the rationale of this prediction, a study by Myers et al. (2014) has shown that natural fluctuations in neural excitability are correlated with the accuracy of WM recall.

A recent study by Emrich, Lockhart and Al-Aidroos (2017) suggested that the allocation of spatial attention during WM encoding determines the resolution with which the information is stored. In keeping with previous findings suggesting that attention samples between different locations in space approximately once every 200 ms (~4-8 Hz; e.g., Landau & Fries, 2012; Song et al., 2014; VanRullen, Carlson, & Cavanagh, 2007), Experiment 3 aimed to determine whether the phase of the cycle underlying attentional sampling of space affects the encoding of

information into WM. To do this, to-be-encoded information was presented at one of two sampled locations at different time intervals following an attention-resetting stimulus. I predicted that information would be encoded more efficiently during particular phases of an ongoing oscillation. This would be evidenced by a pattern of rhythmic fluctuations in the fidelity of memory recall with respect to the location of the resetting stimulus (flash-congruent and flash-incongruent) and the time elapsed between the reset and the presentation of the information (SOA).

Methods and Materials

Participants. Twenty undergraduate and graduate students (7 male, age: $M = 19.05$, $SD = 1.36$) were recruited from North Dakota State University to participate in this study for course credit or monetary compensation ($10/h). Participant selection criteria and recruitment procedures were the same as described in Experiment 1.

Materials and procedure. Stimulus presentation and response recording were controlled by a PC running Matlab (Mathworks, Inc.) with Psychophysics Toolbox extensions (Brainard, 1997; D.G. Pelli, 1997). Stimuli were presented on the surface of a 24" of a LCD monitor with a refresh rate of 144 Hz, at a viewing distance of 57 cm.

The behavioral task consisted of a short-term memory recall task. The experimental stimuli consisted of two circular gray placeholders (R=140, G=140, B=140) subtending 4° of visual angle in diameter presented 5° eccentrically to the left or right of central fixation against medium gray background (R=128, G=128, B=128) filled with black and white noise patches (black R=0, G=0, B=0; white R=255, G=255, B=255). The sample stimulus consisted of one oriented grating (black R=0, G=0, B=0; white R=255, G=255, B=255) subtending 3.8° of visual angle in diameter presented inside one of the two placeholders. Orientation of the grating was

randomly drawn from 180° orientation space. The stimulus was overlaid with a semi-transparent Gaussian mask (R=128, G=128, B=128; alpha = 220) to reduce afterimages. A contrasting task-irrelevant flash (R=180, G=180, B=180) was used to reset attentional sampling prior to the presentation of the sample display. The flash was presented with equal likelihood and in a random order over one of the placeholders, producing flash-congruent and flash-incongruent trials. At test, participants were asked to recall the orientation of the sample grating by moving mouse crosshairs around the outline of the placeholder to adjust the orientation of the grating to match the orientation of the sample grating. The orientation of the grating was updated as the participant moved the crosshairs.

Experimental procedure. The sequence of trial events can be seen in Figure 14. Prior to the beginning of each block, participants were asked to place their chin in a chin rest and were instructed to maintain fixation on a fixation cross positioned at the center of the screen. For each block, following the appearance of the fixation cross, two unfilled circles were presented to the left and right of the fixation cross. At the beginning of each trial, the two circles were filled with random noise. At a variable time after the appearance of the noise patches (1000 - 1500 ms), one of the two circles briefly flashed (33 ms), generating a task-irrelevant resetting event. Following a variable SOA (randomly selected from 10 different time bins spanning the interval 200-700 ms after the resetting event: 200 ms, 256 ms, 311 ms, 367 ms, 422 ms, 478 ms, 533 ms, 589 ms, 644 ms, 700 ms), a sample display was presented for 100 ms. The sample display consisted of a single grating presented inside one of the two circles to the left or right of fixation. Participants were asked to recall the orientation of the grating following a 1000-ms delay interval. After providing their answer by clicking the mouse, participants received feedback in the form of a red bar marking the true orientation of the sample grating. The experiment consisted of 1200 total

trials separated into 40 blocks split into two experimental sessions that were completed on separate days. Participants completed 30 practice trials prior to the experiment. The full experiment took ~3 h to complete.

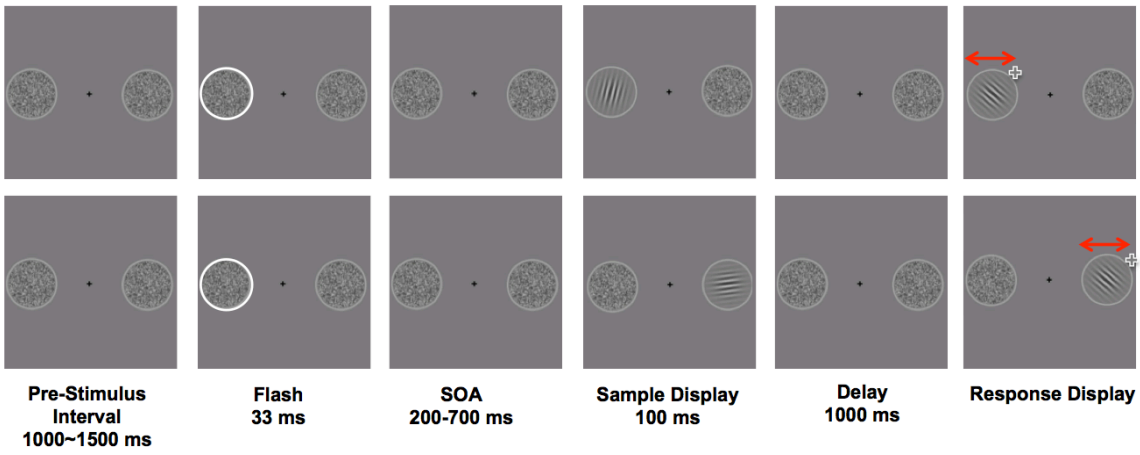

Figure 14. Behavioral task trial sequence for flash-congruent (top) and flash-incongruent (bottom) conditions for Experiment 3. Each trial started with the presentation of two circular noise patches to the left and right of fixation. Following a variable pre-stimulus interval, a task-irrelevant flash surrounding one of the two locations was used to reset attentional sampling. Following a variable SOA, a sample grating was presented at one of the two locations. Following a 1000 ms delay, the participants were asked to recall the orientation of the sample stimulus.

Angular error. A measure of WM accuracy was calculated as the mean absolute angular error between the sample and reported orientation (0-90 degrees). Angular error was calculated separately for each SOA, congruency (flash-congruent, flash-incongruent) and visual field (left, right). A difference time-series was calculated by subtracting flash-incongruent from flash-congruent angular error and averaging across visual fields.

Spectral analysis. To test whether WM performance (i.e., angular error) varied with respect to the task-irrelevant flash, spectral amplitude for a range of frequencies was calculated. To extract spectral amplitude, Fourier transform (fft; EEGLAB; Delorme and Makeig, 2004) was applied to an epoch of data (values of angular error) in an ascending order of SOAs from 200-700 ms, detrended, Hanning tapered and zero-padded (50 points before and after). The absolute

value of the resulting complex number represented amplitude values for frequencies, which were determined as in Experiment 1.

Statistical significance of the observed amplitude values was evaluated using a permutation test (for similar approach, see Dugué, Xue, & Carrasco, 2017; Dugué, Roberts, & Carrasco, 2016). A null distribution of spectral amplitude was generated by randomly assigning SOAs to the angular error values for each condition and for each participant separately. After randomization, the same analysis as the one described above was performed on the randomized data. This procedure was repeated 10,000 times and the resulting amplitude values were ordered from lowest to highest separately for each frequency. Spectral amplitude was considered statistically significant if the amplitude extracted from the real data was higher than the 95% confidence interval (CI) determined based on the 9,500th amplitude generated from the permuted data (corresponds to one-tailed p-value of .05). Benjamini-Hochberg correction for multiple comparisons was implemented. Probability less than $p = .05$ was considered statistically significant.

Phase-lag analysis. In addition to analyzing the spectral amplitude of angular error fluctuations in the *flash-congruent* and *flash-incongruent* conditions, the phase relationship between these two conditions was examined using the analysis described in Experiment 1.

Results

Average angular error. The angular difference between the sample and reported orientation across all SOAs and congruency conditions, i.e., the mean average angular error, was 10.67 ± 3.61 degrees. The resetting flash resulted in a significantly lower mean average angular error, $t(19) = -3.078$, $p = .006$, d = 0.694, CI [-0.906, -0.173], for the flash-congruent condition ($M = 10.40$, $SD = 3.55$) compared to flash-incongruent condition ($M = 10.94$, $SD = 3.71$; Figure

15A), This means that the sample orientations appearing in the same location as the flash were recalled more precisely compared to sample orientations appearing in the location opposite to the resetting flash. As expected for non-predictive cues, the cueing benefit was short-lived and the significant difference between flash-congruent and flash-incongruent conditions was driven by a significant advantage in the congruent condition in the two shortest flash-to-sample SOAs [200 ms: p = .007, 260 ms: p = .029; Benjamini-Hochberg corrected for multiple comparisons; Figure 15B].

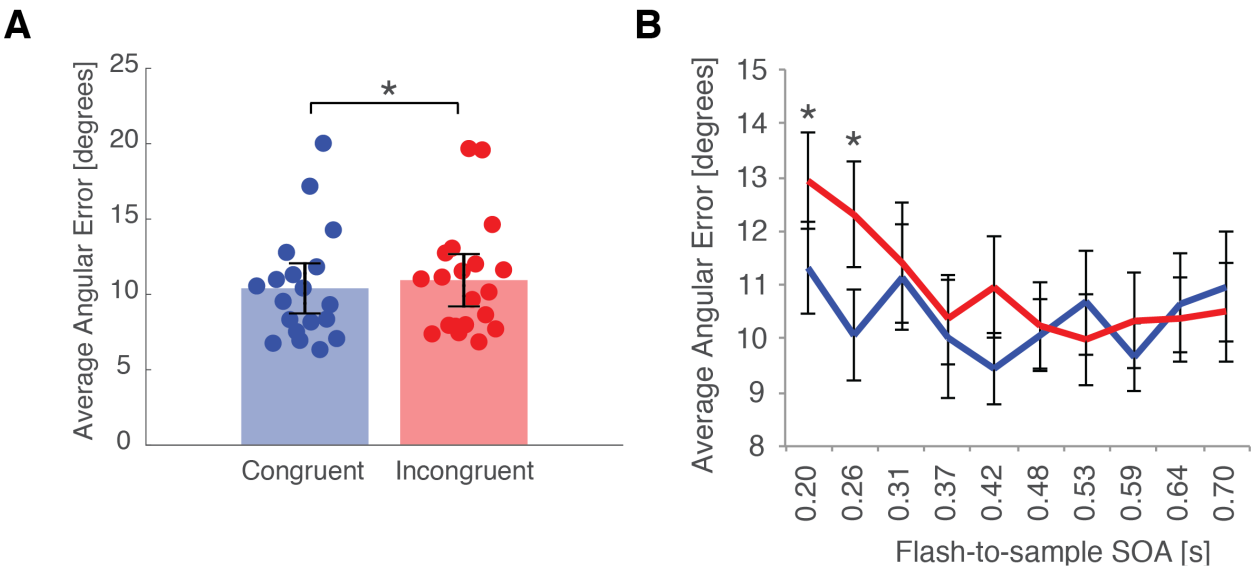

Figure 15. Behavioral performance for flash-congruent and flash-incongruent conditions. (A) Mean average angular error for flash-congruent and flash-incongruent conditions averaged across LVF and RVF and all SOAs. Error bars correspond to 95% CI. (B) Average angular error for different flash-to-sample SOAs for flash-congruent and flash-incongruent conditions (averaged across LVF and RVF). Flash-to-sample SOAs that were significantly different are marked with '*' (Benjamini-Hochberg corrected for multiple comparisons). Error bars correspond to ±1 SEM.

Spectral analysis of angular error. In order to test whether WM recall accuracy varied rhythmically at theta frequency (4-8 Hz) as a function of flash location and the length of the SOA, mirroring the attentional cycle, the time series of angular error differences between flash-congruent and flash-incongruent conditions was subjected to spectral analysis. The results

suggested that recall accuracy varied rhythmically in theta frequency: 6.6 Hz ($p < .001$ against null-distribution generated using permutation testing, Figure 16A). This finding supports the hypothesis that fluctuations in external attention rhythmically affect the encoding of information into WM.

Phase-lag analysis. If attention samples spatial locations in a serial manner, sampling of each location is expected to happen at opposite phases (180°) of the attentional cycle, resulting in an anti-phase relationship in WM recall accuracy between the flash-congruent and flash-incongruent fluctuations. To analyze the phase relationship between flash-congruent and flash-incongruent conditions, phase angle values were extracted for the peak frequency (6.6 Hz) separately for the two conditions (flash-congruent, flash-incongruent) and for each participant. There was a marginally significant phase difference between the flash-congruent and flash-incongruent-conditions (parametric Watson-Williams test: $F = 3.69$, $p = 0.06$) indicating the possible presence of a phase lag. To further evaluate the phase shift, the calculated angle difference was projected onto a unit circle separately for each individual participant. The resulting mean vector direction suggested a phase lag of 104.25° between the flash-congruent and flash-incongruent fluctuation. Rayleigh's test for non-uniformity of circular data showed that the phase angle differences were not distributed uniformly around the circle ($p = .24$), suggesting the presence of clustering. However, a more rigorous comparison of the phase against a null distribution did not provide evidence for a significant phase shift (phase-locking value = 0.27, null distribution phase-locking value = .39, $p > .05$; Figure 16B).

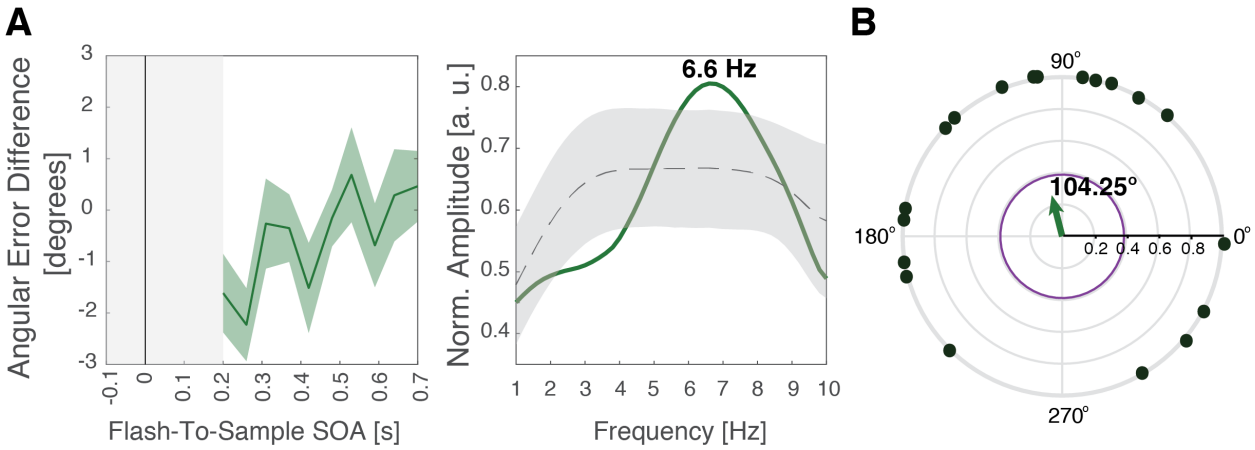

Figure 16. Spectral analysis of the difference in angular error between flash-congruent and flash-incongruent conditions. (A) Difference in angular error time series calculated as a difference between flash-congruent and flash-incongruent angular error collapsed across left and right visual fields. Spectral analysis of the difference in angular error time series showed a significant rhythm in theta range (6.6 Hz). Shaded areas correspond to ±1 SEM. (B) Phase-lag analysis of the phase relationship between the flash-congruent and flash-incongruent conditions. The lag in phase between the flash-congruent and flash-incongruent conditions was 104.25° suggesting a shift in the phase of the rhythms generated by the flash presented at the congruent and incongruent location. This shift was, however, not significant (phase-locking value equal to p = .05 shown in purple, actual phase-locking value shown in green).

Discussion

The goal of Experiment 3 was to test whether rhythmic fluctuations in attentional allocation in space affect the quality with which information is encoded into WM. More specifically, I tested whether presenting to-be-remembered information at different phases of the attentional cycle leads to different recall outcomes depending on whether information is presented in the "good" phase of the cycle and at the currently sampled location. To achieve this, I used an attention-grabbing flash to reset the phase of attentional sampling and presented a to-be-remembered orientation at either the same or opposite location and at different intervals following the flash. The purpose of this manipulation was to obtain samples of behavioral performance at different phases of the attentional cycle. If attentional allocation at encoding

affects the quality with which information is encoded in WM, rhythmic changes in attentional allocation in space should produce rhythmic fluctuations in WM performance.

The results of Experiment 3 showed a significant fluctuation in WM recall performance following an attentional reset for the to-be-remembered orientations presented at both flash-congruent and flash-incongruent locations. This suggested that the phase of attentional sampling, i.e., where attention was allocated at a particular point in time, affected the quality with which the information presented was remembered. In line with previous findings supporting the presence of an attentional rhythm in the theta band, WM recall performance also fluctuated in the theta range with a peak at 6.6 Hz, suggesting that the WM effect observed here was likely driven by the same process.

According to previous evidence, another consequence of rhythmic attentional sampling is that two locations are sampled at the opposite phases of the cycle, i.e., when attention is allocated to one location, less attention is allocated at the other location (Fiebelkorn et al., 2013). The analysis of the phase relationship between the flash-congruent and flash-incongruent conditions has suggested a shift in phase between the two conditions. However the amount (angle) of the phase shift has not been consistent across participants, resulting in an insignificant phase lag of ~104°. An insignificant phase lag could be a result of an incomplete reset of attentional sampling for some participants or could suggest that the two locations were not sampled in a sequential manner. Future studies will be needed to answer this question.

In summary, the results of this experiment further extend findings suggesting that selective spatial attention influences storage of information in WM. It is not only the case that WM is impacted by predictive spatial cues that can improve WM for the information presented at the cued location (and worsen WM for the information presented at the uncued locations), but

WM performance is also affected by rhythmic sampling of attention across space in the absence of predictive cues.

EXPERIMENT FOUR: ASSESSING THE PRESENCE OF RHYTHMIC ATTENTIONAL CYCLING DURING WORKING MEMORY MAINTENANCE

Introduction

In addition to attention playing an important role during the encoding of information into WM, attention also serves to support the active maintenance of information in WM by switching its focus between remembered items to prevent forgetting, a process referred to as attentional refreshing (Barrouillet, Bernardin, & Camos, 2004; Barrouillet, Bernardin, Portrat, Vergauwe, & Camos, 2007; Barrouillet & Camos, 2007, 2012; Vergauwe & Cowan, 2015). In line with the idea that attention supports maintenance, existing evidence suggests that during spatial WM, attention continues to be deployed at the currently maintained locations (Awh & Jonides, 2001). Moreover, decreases in oscillatory alpha-band power have been observed in occipital regions of the hemisphere contralateral to the hemifield of the remembered item (Dijk, Werf, Mazaheri, Medendorp, & Jensen, 2010; Medendorp et al., 2007), which is similar to alpha-band de-synchronization observed when attention is directed during perceptual processing (e.g., Thut, Nietzel, Brandt, & Pascual-Leone, 2006). In fact, these changes in the topographic distribution of alpha-band power are specific enough that the topography of alpha can be used to decode spatial representations being actively held in WM (Foster et al., 2016).

Studies of attentional cueing effects in WM have shown that attention can be selectively directed to specific internal representations in a goal-directed manner, improving memory for task-relevant representations relative to task-irrelevant ones (for review see Souza & Oberauer, 2016). Importantly, representations initially rendered task-irrelevant can be brought back to the focus of attention, resulting in improved representation accessibility (Lewis-Peacock & Postle, 2012). However, the temporal aspect of attentional prioritization in the absence of clear

differences in behavioral relevance of the maintained items remains to be explored. It is possible that attention is distributed equally across the remembered representations, or it could sample periodically between them in a manner similar to attentional sampling in the perceptual world. In line with the second premise, attentional refreshing is thought to be happening sequentially, by cycling through all remembered representations (Portrat & Lemaire, 2015). To address this question, Jafarpour et al. (2017) tracked attentional refreshing of three remembered objects with equal likelihood of being tested and found that resources tended to be directed to the weakest encoded item during maintenance. This finding is in line with a recent computational modeling study suggesting that the process of attentional refreshing likely operates on a schedule, in which the least activated memory trace at a given time is refreshed at that time (Lemaire, Pageot, Plancher, & Portrat, 2017). Even though Jafarpour et al. (2017) did not find evidence for sequential replay of items in WM following the refreshing of the weakest encoded item, their findings do not rule out WM replay as a potential mechanism for maintenance.

A separate line of research that points towards the potential cyclic nature of WM involves studies exploring a theta-based mnemonic code (Heusser, Poeppel, Ezzyat, & Davachi, 2016; Lisman & Jensen, 2013; Lubenov & Siapas, 2009; Vertes, 2005). According to the idea of theta-coupled periodic replay (Fuentemilla, Penny, Cashdollar, Bunzeck, & Düzel, 2010; Lisman, 2010; Lisman & Idiart, 1995), each individual item maintained in WM is represented by a spatial pattern of cells firing in the gamma frequency range (~30-80 Hz) and occurring within a specific phase of an ongoing theta oscillation. This arrangement allows the neural representation of each item to remain distinct because each memory becomes active in a different gamma cycle, and also preserves their sequential order due to the pairing with a specific theta phase. Theta-gamma coupling has been found to support the sequential, periodic replay of maintained items in WM

(Bahramisharif, Jensen, Jacobs, & Lisman, 2018; Fuentemilla et al., 2010), and the strength of theta-gamma coupling was shown to be correlated with the accuracy of later memory recall (Osipova et al., 2006; Tort, Komorowski, Manns, Kopell, & Eichenbaum, 2009).

The idea that *all* items are refreshed within a single cycle of a theta-band oscillation might seem at odds with the idea that attentional sampling occurs at a rate of *one* item per theta cycle. A computational modeling study assessing the plausibility of these two modes in attentional processing has suggested that both modes can be implemented by the brain and may support switching between more exploratory and selective modes of attention (McLelland & VanRullen, 2016). It is possible that maintenance of representations in WM is supported through a theta-based mnemonic code, whereas attention to WM representations may be deployed within individual theta cycles.

The goal of Experiment 4 was to examine the rhythmic properties of attention during WM maintenance. More specifically, I tested whether periodicity observed in external attention is present during the deployment of internal attention to WM representations during active maintenance. A recent pre-print by Peters, Rahm, Kaiser, and Bledowski (2018), provided initial evidence for the possibility that attentional allocation during WM is in fact rhythmic, with an oscillatory cycle of ~6 Hz. Specifically, the authors demonstrated that the speed of participants' ability to determine whether a spatial test probe belonged to one of two remembered objects varied rhythmically. Additionally, these rhythmic fluctuations depended on whether the probe was testing a location within a previously cued (same) or uncued (different) object.

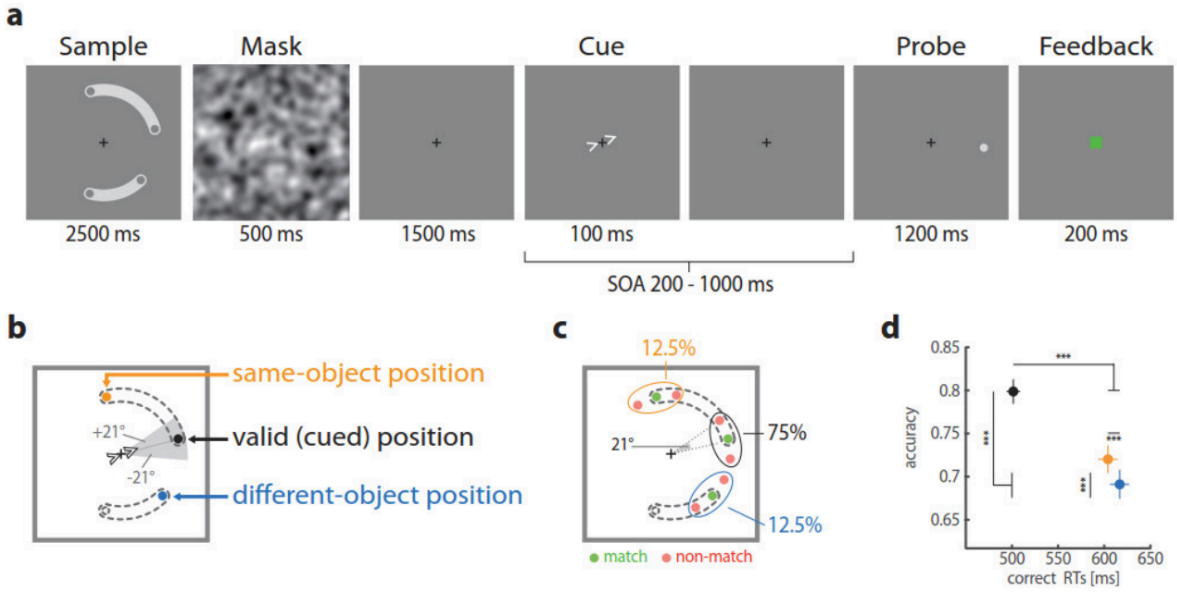

Figure 17. The experimental design and results of Peters et al. (2018)[4]. (A) Participants were asked to remember two sample objects defined by their endpoint positions. An informative cue was presented during maintenance indicating which position (B: same-object position, cued position, different-object position) would likely be tested (percentage of trials testing each position tested shown in C). At test, participants were presented with a probe and were asked to respond whether the probe matched or mismatched the remembered position. (D) As expected, participants responded faster and more accurately to probes presented at the valid position, but also for probes presented at the same-object position. This static effect of attention on RT and accuracy was present in addition to the presence of rhythmic fluctuations in RTs.

One potential shortcoming of this design is that the rhythmic fluctuations in RT observed in this study could be driven by the fact that participants' ability to respond to the test probe depends on the allocation of external attention at the time the test probe appears. More specifically, external attention might be sampling the locations where the target could be presented, leading to faster responses when the test probe appeared at the currently attended location; in other words, this effect could arise purely as a result of spatial attention directed to

[4] Reprinted from Peters et al. (2018) licensed under a CC-BY-NC-ND 4.0 International license and available at https://www.biorxiv.org/content/10.1101/105239v1.

external space. In this scenario, fluctuations in RTs would not necessarily be driven by rhythmic changes in access to the WM representations themselves.

According to prior evidence, allocation of attention during maintenance should affect how well the information is remembered and recalled (e.g., van Moorselaar, Gunseli, Theeuwes, & Olivers, 2015). Indeed, Peters et al. (2018) found a static effect of attention on accuracy, suggesting that participants' memory was, in general, more accurate for the cued versus uncued object. However, WM accuracy was only measured using a standard change detection WM task in which participants were asked to report whether the probe presented at test is the same as or different from the original sample. Because this approach does not provide any information about the quality of the actual memory representation, it remains unclear whether recall precision fluctuates as a result of the rhythmic allocation of attention to the remembered objects. I hypothesized that such periodicity should be reflected in rhythmic changes in the availability of WM representations, which should in turn be reflected in the precision of mnemonic recall. To test this hypothesis, I adopted procedures and analyses that have been used to examine periodic properties of external attention (e.g., Dugué et al., 2016, 2017; Landau & Fries, 2012; Song et al., 2014). After encoding, a task-irrelevant flash was used to reset the sampling of internal attention in a way similar to using spatial retro-cues to bring specific WM representations within the focus of internal attention. I predicted that the accuracy with which information would be recalled would vary rhythmically with respect to the location of the resetting stimulus (flash-congruent and flash-incongruent) and the time elapsed between the reset and the recall of the information (flash-to-test SOA).

Methods and Materials

Participants. Twenty-two undergraduate and graduate students (6 male, age: $M = 18.76$, $SD = 0.77$) were recruited from North Dakota State University to participate in this study for course credit or monetary compensation ($10/hr). One participant was excluded from further analysis due to poor behavioral performance (angular error > 3 *SD* from mean performance). Participant selection criteria and recruitment procedures were the same as described in Experiment 1.

Materials and procedure. Stimulus presentation and response recording were controlled by a PC running Matlab (Mathworks, Inc.) with Psychophysics Toolbox extensions (Brainard, 1997; D.G. Pelli, 1997). Stimuli were presented on the surface of a 24" of a LCD monitor with a refresh rate of 144 Hz, at a viewing distance of 57 cm.

The behavioral task consisted of a short-term memory recall task. The experimental stimuli consisted of two circular gray placeholders (R=140, G=140, B=140) subtending 4° of visual angle in diameter presented 5° eccentrically to the left or right of central fixation against medium gray background (R=128, G=128, B=128) filled with black and white noise patches (black R=0, G=0, B=0; white R=255, G=255, B=255). The sample stimulus consisted of two oriented gratings (black R=0, G=0, B=0; white R=255, G=255, B=255) each subtending 3.8° of visual angle in diameter presented inside the two placeholders. The orientation of each grating was randomly drawn from 180° orientation space. The sample stimuli were overlaid with a semi-transparent Gaussian mask (R=128, G=128, B=128; alpha = 220) to reduce afterimages. A contrasting task-irrelevant flash (R=180, G=180, B=180) was used to reset attentional sampling after the presentation of the sample display. The flash was randomly and equally likely presented over one of the placeholders producing flash-congruent and flash-incongruent trials. At test,

participants were asked to recall the orientation of one of the sample gratings by moving a crosshair around the outline of the placeholder to adjust the orientation of the grating to match the orientation of the sample grating presented at that location. The orientation of the grating was updated as the participant moves the crosshair.

Experimental procedure. The sequence of trial events can be seen in Figure 18. Prior to the beginning of each block, participants were asked to place their chin in a chin rest and were instructed to maintain fixation on a fixation cross positioned at the center of the screen. Each block started with the appearance of a fixation cross in the middle of the screen and two unfilled circles to the left and right of the fixation cross. At the beginning of each trial, the two circles were filled with random noise. Following a 500 ms pre-stimulus interval, a sample display containing two gratings appeared for 500 ms, temporarily replacing the two noise patches. At a variable time after the sample display disappeared (500 - 1000 ms), one of the two circles flashed briefly (33 ms) generating a task-irrelevant resetting event. Following a variable SOA (200-700 ms, 10 different time bins: 200 ms, 256 ms, 311 ms, 367 ms, 422 ms, 478 ms, 533 ms, 589 ms, 644 ms, 700 ms), a test grating was displayed at one of the two locations and participants were asked to recall the orientation of the sample grating presented at this location. After providing their answer by clicking the mouse, participants received feedback in the form of a red bar marking the orientation of the sample grating. The experiment consisted of 1200 total trials separated into 40 blocks and split into two experimental sessions that performed on separate days. Participants completed 30 practice trials prior to the experiment. The full experiment took ~3 h to complete.

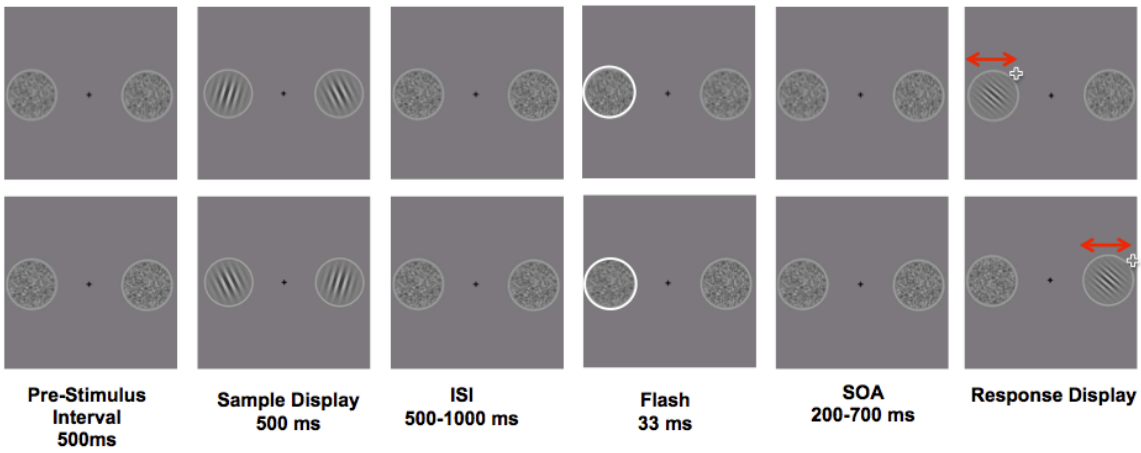

Figure 18. Behavioral task trial sequence for flash-congruent (top) and flash-incongruent (bottom) conditions for Experiment 4. Following a variable pre-stimulus interval, two orientation gratings appeared within two circular noise patches, one to the left and one to the right of the fixations. After a variable inter-stimulus-interval, a flash was used to reset attention to one of the two locations. After a variable SOA, the participants were asked to recall the orientation of one of the gratings.

Data analysis. Amplitude and phase analysis of angular error were performed in the same way as described in Experiment 3.

Results

Average angular error. On average, the angular difference between the sample and reported orientation across all SOAs and across flash-congruent and flash-incongruent conditions was 14.5 ± 3.59 degrees. The resetting flash resulted in a significantly lower mean average angular error, $t(20) = -5.481$, $p < .001$, d = 0.699, CI [-2.361, -1.059], for the flash-congruent orientations ($M = 13.19$, $SD = 3.39$) compared to flash-incongruent orientations ($M = 14.90$, $SD = 3.91$; Figure 19A). This means that the tested orientations appearing in the same location as the flash were recalled more precisely compared to the orientations appearing in the location opposite to the resetting flash. Unlike in Experiment 3, the cueing benefit was more long-lived and was present at both longer and shorter SOAs [640 ms: $p < .001$, 590 ms: $p < .001$, 480 ms: $p = .02$, 370 ms: $p = .02$; Benjamini-Hochberg corrected for multiple comparisons; Figure 19B].

This suggests that the flash produced a more prolonged advantage for the flash-congruent condition similar to an effect expected to be produced by an informative cue.

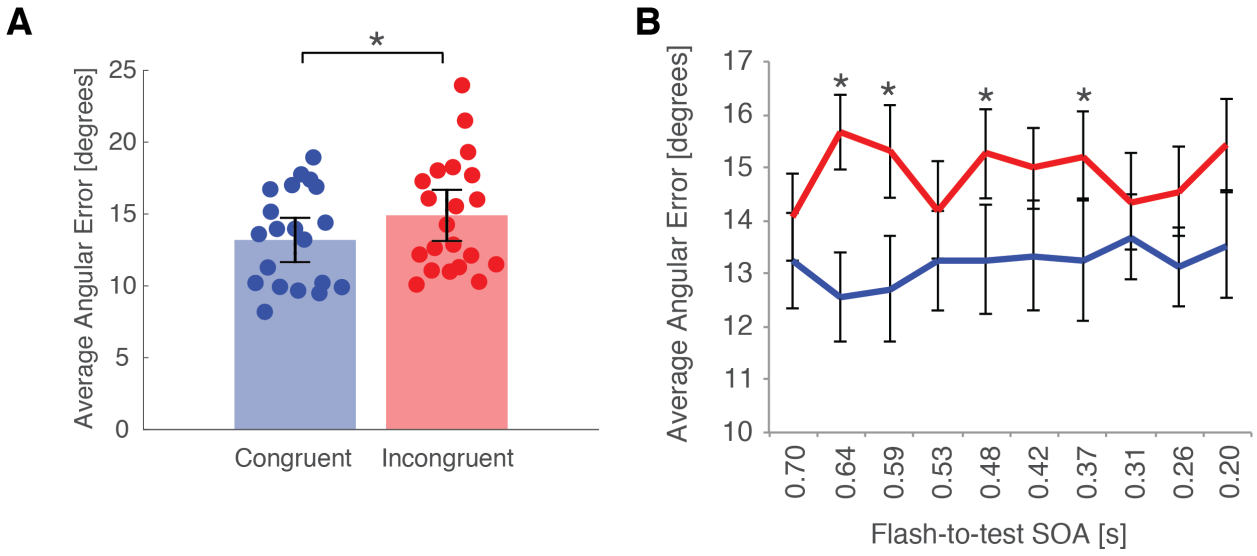

Figure 19. Behavioral performance for flash-congruent and flash incongruent conditions. (A) Mean average angular error for flash-congruent and flash-incongruent conditions averaged across LVF and RVF. Error bars correspond to 95% CI. (B) Average angular error for different flash-to-test SOAs for flash-congruent and flash-incongruent conditions (averaged across LVF and RVF). Flash-to-test SOAs that were significantly different are marked with '*' (Benjamini-Hochberg corrected for multiple comparisons). Error bars correspond to ±1 SEM.

Spectral analysis of angular error. If attention directed to internal representations fluctuates rhythmically, as is the case in externally directed attention, WM recall accuracy should vary rhythmically in theta frequency (4-8 Hz). The results of the spectral analysis of the difference score (congruent-incongruent) time series yielded a peak in the theta band range (5.2 Hz); however, this peak was not significant (z-score = 1.36, p = .09 against null-distribution generated using permutation testing; Figure 20A).

Phase-lag analysis. If attention continues to sample representations stored in WM in a serial manner, sampling of each representation is expected to happen at opposite phases (180°) of the attentional cycle, resulting in an anti-phase relationship in WM recall accuracy between the flash-congruent and flash-incongruent fluctuations. For the purpose of completing all planned

analyses, the phase angle values were extracted for the (non-significant) peak frequency (5.2 Hz) for the flash-congruent and flash-incongruent conditions. There was a significant phase difference between the flash-congruent and flash-incongruent-conditions (parametric Watson-Williams test: $F = 17.12$, $p < 0.001$) indicating the presence of a phase lag. To further evaluate the phase shift, the calculated angle difference was projected onto a unit circle separately for each individual participant. In line with the prediction, the resulting mean vector direction suggested a phase lag of 194.88° between the flash-congruent and flash-incongruent conditions pointing towards an anti-phase relationship. Rayleigh's test for nonuniformity of circular data showed that the phase angle differences were not distributed uniformly around the circle ($p = .24$) suggesting the presence of phase clustering. However, a more rigorous test using permutation showed that this phase lag was not significant (phase-locking value = 0.26, null distribution phase-locking value = 0.37, $p > .05$; Figure 20B).

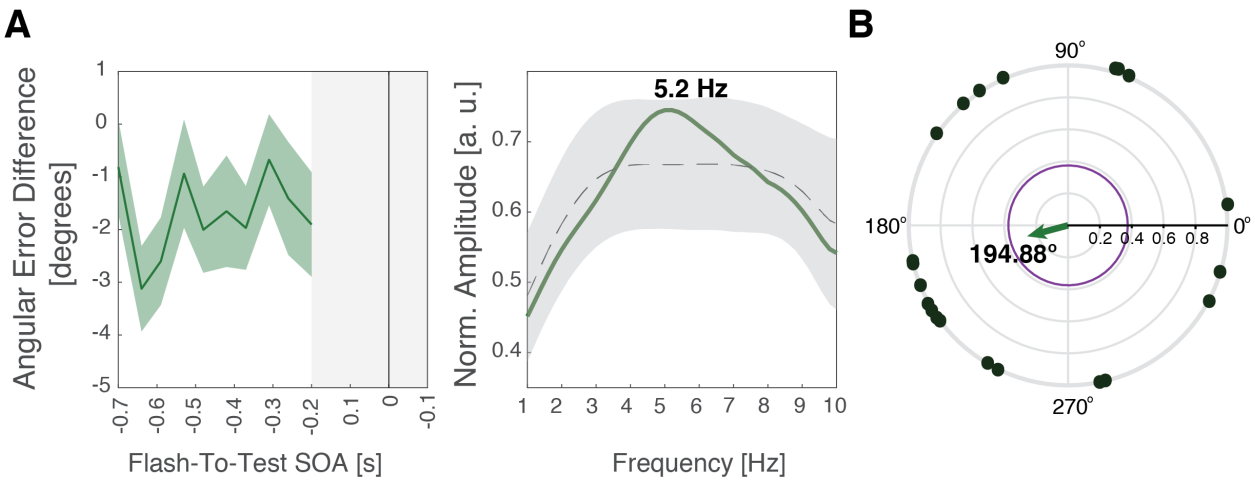

Figure 20. Spectral analysis of the difference in angular error between flash-congruent and flash-incongruent conditions (averaged across LVF and RVF). (A) Angular error difference time series calculated as a difference between the flash-congruent and flash-incongruent angular error plotted for the different flash-to-test SOAs. Results of the spectral analysis of the difference angular error time series showed a peak in theta range (5.2 Hz). The amplitude of this peak was not significantly higher than the amplitude of the null-distribution. Shaded areas correspond to ±1 SEM. (B) Phase-lag analysis of the phase relationship between the flash-congruent and flash-incongruent conditions. The lag in phase between the flash-congruent and flash-incongruent conditions was 194.88° suggesting a shift in the phase of the rhythms generated by the flash presented at the congruent and incongruent location. This shift was, however, not significant (phase-locking value equal to p = .05 shown in purple, actual phase-locking value shown in green).

Discussion

The goal of Experiment 4 was to test for the presence of attentional sampling over representations maintained in WM. Specifically, I examined whether attention is deployed to internal WM representations in a manner similar to rhythmic fluctuations observed in attention directed to visual stimuli currently present in the environment. Similar to Experiment 3 and previous studies, I used a task-irrelevant, non-predictive spatial cue to phase-align the hypothesized rhythmic sampling of WM representations and tested WM recall performance at different phases of the sampling rhythm. If attention samples internal WM representations rhythmically, rhythmic changes in attentional allocation within the internal WM representation space should produce fluctuations in WM performance.

The initial examination of the power spectrum of recall performance for Experiment 4 revealed a spectral peak in the theta frequency band (5.2 Hz); however, this peak was not significant. The results of Experiment 4 therefore failed to provide evidence for the presence of rhythmic sampling over internal WM representations. The lack of a significant peak could suggest that attentional deployment to external representations relies on a different mechanism than attention directed to internal representations. The null result should, however, be taken into consideration with respect to the large body of evidence suggesting similar mechanisms between internal and external attention (Awh & Jonides, 1998, 2001; Dijk et al., 2010; Medendorp et al., 2007). Moreover, a recent study (Balestrieri, Ronconi, & Melcher, 2019, preprint) has shown that when attention was split between monitoring the external flow of information and maintaining information internally, the attentional rhythm was split in a way similar to when two streams of external information have to be monitored. This provides yet another piece of evidence pointing towards a shared resource between external and internal visual attention and the rhythmic allocation of this resource. Additionally, the lack of a significant peak could be due to high between-subject variability in peak sampling frequency, which could have resulted in reduced amplitude of the averaged spectrum. This possibility will have to be tested in an experimental design that allows for individually derived peak frequency (similarly to Experiment 1 and 2).

Interestingly, the task-irrelevant spatial cue generated a prolonged advantage for the orientations presented at the same spatial location as the task-irrelevant flash. Similarly, Peters and colleagues (2018) also observed a static effect of attention on accuracy showing that participants were more accurate in reporting the location of the cued versus uncued object. This potentially suggests that once attention is allocated to a specific WM representation, this

representation remains in the focus of attention until attention is switched to another representation as a result of another cue. In line with this possibility, Wang et al. (2017) showed that a non-predictive retro-cue produced a prolonged advantage in performance for a cued item unless attention was cued away from this item using a central cue. This finding could be taken as an argument against the possibility that attention continues to sample internal representations rhythmically; however, recent studies have raised questions about the role of attention in WM cue-related benefits (Myers, Stokes, & Nobre, 2017). For example, a study by Myers and colleagues (2018) argued that prioritization of an item in WM performance can be achieved by generating a mapping between the representation and the response. According to this interpretation, cue-related improvements in WM performance are a result of the representation-response mapping, rather than reflecting the allocation of attention to this item. This opens up the possibility that attentional sampling is present in WM in addition to the observed stable cue-related benefits arising from response mapping.

Another possible explanation for the lack of significant rhythmic fluctuations in recall performance could be that the time necessary to allocate attentional resources within WM is more time demanding. As a result, the 200-700 ms time window following the flash did not allow enough time for the rhythmic sampling to resume following the initial attentional shift. Support for this possibility is provided by a study by Moorselaar et al. (2015) that tested the role of attention in protection of WM representations against perceptual interference. According to this study, it takes approximately half a second following a cue for attention to be fully deployed towards a WM representation and for the representation to become resistant to interference. This suggests that allocation of attention to internal representations may take longer and as a result,

internal rhythmic sampling may need more time to resume following its reset or may operate at a lower frequency compared to external attention.

Finally, it could be argued that the external cue used to phase-align the attentional rhythm may not be an effective way to reset attentional sampling of internal WM representations. I decided to use an external spatial cue because previous evidence suggests that attention continues to be deployed to locations where remembered items were initially presented (Awh & Jonides, 1998, 2001; Dijk et al., 2010; Medendorp et al., 2007). Additionally, it was recently shown that moving an item stored in WM into the focus of attention involves a gaze bias in the direction of the item's original location and this was the case even when the location was not necessary for recall (Ede, Chekroud, & Nobre, 2019). This study, like many others, provides further evidence for the existence of similarities in the mechanism of attentional selection in external and internal space. Additionally, the fact that the cue produced a behavioral advantage in the flash-congruent condition disputes the possibility that the cue was not effective in capturing and directing attention towards the representation associated with that particular location.

In summary, Experiment 4 provided limited support for the existence of rhythmic sampling in WM. This finding is at odds with the result of Peters et al. (2018), who argue for the existence of rhythmic sampling between objects maintained in WM. As I described in more detail above, I believe that this effect could be driven by rhythmic sampling of external attention deployed to the expected probe locations rather than within WM, as their effect was limited to RT and not recall performance. Future studies will be necessary to further test for the possibility of rhythmic sampling within WM.

GENERAL DISCUSSION

Attention, or the ability to selectively attend to and facilitate the processing of relevant information, is crucial for survival. Numerous studies have been dedicated to studying the effects of attention on behavior and neural processing, and to uncovering the neural substrates supporting this function. It is well established that attention is flexible in its capability to adaptably switch between its targets depending on the current goals (Bosman et al., 2012; Busse, Katzner, & Treue, 2008). However, it was only recently revealed that even when attention is directed to a particular target, it does not remain static but rather its effects fluctuate rhythmically over time (e.g., Landau & Fries, 2012). The work included in this dissertation makes an important contribution to this endeavor by examining the relationship between the observed rhythm and oscillatory signatures of attention, by probing the causal influence of an important attentional hub in the generation of the attentional rhythm and, lastly, by evaluating the consequences of the attentional rhythm on WM.

According to existing evidence, rhythmic fluctuations in the effects of attention reflect rhythmic patterns of neural activity, i.e., neural oscillations. Prior findings suggest that, among these rhythmic patterns, the phase of an ongoing theta-band oscillation influences the extent to which the effects of attention are manifested in behavior and neural activity. For example, it has been shown that theta phase influences participant's ability to perceive hard-to-see targets as well as the power of gamma activity (>30 Hz) related to target processing (Landau et al., 2015). However, the role of suppression supported by alpha band activity, which has been shown to be closely related to attention (e.g., Rihs et al., 2007), in the rhythmic sampling of attention has not been well established. The results of Experiment 1 take a first step in this direction by examining whether rhythmic shifts of attention between two attended locations are reflected in the

topography of alpha-band power changes over time. The results of this study support a role for neural oscillations in the alpha frequency band in the process of attentional sampling of space; in particular, the analysis of behavioral performance and the spatial selectivity of the focus of attention reconstructed from ABOP revealed the presence of rhythmic fluctuations in the theta band (4-8 Hz) over time. This experiment is among the first to demonstrate a relationship between a well-established oscillatory correlate of attention and the attentional rhythms observed in behavior. Continued research related to this topic can help elucidate how neural dynamics give rise to our ability to rhythmically switch our focus of attention to effectively sample task-relevant information in our environment.

Aside from elucidating the role of neural oscillations in the attentional rhythm, this dissertation also took steps towards identifying the neural sources driving the rhythmic sampling of attention. It has been proposed that the attentional rhythm is a reflection of the architecture of the network that supports attention (Helfrich, Breska, & Knight, 2019), and so disruption of one of the network nodes would be expected to affect the ongoing rhythm. Experiment 2 showed that TMS-induced disruptions of the function of the FEF, an important network node involved in attention, leads to a degradation of the attentional rhythm. In particular, the amplitude of the attentional rhythm was greatly attenuated by FEF disruption, supporting a role for this brain area in implementing the attentional rhythm evident in behavior. Future research should replicate this finding and also focus on other specific structures (e.g., the lateral intraparietal cortex; LIP and the thalamus) and their interactions in the control of the attentional rhythm.

Finally, this dissertation also revealed that the effects of attentional rhythms aren't limited to perceptual-level phenomena, such as stimulus detection, but likely also influence the encoding and storage of information in working memory. In particular, Experiment 3 showed

that rhythmic attentional sampling of space affects the precision with which information is encoded into WM. This finding extends prior research of the attentional rhythm into WM and provides further evidence for the close relationship between attention and WM. Experiment 4 then focused on examining whether attention directed to internal representations involves a similar, rhythmic signature. The results replicated previous findings showing prolonged cue-related benefits for attended versus unattended WM representations, but did not provide strong evidence for the existence of rhythmic attentional sampling of representations maintained in WM. Future studies will be needed to elucidate whether the lack of a rhythmic signature is reflective of the nature of attention directed to WM representations, or whether internal attention is rhythmic but elusive using the current paradigm.

Aside from the future directions specific to the individual experiments, this dissertation also highlights the need to critically examine other aspects of the attentional rhythm. First of all, it has been proposed that attention samples spatial locations in a serial manner, which is reflected in an anti-phase relationship (or 180° phase lag) between the rhythms associated with two sampled locations. Here, phase relationships between the flash-congruent and flash-incongruent rhythms were examined for significant peak frequencies in Experiments 1 and 3. In both cases, previously adopted tests of phase relationships (e.g., Dugué et al., 2016, 2017) pointed towards the existence of a significant phase shift between the conditions; however, in the present study, permutation-based tests did not provide support for a significant phase shift. Additionally, the revealed phase lag values were not always consistent with the idea of serial sampling. Given this, it will be important to further examine why this may be the case and to replicate prior findings using permutation-based tests.

Secondly, the results of the studies included in this dissertation revealed considerable variability in the peak frequency of individual participant's attentional rhythm. It has been proposed that the natural attentional 'clock' oscillates at 8 Hz (i.e., every ~125 ms, e.g., Busch & VanRullen, 2010; VanRullen et al., 2007), and that splitting attention between two locations reduces this rhythm to ~4 Hz (for this argument see e.g., VanRullen, 2016). Considering this interpretation, relative differences in the sampling rates of participants could be a result of some participants strategically adopting the approach to only sample from one location rather than divide their attention between the two locations. It is also possible that observed differences in sampling frequency between conditions could have resulted from an unequal distribution of attention. In keeping with this possibility, one previous study has reported that the influence of theta phase on performance is stronger for unattended versus attended locations (Harris, Dux, & Mattingley, 2018). Given that perception naturally varies as a result of fluctuations in cortical excitability, reflected in the phase of alpha oscillations (8-14 hz; Dugué et al., 2011; Harris et al., 2018; Mathewson et al., 2009; Senoussi, Moreland, Busch, & Dugue, 2018-preprint; Sherman, Kanai, Seth, & VanRullen, 2016), this perceptual alpha rhythm may be more strongly represented in the sampling frequency of the currently attended location. This, in turn, may lead to an overall higher frequency peak for the currently attended location. In order to address this possibility, the interaction between the perceptual and attentional rhythms will need to be explored in a more strategic manner in the future.

In summary, this dissertation makes an important contribution to extending our understating of the attentional rhythm. Specifically, it considers the importance of sensory suppression supported by alpha band power in rhythmic shifts of attention, it probes the causal influence of the FEF in the generation of the attentional rhythm, and, finally, it characterizes the

consequences of the attentional rhythm on WM. Overall, the work included in this dissertation makes a valuable contribution to research aimed at testing a very interesting perspective, that cognition in general, and attention in particular, is rhythmic in nature, and this rhythmicity is a reflection of the nature of the neural activity supporting it.

REFERENCES

Awh, E., & Jonides, J. (1998). Spatial working memory and spatial selective attention. In R. Parasuraman (Ed.), *The Attentive Brain* (pp. 71–94). Cambridge, MA: MIT Press.

Awh, E., & Jonides, J. (2001). Overlapping mechanisms of attention and spatial working memory. *Trends in Cognitive Sciences*, *5*(3), 119–126. https://doi.org/10.1016/S1364-6613(00)01593-X

Awh, E., Jonides, J., & Reuter-Lorenz, P. A. (1998). Rehearsal in spatial working memory. *Journal of Experimental Psychology: Human Perception and Performance*, *24*(3), 780–790. https://doi.org/10.1037/0096-1523.24.3.780

Awh, E., & Pashler, H. (2000). Evidence for split attentional foci. *Journal of Experimental Psychology. Human Perception and Performance*, *26*(2), 834–846.

Baddeley, A. D. (1992). Working memory. *Science*, *255*(5044), 556–559. https://doi.org/10.1126/science.1736359

Bahramisharif, A., Jensen, O., Jacobs, J., & Lisman, J. (2018). Serial representation of items during working memory maintenance at letter-selective cortical sites. *PLOS Biology*, *16*(8), e2003805. https://doi.org/10.1371/journal.pbio.2003805

Balestrieri, E., Ronconi, L., & Melcher, D. (2019). Shared resources between visual attention and visual working memory are allocated through rhythmic sampling. *BioRxiv*, 567602. https://doi.org/10.1101/567602

Barrouillet, P., Bernardin, S., & Camos, V. (2004). Time constraints and resource sharing in adults' working memory spans. *Journal of Experimental Psychology. General*, *133*(1), 83–100. https://doi.org/10.1037/0096-3445.133.1.83

Barrouillet, P., Bernardin, S., Portrat, S., Vergauwe, E., & Camos, V. (2007). Time and cognitive load in working memory. *Journal of Experimental Psychology. Learning, Memory, and Cognition*, *33*(3), 570–585. https://doi.org/10.1037/0278-7393.33.3.570

Barrouillet, P., & Camos, V. (2007). The time-based resource-sharing model of working memory. In *The Cognitive Neuroscience of Working Memory* (pp. 59–80).

Barrouillet, P., & Camos, V. (2012). As Time Goes By: Temporal Constraints in Working Memory. *Current Directions in Psychological Science*, *21*(6), 413–419. https://doi.org/10.1177/0963721412459513

Bosman, C. A., Schoffelen, J.-M., Brunet, N., Oostenveld, R., Bastos, A. M., Womelsdorf, T., … Fries, P. (2012). Attentional stimulus selection through selective synchronization between monkey visual areas. *Neuron*, *75*(5), 875–888. https://doi.org/10.1016/j.neuron.2012.06.037

Brainard, D. H. (1997). The psychophysics toolbox. *Spatial Vision*, *10*, 433–436.

Busch, N. A., Dubois, J., & VanRullen, R. (2009). The Phase of Ongoing EEG Oscillations Predicts Visual Perception. *Journal of Neuroscience*, *29*(24), 7869–7876. https://doi.org/10.1523/JNEUROSCI.0113-09.2009

Busch, N. A., & VanRullen, R. (2010). Spontaneous EEG oscillations reveal periodic sampling of visual attention. *Proceedings of the National Academy of Sciences*, *107*(37), 16048–16053. https://doi.org/10.1073/pnas.1004801107

Buschman, T. J., & Kastner, S. (2015). From Behavior to Neural Dynamics: An Integrated Theory of Attention. *Neuron*, *88*(1), 127–144. https://doi.org/10.1016/j.neuron.2015.09.017

Buschman, T. J., & Miller, E. K. (2009). Serial, Covert Shifts of Attention during Visual Search Are Reflected by the Frontal Eye Fields and Correlated with Population Oscillations. *Neuron*, *63*(3), 386–396. https://doi.org/10.1016/j.neuron.2009.06.020

Busse, L., Katzner, S., & Treue, S. (2008). Temporal dynamics of neuronal modulation during exogenous and endogenous shifts of visual attention in macaque area MT. *Proceedings of the National Academy of Sciences*, *105*(42), 16380–16385. https://doi.org/10.1073/pnas.0707369105

Carvalhaes, C., & de Barros, J. A. (2015). The surface Laplacian technique in EEG: Theory and methods. *International Journal of Psychophysiology*, *97*(3), 174–188. https://doi.org/10.1016/j.ijpsycho.2015.04.023

Cavanagh, J. F., & Frank, M. J. (2014). Frontal theta as a mechanism for cognitive control. *Trends in Cognitive Sciences*, *18*(8), 414–421. https://doi.org/10.1016/j.tics.2014.04.012

Chanes, L., Quentin, R., Tallon-Baudry, C., & Valero-Cabré, A. (2013). Causal Frequency-Specific Contributions of Frontal Spatiotemporal Patterns Induced by Non-Invasive Neurostimulation to Human Visual Performance. *The Journal of Neuroscience*, *33*(11), 5000–5005. https://doi.org/10.1523/JNEUROSCI.4401-12.2013

Chun, M. M., & Johnson, M. K. (2011). Memory: Enduring Traces of Perceptual and Reflective Attention. *Neuron*, *72*(4), 520–535. https://doi.org/10.1016/j.neuron.2011.10.026

Clayton, M. S., Yeung, N., & Cohen Kadosh, R. (2015). The roles of cortical oscillations in sustained attention. *Trends in Cognitive Sciences*, *19*(4), 188–195. https://doi.org/10.1016/j.tics.2015.02.004

Cohen, M. X. (2014). *Analyzing Neural Time Series Data: Theory and Practice*. MIT Press.

Corbetta, M., & Shulman, G. L. (2002). Control of Goal-Directed and Stimulus-Driven Attention in the Brain. *Nature Reviews Neuroscience*, *3*(3), 215–229. https://doi.org/10.1038/nrn755

Cowan, N. (2001). The magical number 4 in short-term memory: A reconsideration of mental storage capacity. *Behavioral and Brain Sciences*, *24*, 87–185.

Crick, F. (1984). Function of the thalamic reticular complex: the searchlight hypothesis. *Proceedings of the National Academy of Sciences*, *81*(14), 4586–4590. https://doi.org/10.1073/pnas.81.14.4586

Crouzet, S. M., & VanRullen, R. (2017). The rhythm of attentional stimulus selection during visual competition. *BioRxiv*, 105239. https://doi.org/10.1101/105239

Delorme, A., & Makeig, S. (2004). EEGLAB: an open source toolbox for analysis of single-trial EEG dynamics including independent component analysis. *Journal of Neuroscience Methods*, *134*, 9–21.

Deouell, L. Y., Sacher, Y., & Soroker, N. (2005). Assessment of spatial attention after brain damage with a dynamic reaction time test. *Journal of the International Neuropsychological Society*, *11*(6), 697–707. https://doi.org/10.1017/S1355617705050824

Desimone, R., & Duncan, J. (1995). Neural mechanisms of selective visual attention. *Annual Review of Neuroscience*, *18*, 193–222.

D'Esposito, M., & Postle, B. R. (2015). The Cognitive Neuroscience of Working Memory. *Annual Review of Psychology*, *66*(1), 115–142. https://doi.org/10.1146/annurev-psych-010814-015031

Dijk, H. van, Werf, J. van der, Mazaheri, A., Medendorp, W. P., & Jensen, O. (2010). Modulations in oscillatory activity with amplitude asymmetry can produce cognitively relevant event-related responses. *Proceedings of the National Academy of Sciences*, *107*(2), 900–905. https://doi.org/10.1073/pnas.0908821107

Downing, P. (2000). Interactions Between Visual Working Memory and Selective Attention. *Psychological Science*, *11*(6), 467–473. https://doi.org/10.1111/1467-9280.00290

Downing, P., & Dodds, C. (2004). Competition in visual working memory for control of search. *Visual Cognition*, *11*(6), 689–703. https://doi.org/10.1080/13506280344000446

Dugue, L., Beck, A.-A., Marque, P., & VanRullen, R. (2018). Contribution of FEF to attentional periodicity during visual search: a TMS study. *BioRxiv*, 414383. https://doi.org/10.1101/414383

Dugué, L., Marque, P., & VanRullen, R. (2011). The Phase of Ongoing Oscillations Mediates the Causal Relation between Brain Excitation and Visual Perception. *Journal of Neuroscience*, *31*(33), 11889–11893. https://doi.org/10.1523/JNEUROSCI.1161-11.2011

Dugué, L., Roberts, M., & Carrasco, M. (2016). Attention Reorients Periodically. *Current Biology*, *26*(12), 1595–1601. https://doi.org/10.1016/j.cub.2016.04.046

Dugué, L., Xue, A. M., & Carrasco, M. (2017). Distinct perceptual rhythms for feature and conjunction searches. *Journal of Vision*, *17*(3), 22. https://doi.org/10.1167/17.3.22

Ede, F. van, Chekroud, S. R., & Nobre, A. C. (2019). Human gaze tracks attentional focusing in memorized visual space. *Nature Human Behaviour*, 1. https://doi.org/10.1038/s41562-019-0549-y

Emrich, S. M., Lockhart, H. A., & Al-Aidroos, N. (2017). Attention mediates the flexible allocation of visual working memory resources. *Journal of Experimental Psychology.*

Human Perception and Performance, *43*(7), 1454–1465. https://doi.org/10.1037/xhp0000398

Esterman, M., Liu, G., Okabe, H., Reagan, A., Thai, M., & DeGutis, J. (2015). Frontal eye field involvement in sustaining visual attention: Evidence from transcranial magnetic stimulation. *NeuroImage*, *111*, 542–548. https://doi.org/10.1016/j.neuroimage.2015.01.044

Fiebelkorn, I., Pinsk, M. A., & Kastner, S. (2018). A Dynamic Interplay within the Frontoparietal Network Underlies Rhythmic Spatial Attention. *Neuron*, *99*(4), 842-853.e8. https://doi.org/10.1016/j.neuron.2018.07.038

Fiebelkorn, I., Saalmann, Y. B., & Kastner, S. (2013). Rhythmic Sampling within and between Objects despite Sustained Attention at a Cued Location. *Current Biology*, *23*(24), 2553–2558. https://doi.org/10.1016/j.cub.2013.10.063

Foster, J. J., Bsales, E. M., Jaffe, R. J., & Awh, E. (2017). Alpha-Band Activity Reveals Spontaneous Representations of Spatial Position in Visual Working Memory. *Current Biology*, *27*(20), 3216-3223.e6. https://doi.org/10.1016/j.cub.2017.09.031

Foster, J. J., Sutterer, D. W., Serences, J. T., Vogel, E. K., & Awh, E. (2016). The topography of alpha-band activity tracks the content of spatial working memory. *Journal of Neurophysiology*, *115*(1), 168–177. https://doi.org/10.1152/jn.00860.2015

Foster, J. J., Sutterer, D. W., Serences, J. T., Vogel, E. K., & Awh, E. (2017). Alpha-Band Oscillations Enable Spatially and Temporally Resolved Tracking of Covert Spatial Attention. *Psychological Science*, 0956797617699167. https://doi.org/10.1177/0956797617699167

Fries, P. (2005). A mechanism for cognitive dynamics: neuronal communication through neuronal coherence. *Trends in Cognitive Sciences*, *9*(10), 474–480. https://doi.org/10.1016/j.tics.2005.08.011

Fries, P. (2015). Rhythms for Cognition: Communication through Coherence. *Neuron*, *88*(1), 220–235. https://doi.org/10.1016/j.neuron.2015.09.034

Fries, P., Reynolds, J. H., Rorie, A. E., & Desimone, R. (2001). Modulation of Oscillatory Neuronal Synchronization by Selective Visual Attention. *Science*, *291*(5508), 1560–1563. https://doi.org/10.1126/science.1055465

Fuentemilla, L., Penny, W. D., Cashdollar, N., Bunzeck, N., & Düzel, E. (2010). Theta-Coupled Periodic Replay in Working Memory. *Current Biology*, *20*(7), 606–612. https://doi.org/10.1016/j.cub.2010.01.057

Harris, A. M., Dux, P. E., & Mattingley, J. B. (2018). Detecting Unattended Stimuli Depends on the Phase of Prestimulus Neural Oscillations. *Journal of Neuroscience*, *38*(12), 3092–3101. https://doi.org/10.1523/JNEUROSCI.3006-17.2018

Heinen, K., Feredoes, E., Ruff, C. C., & Driver, J. (2017). Functional connectivity between prefrontal and parietal cortex drives visuo-spatial attention shifts. *Neuropsychologia*, *99*, 81–91. https://doi.org/10.1016/j.neuropsychologia.2017.02.024

Helfrich, R. F., Breska, A., & Knight, R. T. (2019). Neural entrainment and network resonance in support of top-down guided attention. *Current Opinion in Psychology*, *29*, 82–89. https://doi.org/10.1016/j.copsyc.2018.12.016

Helfrich, R. F., Fiebelkorn, I., Szczepanski, S. M., Lin, J. J., Parvizi, J., Knight, R. T., & Kastner, S. (2018). Neural Mechanisms of Sustained Attention Are Rhythmic. *Neuron*, *99*(4), 854-865.e5. https://doi.org/10.1016/j.neuron.2018.07.032

Helfrich, R. F., & Knight, R. T. (2016). Oscillatory Dynamics of Prefrontal Cognitive Control. *Trends in Cognitive Sciences*, *20*(12), 916–930. https://doi.org/10.1016/j.tics.2016.09.007

Herbst, S. K., & Landau, A. N. (2016). Rhythms for cognition: the case of temporal processing. *Current Opinion in Behavioral Sciences*, *8*, 85–93. https://doi.org/10.1016/j.cobeha.2016.01.014

Heusser, A. C., Poeppel, D., Ezzyat, Y., & Davachi, L. (2016). Episodic sequence memory is supported by a theta-gamma phase code. *Nature Neuroscience*, *19*(10), 1374–1380. https://doi.org/10.1038/nn.4374

Hung, J., Driver, J., & Walsh, V. (2011). Visual Selection and the Human Frontal Eye Fields: Effects of Frontal Transcranial Magnetic Stimulation on Partial Report Analyzed by Bundesen's Theory of Visual Attention. *Journal of Neuroscience*, *31*(44), 15904–15913. https://doi.org/10.1523/JNEUROSCI.2626-11.2011

Jafarpour, A., Penny, W., Barnes, G., Knight, R. T., & Duzel, E. (2017). Working Memory Replay Prioritizes Weakly Attended Events. *ENeuro*, *4*(4). https://doi.org/10.1523/ENEURO.0171-17.2017

Jensen, O., & Vissers, M. E. (2017). Multiple visual objects are sampled sequentially. *PLOS Biology*, *15*(7), e2003230. https://doi.org/10.1371/journal.pbio.2003230

Jia, J., Liu, L., Fang, F., & Luo, H. (2017). Sequential sampling of visual objects during sustained attention. *PLOS Biology*, *15*(6), e2001903. https://doi.org/10.1371/journal.pbio.2001903

Kelly, S. P., Lalor, E. C., Reilly, R. B., & Foxe, J. J. (2006). Increases in alpha oscillatory power reflect an active retinotopic mechanism for distracter suppression during sustained

visuospatial attention. *Journal of Neurophysiology*, *95*(6), 3844–3851. https://doi.org/10.1152/jn.01234.2005

Kienitz, R., Schmiedt, J. T., Shapcott, K. A., Kouroupaki, K., Saunders, R. C., & Schmid, M. C. (2018). Theta Rhythmic Neuronal Activity and Reaction Times Arising from Cortical Receptive Field Interactions during Distributed Attention. *Current Biology*. https://doi.org/10.1016/j.cub.2018.05.086

Klimesch, W. (2012). Alpha-band oscillations, attention, and controlled access to stored information. *Trends in Cognitive Sciences*, *16*(12), 606–617. https://doi.org/10.1016/j.tics.2012.10.007

Landau, A. N., & Fries, P. (2012). Attention Samples Stimuli Rhythmically. *Current Biology*, *22*(11), 1000–1004. https://doi.org/10.1016/j.cub.2012.03.054

Landau, A. N., Schreyer, H. M., van Pelt, S., & Fries, P. (2015). Distributed Attention Is Implemented through Theta-Rhythmic Gamma Modulation. *Current Biology*, *25*(17), 2332–2337. https://doi.org/10.1016/j.cub.2015.07.048

Lemaire, B., Pageot, A., Plancher, G., & Portrat, S. (2017). What is the time course of working memory attentional refreshing? *Psychonomic Bulletin & Review*, 1–16. https://doi.org/10.3758/s13423-017-1282-z

Lewis-Peacock, J. A., & Postle, B. R. (2012). Decoding the internal focus of attention. *Neuropsychologia*, *50*(4), 470–478. https://doi.org/10.1016/j.neuropsychologia.2011.11.006

Lisman, J. E. (2010). Working Memory: The Importance of Theta and Gamma Oscillations. *Current Biology*, *20*(11), R490–R492. https://doi.org/10.1016/j.cub.2010.04.011

Lisman, J. E., & Idiart, M. A. (1995). Storage of 7 +/- 2 short-term memories in oscillatory subcycles. *Science*, *313*, 1512–1515.

Lisman, J. E., & Jensen, O. (2013). The Theta-Gamma Neural Code. *Neuron*, *77*(6), 1002–1016. https://doi.org/10.1016/j.neuron.2013.03.007

Lubenov, E. V., & Siapas, A. G. (2009). Hippocampal theta oscillations are travelling waves. *Nature*, *459*(7246), 534–539. https://doi.org/10.1038/nature08010

Luck, S. J., & Vogel, E. K. (1997). The capacity of visual working memory for features and conjunctions. *Nature*, *390*(6657), 279–281. https://doi.org/10.1038/36846

Makovski, T., & Jiang, Y. V. (2007). Distributing versus focusing attention in visual short-term memory. *Psychonomic Bulletin & Review*, *14*(6), 1072–1078. https://doi.org/10.3758/BF03193093

Marshall, T. R., O'Shea, J., Jensen, O., & Bergmann, T. O. (2015). Frontal Eye Fields Control Attentional Modulation of Alpha and Gamma Oscillations in Contralateral Occipitoparietal Cortex. *The Journal of Neuroscience*, *35*(4), 1638–1647. https://doi.org/10.1523/JNEUROSCI.3116-14.2015

Mathewson, K. E., Gratton, G., Fabiani, M., Beck, D. M., & Ro, T. (2009). To see or not to see: prestimulus alpha phase predicts visual awareness. *The Journal of Neuroscience*, *29*, 2725–2732.

McLelland, D., & VanRullen, R. (2016). Theta-Gamma Coding Meets Communication-through-Coherence: Neuronal Oscillatory Multiplexing Theories Reconciled. *PLOS Computational Biology*, *12*(10), e1005162. https://doi.org/10.1371/journal.pcbi.1005162

Medendorp, W. P., Kramer, G. F. I., Jensen, O., Oostenveld, R., Schoffelen, J.-M., & Fries, P. (2007). Oscillatory Activity in Human Parietal and Occipital Cortex Shows Hemispheric

Lateralization and Memory Effects in a Delayed Double-Step Saccade Task. *Cerebral Cortex*, *17*(10), 2364–2374. https://doi.org/10.1093/cercor/bhl145

Myers, N. E., Chekroud, S. R., Stokes, M. G., & Nobre, A. C. (2018). Benefits of Flexible Prioritization in Working Memory Can Arise Without Costs. *Journal of Experimental Psychology. Human Perception and Performance*, *44*(3), 398–411. https://doi.org/10.1037/xhp0000449

Myers, N. E., Stokes, M. G., & Nobre, A. C. (2017). Prioritizing Information during Working Memory: Beyond Sustained Internal Attention. *Trends in Cognitive Sciences*, *0*(0). https://doi.org/10.1016/j.tics.2017.03.010

Myers, N. E., Stokes, M. G., Walther, L., & Nobre, A. C. (2014). Oscillatory Brain State Predicts Variability in Working Memory. *The Journal of Neuroscience*, *34*(23), 7735–7743. https://doi.org/10.1523/JNEUROSCI.4741-13.2014

Nyffeler, T., Wurtz, P., Lüscher, H.-R., Hess, C. W., Senn, W., Pflugshaupt, T., … Müri, R. M. (2006). Repetitive TMS over the human oculomotor cortex: comparison of 1-Hz and theta burst stimulation. *Neuroscience Letters*, *409*(1), 57–60. https://doi.org/10.1016/j.neulet.2006.09.011

Olivers, C. N. L., Peters, J., Houtkamp, R., & Roelfsema, P. R. (2011). Different states in visual working memory: when it guides attention and when it does not. *Trends in Cognitive Sciences*, *15*(7), 327–334. https://doi.org/10.1016/j.tics.2011.05.004

Oostenveld, R., Fries, P., Maris, E., & Schoffelen, J. M. (2011). FieldTrip: Open source software for advanced analysis of MEG, EEG, and invasive electrophysiological data. *Computational Intelligence and Neuroscience*, *2011*. https://doi.org/10.1155/2011/156869

Osipova, D., Takashima, A., Oostenveld, R., Fernández, G., Maris, E., & Jensen, O. (2006). Theta and Gamma Oscillations Predict Encoding and Retrieval of Declarative Memory. *The Journal of Neuroscience*, *26*(28), 7523–7531. https://doi.org/10.1523/JNEUROSCI.1948-06.2006

Pascual-Leone, A., Bartres-Faz, D., & Keenan, J. P. (1999). Transcranial magnetic stimulation: studying the brain-behaviour relationship by induction of "virtual lesions". *Philosophical Transactions of the Royal Society B: Biological Sciences*, *354*(1387), 1229–1238.

Pashler, H., & Shiu, L. (1999). Do images involuntarily trigger search? A test of Pillsbury's hypothesis. *Psychonomic Bulletin & Review*, *6*(3), 445–448. https://doi.org/10.3758/BF03210833

Paus, T. (1996). Location and function of the human frontal eye-field: A selective review. *Neuropsychologia*, *34*(6), 475–483. https://doi.org/10.1016/0028-3932(95)00134-4

Pelli, Denis G., & Farell, B. (1995). Psychophysical methods. *Handbook of Optics*, 29.21-29.31.

Pelli, D.G. (1997). The VideoToolbox software for visual psychophysics: Transforming numbers into movies. *Spatial Vision*, *10*, 437–442.

Peters, B., Rahm, B., Kaiser, J., & Bledowski, C. (2018). Attention samples objects held in working memory at a theta rhythm. *BioRxiv*, 369652. https://doi.org/10.1101/369652

Phillips, J. M., Vinck, M., Everling, S., & Womelsdorf, T. (2014). A Long-Range Fronto-Parietal 5- to 10-Hz Network Predicts "Top-Down" Controlled Guidance in a Task-Switch Paradigm. *Cerebral Cortex*, *24*(8), 1996–2008. https://doi.org/10.1093/cercor/bht050

Popov, T., Kastner, S., & Jensen, O. (2017). FEF-Controlled Alpha Delay Activity Precedes Stimulus-Induced Gamma-Band Activity in Visual Cortex. *The Journal of Neuroscience:*

The Official Journal of the Society for Neuroscience, *37*(15), 4117–4127. https://doi.org/10.1523/JNEUROSCI.3015-16.2017

Portrat, S., & Lemaire, B. (2015). Is Attentional Refreshing in Working Memory Sequential? A Computational Modeling Approach. *Cognitive Computation*, *7*(3), 333–345. https://doi.org/10.1007/s12559-014-9294-8

Posner, M. I., & Petersen, S. E. (1990). The Attention System of the Human Brain. *Annual Review of Neuroscience*, *13*(1), 25–42. https://doi.org/10.1146/annurev.ne.13.030190.000325

Rihs, T. A., Michel, C. M., & Thut, G. (2007). Mechanisms of selective inhibition in visual spatial attention are indexed by alpha-band EEG synchronization. *The European Journal of Neuroscience*, *25*(2), 603–610. https://doi.org/10.1111/j.1460-9568.2007.05278.x

Ro, T., Farnè, A., & Chang, E. (2002). Locating the Human Frontal Eye Fields With Transcranial Magnetic Stimulation. *Journal of Clinical and Experimental Neuropsychology*, *24*(7), 930–940. https://doi.org/10.1076/jcen.24.7.930.8385

Ruff, C. C., Blankenburg, F., Bjoertomt, O., Bestmann, S., Weiskopf, N., & Driver, J. (2008). Hemispheric Differences in Frontal and Parietal Influences on Human Occipital Cortex: Direct Confirmation with Concurrent TMS–fMRI. *Journal of Cognitive Neuroscience*, *21*(6), 1146–1161. https://doi.org/10.1162/jocn.2009.21097

Sauseng, P., Feldheim, J. F., Freunberger, R., & Hummel, F. C. (2011). Right Prefrontal TMS Disrupts Interregional Anticipatory EEG Alpha Activity during Shifting of Visuospatial Attention. *Frontiers in Psychology*, *2*, 241. https://doi.org/10.3389/fpsyg.2011.00241

Sauseng, P., Klimesch, W., Stadler, W., Schabus, M., Doppelmayr, M., Hanslmayr, S., … Birbaumer, N. (2005). A shift of visual spatial attention is selectively associated with

human EEG alpha activity. *European Journal of Neuroscience*, *22*(11), 2917–2926. https://doi.org/10.1111/j.1460-9568.2005.04482.x

Schmidt, B. K., Vogel, E. K., Woodman, G. F., & Luck, S. J. (2002). Voluntary and automatic attentional control of visual working memory. *Perception & Psychophysics*, *64*(5), 754–763. https://doi.org/10.3758/BF03194742

Sellers, K. K., Yu, C., Zhou, Z. C., Stitt, I., Li, Y., Radtke-Schuller, S., … Fröhlich, F. (2016). Oscillatory Dynamics in the Frontoparietal Attention Network during Sustained Attention in the Ferret. *Cell Reports*, *16*(11), 2864–2874. https://doi.org/10.1016/j.celrep.2016.08.055

Senoussi, M., Moreland, J. C., Busch, N. A., & Dugue, L. (2018). Attention explores space periodically at the theta frequency. *BioRxiv*, 443341. https://doi.org/10.1101/443341

Sherman, M. T., Kanai, R., Seth, A. K., & VanRullen, R. (2016). Rhythmic Influence of Top–Down Perceptual Priors in the Phase of Prestimulus Occipital Alpha Oscillations. *Journal of Cognitive Neuroscience*, *28*(9), 1318–1330. https://doi.org/10.1162/jocn_a_00973

Siegel, M., Donner, T. H., & Engel, A. K. (2012). Spectral fingerprints of large-scale neuronal interactions. *Nature Reviews Neuroscience*, *13*(2), 121–134. https://doi.org/10.1038/nrn3137

Siegel, M., Donner, T. H., Oostenveld, R., Fries, P., & Engel, A. K. (2008). Neuronal Synchronization along the Dorsal Visual Pathway Reflects the Focus of Spatial Attention. *Neuron*, *60*(4), 709–719. https://doi.org/10.1016/j.neuron.2008.09.010

Silvanto, J., Lavie, N., & Walsh, V. (2006). Stimulation of the Human Frontal Eye Fields Modulates Sensitivity of Extrastriate Visual Cortex. *Journal of Neurophysiology*, *96*(2), 941–945. https://doi.org/10.1152/jn.00015.2006

Song, K., Meng, M., Chen, L., Zhou, K., & Luo, H. (2014). Behavioral Oscillations in Attention: Rhythmic α Pulses Mediated through θ Band. *The Journal of Neuroscience*, *34*(14), 4837–4844. https://doi.org/10.1523/JNEUROSCI.4856-13.2014

Souza, A. S., & Oberauer, K. (2016). In search of the focus of attention in working memory: 13 years of the retro-cue effect. *Attention, Perception, & Psychophysics*, *78*(7), 1839–1860. https://doi.org/10.3758/s13414-016-1108-5

Spaak, E., Bonnefond, M., Maier, A., Leopold, D. A., & Jensen, O. (2012). Layer-Specific Entrainment of Gamma-Band Neural Activity by the Alpha Rhythm in Monkey Visual Cortex. *Current Biology*, *22*(24), 2313–2318. https://doi.org/10.1016/j.cub.2012.10.020

Szczepanski, S. M., Crone, N. E., Kuperman, R. A., Auguste, K. I., Parvizi, J., & Knight, R. T. (2014). Dynamic Changes in Phase-Amplitude Coupling Facilitate Spatial Attention Control in Fronto-Parietal Cortex. *PLOS Biology*, *12*(8), e1001936. https://doi.org/10.1371/journal.pbio.1001936

Thut, G., Nietzel, A., Brandt, S. A., & Pascual-Leone, A. (2006). Alpha-Band Electroencephalographic Activity over Occipital Cortex Indexes Visuospatial Attention Bias and Predicts Visual Target Detection. *The Journal of Neuroscience*, *26*(37), 9494–9502. https://doi.org/10.1523/jneurosci.0875-06.2006

Tort, A. B. L., Komorowski, R. W., Manns, J. R., Kopell, N. J., & Eichenbaum, H. (2009). Theta-gamma coupling increases during the learning of item-context associations. *Proceedings of the National Academy of Sciences of the United States of America*, *106*(49), 20942–20947. https://doi.org/10.1073/pnas.0911331106

Treisman, A. (1982). Perceptual grouping and attention in visual search for features and for objects. *Journal of Experimental Psychology. Human Perception and Performance*, *8*(2), 194–214.

van Moorselaar, D., Gunseli, E., Theeuwes, J., & Olivers, C. N. L. (2015). The time course of protecting a visual memory representation from perceptual interference. *Frontiers in Human Neuroscience*, *8*. https://doi.org/10.3389/fnhum.2014.01053

VanRullen, R. (2016). Perceptual Cycles. *Trends in Cognitive Sciences*, *20*(10), 723–735. https://doi.org/10.1016/j.tics.2016.07.006

VanRullen, R., Carlson, T., & Cavanagh, P. (2007). The blinking spotlight of attention. *Proceedings of the National Academy of Sciences of the United States of America*, *104*(49), 19204–19209. https://doi.org/10.1073/pnas.0707316104

Vergauwe, E., & Cowan, N. (2015). Attending to items in working memory: evidence that refreshing and memory search are closely related. *Psychonomic Bulletin & Review*, *22*(4), 1001–1006. https://doi.org/10.3758/s13423-014-0755-6

Vernet, M., Quentin, R., Chanes, L., Mitsumasu, A., & Valero-Cabré, A. (2014). Frontal eye field, where art thou? Anatomy, function, and non-invasive manipulation of frontal regions involved in eye movements and associated cognitive operations. *Frontiers in Integrative Neuroscience*, *8*. https://doi.org/10.3389/fnint.2014.00066

Vertes, R. P. (2005). Hippocampal theta rhythm: A tag for short-term memory. *Hippocampus*, *15*(7), 923–935. https://doi.org/10.1002/hipo.20118

Vogel, E.K., Woodman, G. F., & Luck, S. J. (2005). Pushing around the Locus of Selection: Evidence for the Flexible-selection Hypothesis. *Journal of Cognitive Neuroscience*, *17*(12), 1907–1922. https://doi.org/10.1162/089892905775008599

Vogel, E.K., McCollough, A. W., & Machizawa, M. G. (2005). Neural measures reveal individual differences in controlling access to working memory. *Nature*, *438*, 368–387.

Wang, B., Yan, C., Wang, Z., Olivers, C. N. L., & Theeuwes, J. (2017). Adverse orienting effects on visual working memory encoding and maintenance. *Psychonomic Bulletin & Review*, *24*(4), 1261–1267. https://doi.org/10.3758/s13423-016-1205-4

Watson, A. B., & Pelli, D. G. (1983). Quest: A Bayesian adaptive psychometric method. *Perception & Psychophysics*, *33*(2), 113–120. https://doi.org/10.3758/BF03202828

Wen, H., & Liu, Z. (2016). Separating Fractal and Oscillatory Components in the Power Spectrum of Neurophysiological Signal. *Brain Topography*, *29*(1), 13–26. https://doi.org/10.1007/s10548-015-0448-0

Woodman, G. F., & Luck, S. J. (2002). Interactions between perception and working memory during visual search. *Journal of Vision*, *2*(7), 732–732. https://doi.org/10.1167/2.7.732

Woodman, G. F., Vecera, S. P., & Luck, S. J. (2003). Perceptual organization influences visual working memory. *Psychonomic Bulletin & Review*, *10*(1), 80–87. https://doi.org/10.3758/BF03196470

Zoefel, B., & VanRullen, R. (2017). Oscillatory Mechanisms of Stimulus Processing and Selection in the Visual and Auditory Systems: State-of-the-Art, Speculations and Suggestions. *Frontiers in Neuroscience*, *11*. https://doi.org/10.3389/fnins.2017.00296

APPENDIX. SUPPLEMENTAL FIGURES

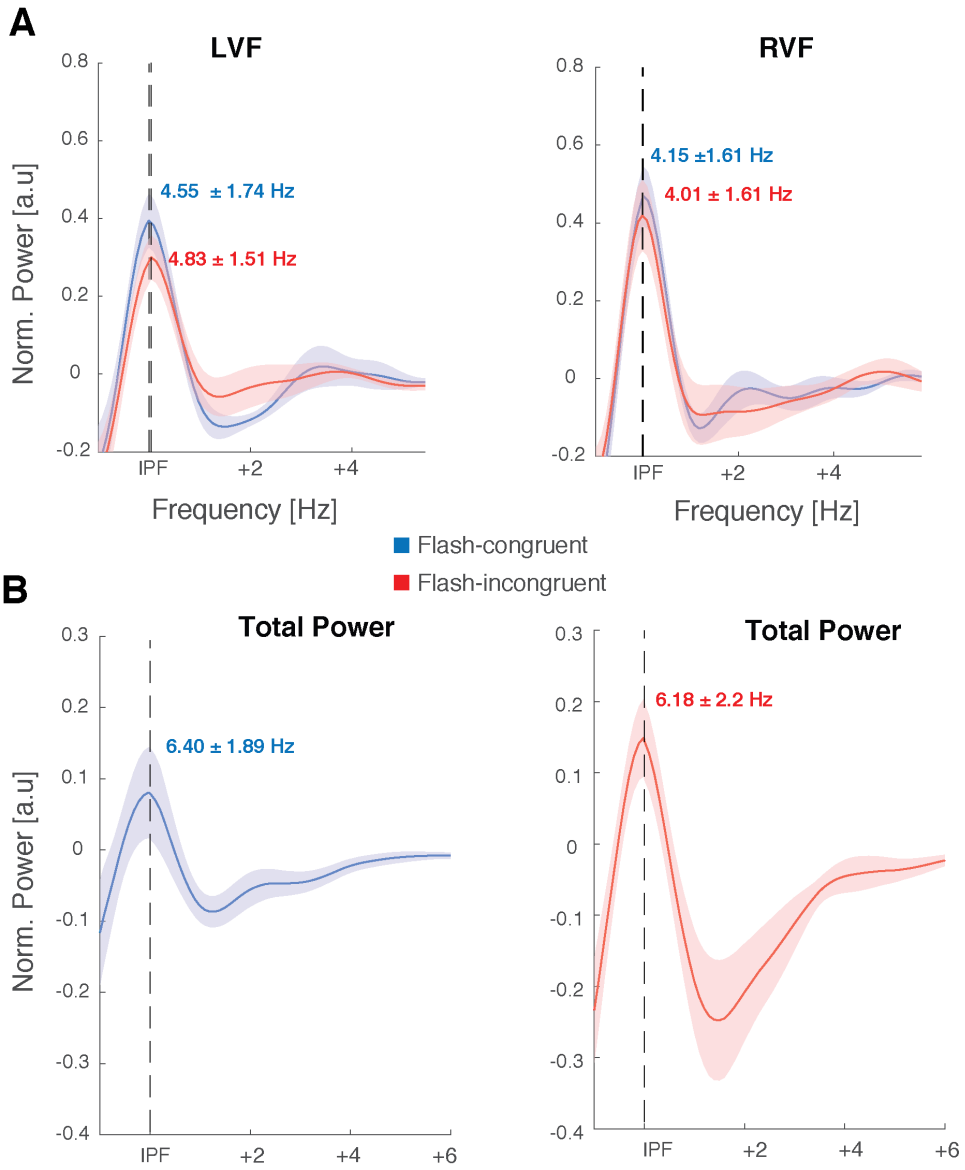

Figure A1. Peak aligned power spectral density for flash-congruent (blue) and flash-incongruent (red) detection accuracy (A) and CTF selectivity (B) estimated using IRASA procedure. Similarly to the permutation-based estimated peaks, IRASA-based peaks in theta range (4-8Hz) provide evidence for the presence of rhythmic fluctuations in detection accuracy and CTF selectivity.

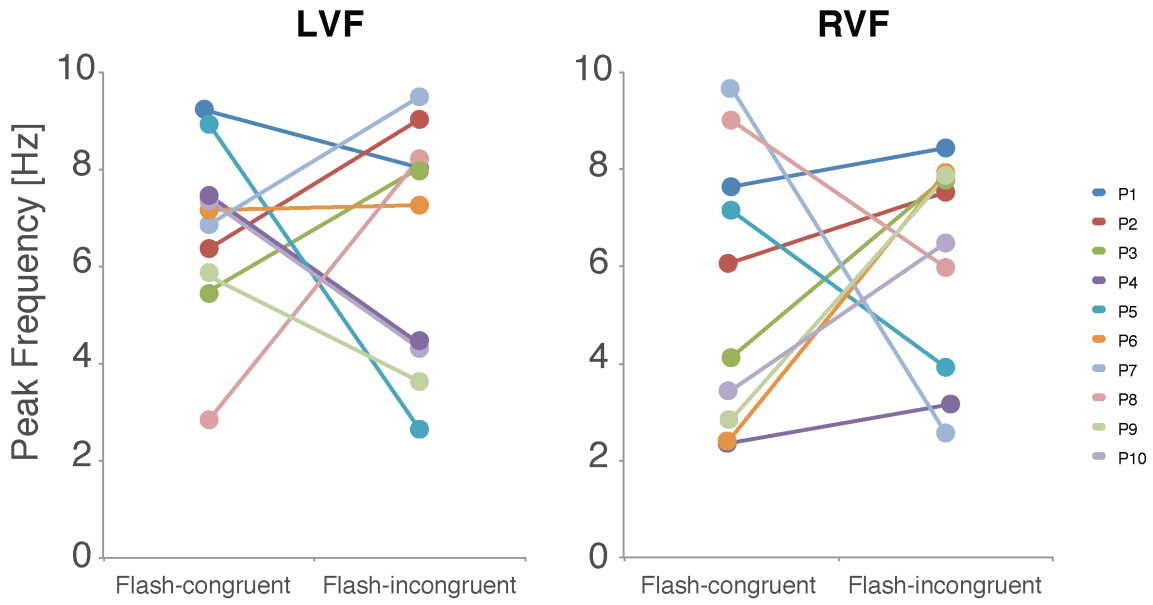

Figure A2. Individual participant peak frequencies for flash-congruent and flash-incongruent detection accuracy for LVF (left) and RVF (right).

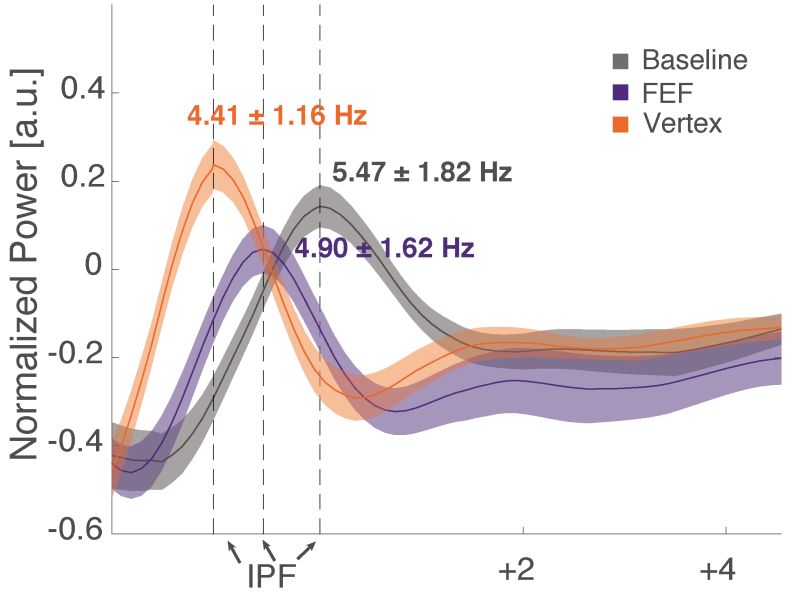

Figure A3. Peak aligned power spectral density for baseline, FEF and vertex conditions estimated using the IRASA procedure. Similarly to the permutation-based analysis, there were no significant differences in peak frequency between the different conditions and no significant differences in the peak power. It is important to note, however, that normalized power for the FEF peak (M = .05, SD = .20) was not significantly different from zero [one-tailed one-sample t-test, $t(11)$= 0.82, p = .21], whereas both baseline [M = .14, SD = .17; $t(11)$= 2.84, p = .008] and vertex [M = .24, SD = .20; $t(11)$= 4.16, p < .001] peaks were significantly larger than zero.

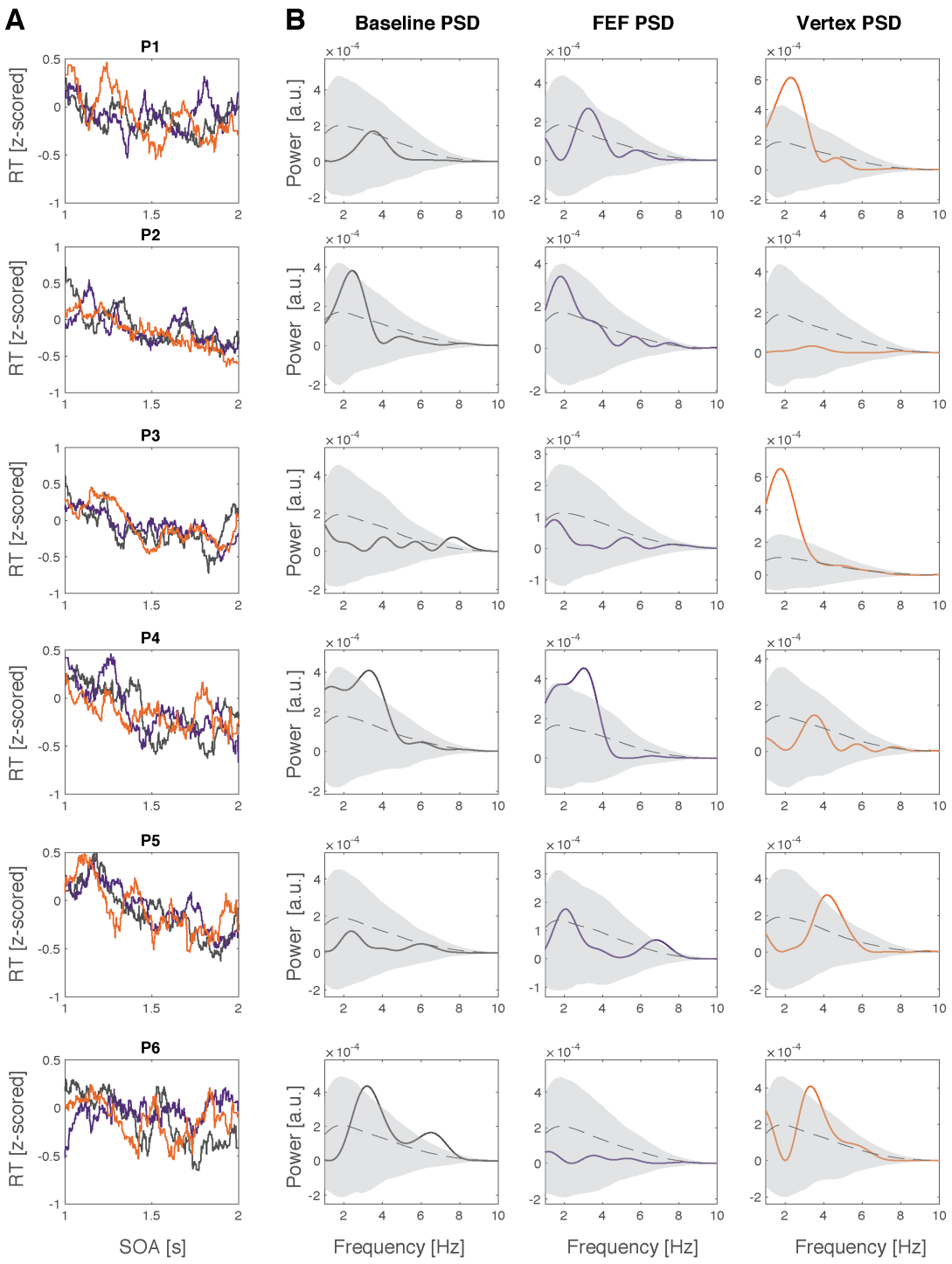

Figure A4. Individual participant data and the results of the spectral analysis for the baseline (gray), FEF (purple) and vertex (orange) conditions. (A) Time-series of z-scored RTs for the three experimental conditions. (B) PSD for the three experimental conditions. Dashed lines represent mean PSD for the null-distribution. Shaded areas correspond to 95% CI.

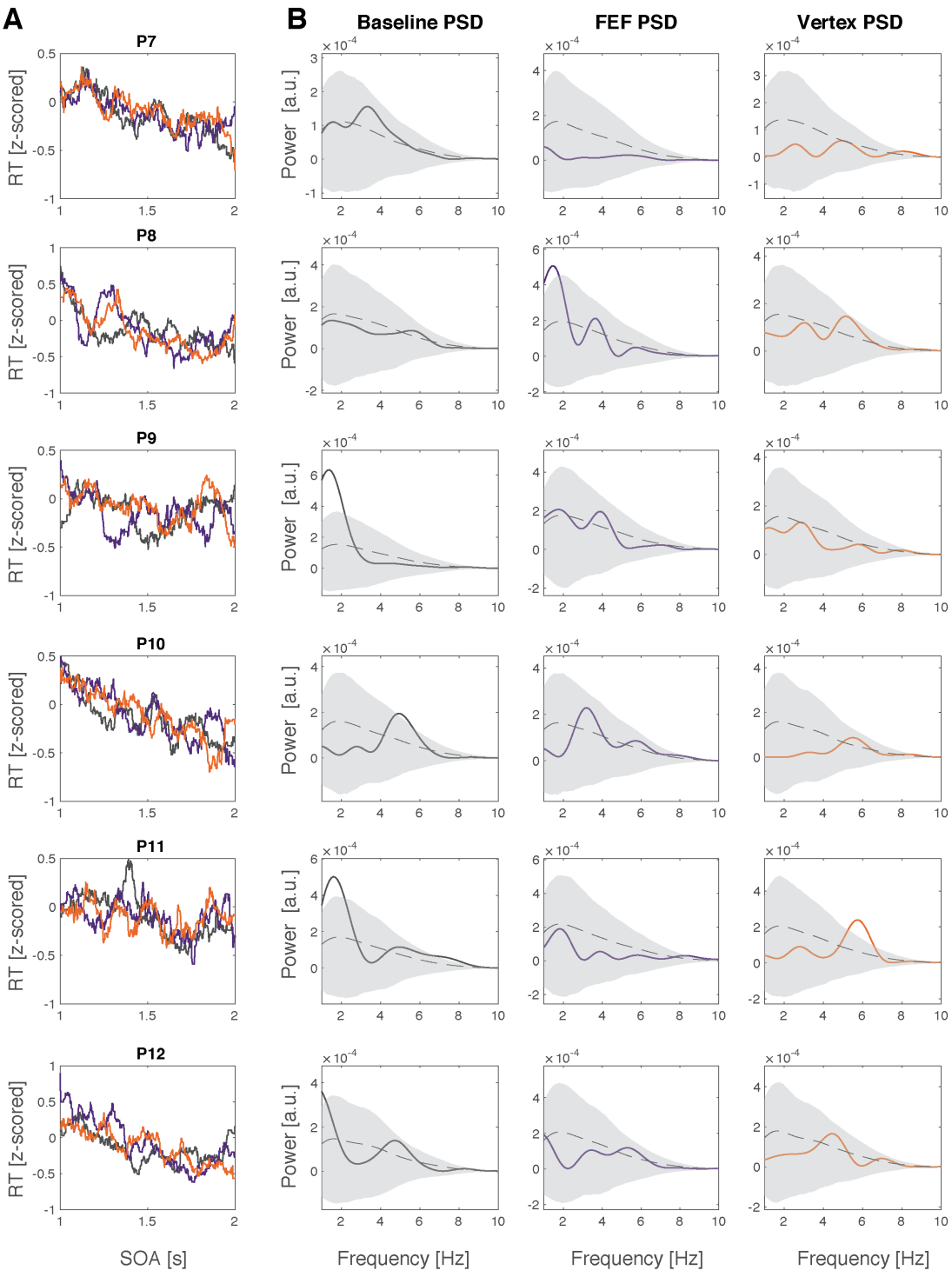

Figure A4. Individual participant data and the results of the spectral analysis for the baseline (gray), FEF (purple) and vertex (orange) conditions (continued). (A) Time-series of z-scored RTs for the three experimental conditions. (B) PSD for the three experimental conditions. Dashed lines represent mean PSD for the null-distribution. Shaded areas correspond to 95% CI.